FUNDAMENTAL STUDY ON TIN RECOVERY IN ACIDIC AQUEOUS SYSTEMS

by

Tao Hong

BSc., Nanjing University, China, 2013

A THESIS SUBMITTED IN PARTIAL FULFILMENT OF

THE REQUIREMENTS FOR THE DEGREE OF

MASTER OF APPLIED SCIENCE

in

THE FACULTY OF GRADUATE AND POSTDOCTORAL STUDIES

(Materials Engineering)

THE UNIVERSITY OF BRITISH COLUMBIA

(Vancouver)

October 2015

Abstract

Tin is widely used in solder, tin plating and tin alloys. The current recovery rate of tin metal is low and insufficient with just over 300,000 tonnes annually. The grade of tin concentrates in traditional smelting methods needs to be at least 60%. Otherwise, iron, the chief impurity in tin concentrates can form tin-iron alloys and result in inefficient recovery of tin. Therefore, a hydrometallurgical technology to treat lower grade tin concentrates is proposed to solve the problem and close the demand gap for tin.

The electrochemical reduction of chromium(III) solutions was conducted with a graphite felt cathode in acidic aqueous systems (chloride, sulfate and MSA). The parameters of acid concentration, current density, graphite felt thickness, graphite felt surface condition and graphite felt usage frequency were investigated. It was found that acid concentration has a significant influence on chromium(III) reduction in the sulfate and MSA system, while slight effect in the chloride system. In addition, the lifetime of the graphite felt in the sulfate and MSA system was shorter than that in the chloride system. These electrochemical differences may result from the pathway difference in electron transfer between the electrode and the chromium(III) ions. In general, chromium(III) ions in the chloride system showed the best electrochemical reduction activity.

The chromium(II) ions synthesized from electrochemical reduction of chromium(III) ions were then used to effect the reduction of SnO_2 powder. The effect of temperature on the recovery test in the chloride, sulfate and MSA system was investigated. It was found that under the conditions of this thesis, the predominant recovery product of SnO_2 is Sn metal, rather than Sn(II). Generally, the recovery kinetics and total conversion were low in the sulfate and MSA system; however, the chloride system showed significantly better recovery results. This may be attributed to the catalysis effect of the chloride ions on the recovery process.

Preface

This thesis is original, unpublished, independent work by the author, Tao Hong.

Table of Contents

List of Tables

List of Figures

Nomenclature

ΔG^o	Standard Gibbs free energy, in kJ/mol
E^o	Standard potential, in volts (V)
Eh	Potential, in volts (V)
SHE	Standard hydrogen electrode
SCE	Saturated calomel electrode
HMDE	Hanging mercury drop electrode
CE	Current efficiency
CR	Conversion of Reaction 1 or Reaction 2
XRD	X-ray powder diffraction
AAS	Atomic absorption spectrometer
M	Molarity, in mol/L
N	Normality, in Eq/L
e	Electron
α_{app}	Apparent transfer coefficient
rpm	Rotations per minutes
ppm	mg/kg
ΔV_m	Change of molar volume, in cm^3/mol
T	Temperature, in ℃ or K
i	Current density, in A/m^2
I	Current, in A
t	Time, in seconds (s)
V	Volume, in liters (L)
F	Faraday constant, equal to 96485 C/mol electron
n	Number of moles of electrons passed for a half reaction
[ ]	Molarity concentration, in mol/L
R	Universal gas constant, $R = 8.314\,472(15)\ J\ K^{-1}\ mol^{-1}$
K	Stablity constant

oHp	Outer Helmholtz plane
RVC	Reticulated vitreous carbon
MSA	Methanesulfonic acid
EDTA	Ethylenediaminetetraacetic acid
CyDTA	Trans-1,2-Diaminocyclohexane-N,N,N',N'-tetraacetic acid
DTPA	Diethylene triamine pentaacetic acid
EGTA	Ethylene glycol tetraacetic acid

Acknowledgements

First of all, I would like to express my sincere gratitude to my supervisor, Dr. David Dreisinger for all the inspiring discussions, instructive advices, and continuous encouragement throughout my graduate studies. Without his guidance, this work would never have been completed. His great talent, rich experiences and strong passion to hydrometallurgy also greatly inspired me.

I highly appreciate the help from Dr. Jianming Lu for his invaluable suggestions and instructions on my electrochemical researches. I'm also thankful for Dr. Berend Wassink`s patient assistance with my analytical techniques and safety suggestions.

Great thanks to Dr. David Dixon, Dr. Edouard Asselin, Dr. Wenying Liu and any other faculty and staff in the department for their kind help during my graduate study.

I wish to thank all the members of the Hydrometallurgy Group at UBC for their help. Thanks to Dr. Zihe Ren for his kind help on the XRD interpretation.

In addition, thank you to Dr. Dreisinger, the Department of Materials Engineering at UBC, BASF Company (Germany) for providing the financial assistance necessary to undertake this thesis.

Many thanks to all my friends in Vancouver. Life in foreign country is lonely and not easy. Thank you all for making my days in Vancouver beautiful and unforgettable.

Finally, special thanks to my family for their understanding and support throughout my years of education. Without their love, I wouldn't have come this far.

Chapter 1 Introduction

As one of the most ancient metals known to humans, tin extraction and use can be dated to the beginnings of the Bronze Age around 3,000 BC, when it was observed that copper objects formed of polymetallic ores with different metal contents had different physical properties. The extractive metallurgy of tin is based on the recovery of the tin oxide mineral, cassiterite, which is the most important source of tin ore throughout history. In practice, cassiterite is always reduced by carbon or carbonaceous matter[1]. Several problems may occur for this process:

(1) The temperature of reduction is so high that other metals are reduced at the same time, and alloy with the reduced tin. This applies especially to iron. Tin-iron alloys can cause many difficulties in the effective recovery of tin. Typically, the grade of tin concentrates for smelting should be very high, at least 60%.

(2) The tin ore must be contained in a furnace capable of resisting the high temperature required; hence the furnace lining must be either acidic, consisting of silica or silicates, or basic, consisting of lime or magnesia. In both cases silico-stannates are likely produced[1]. Therefore, the slags produced are too rich in tin to be thrown away, and they require further treatment; otherwise great values will be lost.

(3) The release of carbon dioxide, carbon monoxide and other harmful gases during the smelting process of tin pyrometallurgical recovery has caused several environmental problems.

In order to solve the problems mentioned above, an alternative process for the hydrometallurgical treatment of cassiterite has been proposed.

Tin can be possibly reductively extracted at a moderate pH by reducing tin dioxide to the stannous state or metallic tin. There are many reducing reagents that could be used. Ideally, the reagent should be recyclable. One such system that may be useful is the chromous/chromic system (Cr^{3+}/Cr^{2+}). The benefit of the chromium system is that Cr^{2+}

can be electrochemically regenerated at a cathode and is thus fully recyclable. The tin extraction reactions with Cr^{2+} are described in **Equation 1.1** and **Equation 1.2**.

Reaction 1 $SnO_2 + 4H^+ + 2Cr^{2+} \longrightarrow Sn^{2+} + 2Cr^{3+} + 2H_2O$ **Equation 1.1**

Reaction 2 $SnO_2 + 4H^+ + 4Cr^{2+} \longrightarrow Sn + 4Cr^{3+} + 2H_2O$ **Equation 1.2**

Compared to traditional inorganic acids (HCl, H_2SO_4 and HNO_3), methanesulfonic acid (MSA) has many attractive features such as a high solubility of salts, non-oxidizing, readily biodegradable and odorless. The high solubility of tin in the MSA (3.73 mol/L Sn^{2+}, 22 ℃) lends itself to potential novel applications for recovery and refining of tin[2].

The electrochemical reduction kinetics of chromium(III) in the chloride system has been widely studied[3, 4] and some research has also focused on the sulfate system[4]. However, there are few published results on the current efficiency of chromium(III) reduction in batch electrochemical reactors in these two systems. In addition, no work on chromium(III) electrochemical reduction in the MSA system has ever been reported.

Although several studies on the hydrometallurgical recovery of tin have been reported[5-7], pyrometallurgical steps such as roasting and calcination, are usually involved in these processes, where SnO_2 is reduced by carbon or carbonaceous matter at high temperatures. No work on reductive extraction of tin in acidic aqueous systems has been reported.

A fundamental study on electrochemical reduction of chromium(III) ions and reductive extraction of tin in chloride, sulfate and MSA systems was performed. The objectives of this project are:

(1) To study the effect of acid concentration, current density, graphite felt thickness, graphite felt surface condition and graphite felt usage frequency on the current efficiency of electrochemical reduction of chromium(III) ions in acidic aqueous solutions (chloride, sulfate and MSA systems).

(2) To compare the three acid systems in the performance of electrochemical reduction of chromium(III) ions.

(3) To investigate whether tin could be reductively extracted from synthetic tin(IV) oxide with electrochemically synthesized chromium(II) ions in acidic aqueous solutions.

(4) To explore whether Sn(II) can be the predominant recovery product and evaluate the recovery conversion of SnO_2 in acidic aqueous solutions.

(5) To compare HCl, H_2SO_4 and MSA in the ability to recover tin from synthetic tin dioxide with electrochemically synthesized chromium(II) ions.

In this thesis, previous studies on the electrochemical reduction of Cr(III) ions, reactions of inorganic solids with Cr(II), hydrometallurgical recovery of tin and other background information are reviewed in **Chapter 2**. **Chapter 3** describes the results of electrochemical reduction of Cr(II) ions in acidic aqueous solutions. The experimental study results of tin recovery in acidic aqueous systems are presented in **Chapter 4**. Finally, conclusions and recommendations of this research are talked in **Chapter 5**.

Chapter 2 Literature Review

2.1 Previous Studies on Electrochemical Reduction of Chromium(III) Ions

As a strong reducing reagent, chromium(II) has been extensively studied for its application in organic synthesis[8], energy storage[9, 10] and chromium electroplating[4]. Meanwhile, Cr(II) has also been used in the novel hydrometallurgical processes. For example, Zabin and Taube investigated the reduction of metal oxides with Cr(II) and Kelsall studied the sulfide minerals reduction with Cr(II) in the acidic aqueous systems [11, 12]. Chromium(III) species are substitution inert, which can provide evidence of bridging group involvement in homogeneous electron transfer reactions. Due to this specific property, Cr(III)/Cr(II) couple has also been used in mechanistic studies of inorganic reactions[13].

In order to employ chromium(II) ions as the reductant in the fields mentioned above, the electrochemical synthesis of chromium(II) ions with a high current efficiency is a prerequisite. However, the standard potential for chromium(III) reduction is 0.42 V lower than that of hydrogen evolution (See **Equation 2.1**). Thermodynamically, the proton is much easier to reduce than the chromium(III) ion (See **Equation 2.2**).

$$Cr^{3+} + e^- \rightarrow Cr^{2+} \qquad E^0 = -0.42 \text{ V vs SHE} \qquad \textbf{Equation 2.1}$$

$$2H^+ + 2e^- \rightarrow H_2 \qquad E^0 = 0 \text{ V vs SHE} \qquad \textbf{Equation 2.2}$$

To avoid the hydrogen evolution reaction, cathode materials for Cr(II) synthesis must have a small exchange current and a high overpotential for hydrogen generation. Hanging mercury drop, dropping mercury, lead and carbon electrodes have been widely investigated for the electrochemical reduction of chromium(III) ions in the past few decades[4, 14-18].

However, most of the previous studies were focused on the electrogeneration of chromium(II) ions in the chloride system. Few research on the electrochemical reduction in sulfate and MSA systems has been reported.

2.1.1 Eh-pH Diagram for the Cr-H_2O System

The thermodynamics of electrochemical reduction of chromium(III) ions in aqueous solution can be discussed in terms of the Eh-pH diagram for the Cr-H_2O system.

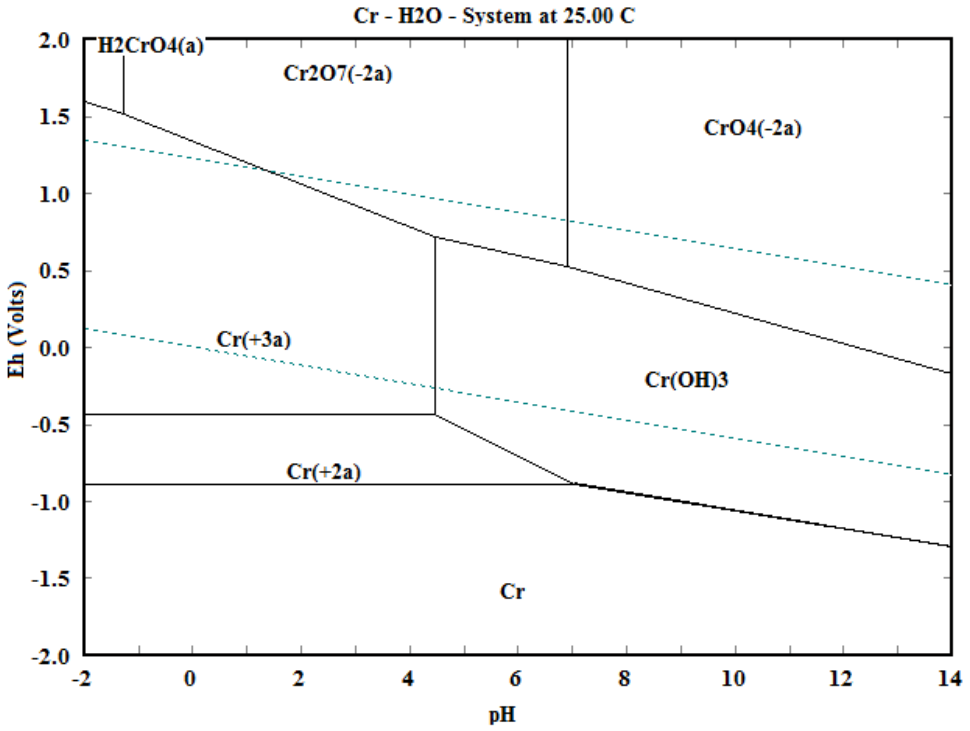

Figure 2.1 The Cr-H_2O Eh-pH diagram at 25 ℃ and 0.1 M Cr species

Figure 2.1 indicates that in the aqueous solution, Cr(III) ions are only stable when the pH is below 2.4. Beyond that point, Cr(III) will convert to $Cr(OH)_3$, which is a precipitate in the solution. Thermodynamically, it is possible to reduce Cr(III) ions to Cr(II) ions in the aqueous solution at the potential of -0.42 V with the pH less than 2.4.

The long term stability of the aqueous Cr(II) ion is of concern because thermodynamically it is unstable at a low pH, where it could possibly be oxidized by H^+ and cause self-discharge (See **Equation 2.3**)

$$2Cr^{2+} + 2H^+ \rightarrow 2Cr^{3+} + H_2 \qquad \Delta G^0 = -81.0 \text{ kJ/mol} \qquad \textbf{Equation 2.3}$$

However, long term(~600 hours) stability of Cr(II) ions in chloride solution has been evaluated by NASA; they found that the thermodynamically feasible direct oxidation of Cr(II) ions by hydrogen ions is kinetically inhibited[19].

2.1.2 Chromium(III) Ions Reduction in the Basic Molten Salt System

Mixtures of aluminum chloride ($AlCl_3$) and certain anhydrous organic halide salts (RCl) such as N-butylpyridium chloride (BupyCl), 1-methyl-3-ethylimidazolium chloride (MeEtimCl) and 1,2 dimethyl-3-propylimidazolium chloride (DMPrimCl) can form molten salts at room temperature. These ionic liquids have proven to be useful solvents for electrochemical studies of many inorganic, organometallic, and organic compounds[20, 21].

Chromium compounds in molten salts and especially in chloride electrolytes are used as cathode materials in thermally activated batteries. In LiCl-KCl melt, Cr(III) can be reduced to chromium metal via a two-step process in which the intermediate species is precipitated as $CrCl_2$[22]. Through the study on the electrochemical behavior of Cr(III) in the sodium chloride-saturated $AlCl_3$-NaCl electrolyte, Hussey reported that Cr(III) was reduced to Cr(II) through a quasi-reversible charge-transfer process and that Cr(II) could be further reduced to chromium metal[23]. The electrochemistry of Cr(III) in basic $AlCl_3$-MeEtimCl melts was also examined at a glassy carbon electrode by Hussey[24]. Scheffler reported earlier that all traces of proton impurities in the melts had to be removed, otherwise the reduction of Cr(III) chloride would be complicated and the stable products of this reduction process could neither be obtained nor characterized in these melts[24]. It was found that in proton free basic $AlCl_3$-MeEtimCl melt, $[CrCl_6]^{3-}$ could be reduced to $[CrCl_4]^{2-}$, which was stable in the melt unless exposed to trace amounts of oxygen[24]. The electrochemical behavior of chromium chloride complex species in basic $AlCl_3$-MeEtimCl melt is different from those observed in the alkali metal chloride-based melts. In both LiCl-KCl and $AlCl_3$-NaCl melts, Cr(III) can be reduced successively to Cr(II) and Cr metal, whereas in basic $AlCl_3$-MeEtimCl melt, Cr(III) can only be reduced to Cr(II)[24].

2.1.3 Chromium(III) Ions Reduction in the Chloride System

As mentioned earlier, the standard potential for Cr(III) reduction is 0.42 V lower than that of hydrogen evolution. Hydrogen evolution is the main side reaction when the Cr(III) reduction occurs in acidic aqueous solutions. The half cell reactions of Cr(III) electrochemical reduction in the acid solution can be described as **Equation 2.1**, **Equation 2.2** and **Equation 2.4**.

Cathode $Cr^{3+} + e^- \rightarrow Cr^{2+}$ **Equation 2.1**

$2H^+ + 2e^- \rightarrow H_2$ **Equation 2.2**

Anode $2H_2O \rightarrow O_2 + 4H^+ + 4e^-$ **Equation 2.4**

Kelsall investigated the electrochemical reduction of Cr(III) to Cr(II) on vitreous carbon and graphite felt electrodes, and found that the electrochemical reduction of Cr(III) on vitreous carbon electrodes was mainly controlled by charge transfer rather than mass transfer[4]. Specifically, in 0.1 M Cr(III) + 1M hydrochloric acid over an electrode potential range from -0.8 V to 0.8 V vs SCE, the electrochemical reaction at carbon electrodes was essentially a surface process of proton adsorption and desorption, without significant hydrogen evolution and Cr(II) formation. At electrode potentials more negative than -0.8 V vs SCE, both hydrogen evolution and Cr(II) formation occurred simultaneously.

Kelsall also predicted the Cr(III) reduction kinetics by the extended high field approximation of the Butler-Volmer equation[21]. In his prediction, a term involving the mass transfer and the conversion of Cr(III) to Cr(II) was incorporated to allow for local depletion of Cr(III) concentration. The relationship between the electrode potential, Cr(III) concentration and current efficiency may be predicted as illustrated by **Figure 2.2**[21]. It was indicated that when the electrode potential was controlled at around -1.1 V vs SCE, the current efficiency for Cr(III) reduction to Cr(II) could reach about 0.85 with a fractional conversion of 0.8 starting with 0.1 M Cr(III) ions.

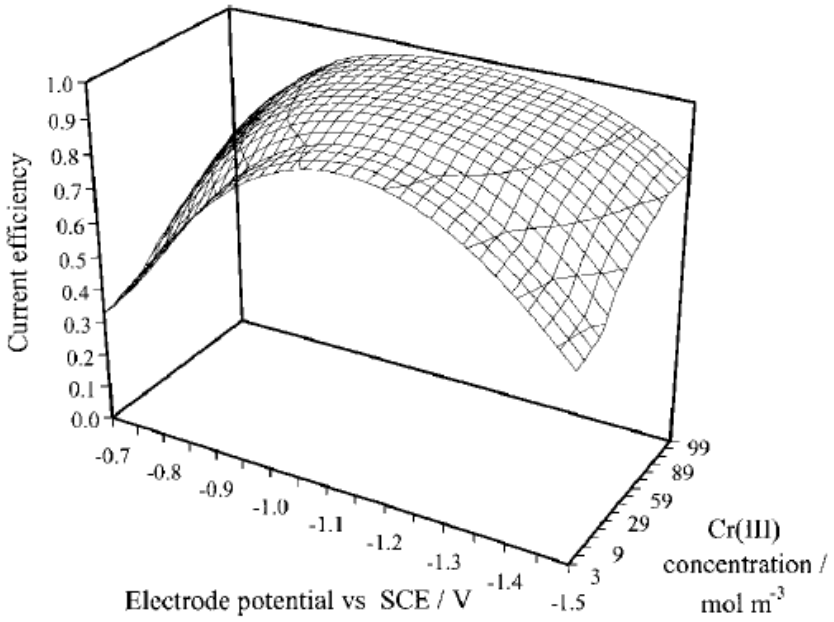

Figure 2.2 Predicted relationship between electrode potential, current efficiency and concentration of Cr(III) in 1 M HCl + 0.1 M Cr(total) at a vitreous carbon electrode[21]

Gudyanga and his coworkers also studied the chemical and electrochemical equilibria and kinetics in aqueous Cr(III)/Cr(II) chloride system. The heterogeneous rate constants were determined for the $CrCl_2^+/Cr^{2+}$, $CrCl^{2+}/Cr^{2+}$ and Cr^{3+}/Cr^{2+} couples from the results of cyclic voltammetry at a hanging mercury drop electrode (HMDE), which are summarized in **Table 2.1**[11] .

The kinetics of these couples was found to be irreversible or quasi-reversible, depending on the initial Cr(III) species and the electrolyte composition[11]. The reduction of $CrCl_2^+$ ions occurs via an ECE mechanism, where E and C present electrochemical and chemical reactions respectively. Specifically, the reduction of $CrCl_2^+$ ions occurs via a $CrCl^{2+}$ intermediate and successive elimination of Cl^- ligands (See **Equation 2.5**), the presence of which can greatly enhance the electrode kinetics.

$$Cr^{2+} + CrCl_2^+ \rightarrow CrCl^{2+} + Cr^{2+} + Cl^- \qquad \textbf{Equation 2.5}$$

Table 2.1 Apparent rate constants for Cr(III)/Cr(II) couples at a HMDE, 293 K[11]

Reactant	Electrolyte		k_{app} /m s^{-1}
	[HCl]/ kmol m^{-3}	[KCl]/ kmol m^{-3}	
$CrCl_3$(aq)	10	--	1 x 10^{-4}
$CrCl^{2+}$	3	1	3 x 10^{-5}
$CrCl^{2+}$	3	1	2 x 10^{-5}
$CrCl^{2+}$	5	--	1 x 10^{-5}
$CrCl^{2+}$	3	1	1 x 10^{-5}
$CrCl^{2+}$	1	2.5	7 x 10^{-6}
$CrCl^{2+}$	1	--	5 x 10^{-6}
$CrCl^{2+}$	0.1	0.9	4 x 10^{-6}

It was found that while chloride ions have a very weak complexing effect on Cr^{3+} ions as shown by **Equation 2.6** and **Equation 2.7**, they could greatly enhance the Cr(III)/Cr(II) kinetics.

$$Cr(H_2O)_6^{3+} + Cl^- \rightleftharpoons Cr(H_2O)_5Cl^{2+} + H_2O \qquad K_1 = 0.192 \qquad \textbf{Equation 2.6}$$

$$Cr(H_2O)_5Cl^{2+} + Cl^- \rightleftharpoons Cr(H_2O)_4Cl_2^{+} + H_2O \qquad K_2 = 0.130 \qquad \textbf{Equation 2.7}$$

This is probably caused by the formation of $CrCl_2^+$ and $CrCl^{2+}$ ions in the bulk electrolyte and by the adsorption of Cl^- ions on electrode surfaces acting as electron bridges. However, the slow chemical kinetics of chloride complexation of Cr^{3+} ions, or the aquation of chloro-complexes formed from $CrCl_3$ solid, may cause the Cr(III)/Cr(II) couple to show time dependent electrochemical kinetics.

2.1.4 Chromium(III) Ions Reduction in the Perchlorate System

The kinetics of the Cr^{3+}/Cr^{2+} electrode system in the perchlorate system have been investigated by several researchers. It was reported that in 0.5-1 M perchlorates, the apparent standard rate constant was found to be of the order 10^{-5} cm/s[25]. Anson

investigated the potential dependence of transfer coefficient and discussed the oxidation of Cr(II) catalyzed by adsorbed halides[26, 27].

Galus and his coworkers explored the influence of the water activity in the solution on kinetic parameters of the Cr^{3+}/Cr^{2+} reaction which enabled the determination of the order of electrode reaction with respect to water[15]. Their work is an insight into the electrode processes of aquo-complexes which is important to better understand the nature of electrode processes. The Cr(II)/Cr system at a mercury electrode in concentrated solution of sodium perchlorate and calcium chloride was also studied by these authors.

In their research, the experiments were carried out at constant 10^{-3} M concentration of Cr(III) in different solutions of $NaClO_4$, $HClO_4$, $Ca(ClO_4)_2$ at the HMDE. The rate constant of the Cr(III)/Cr(II) system was found to be practically independent of the perchlorate concentration. The role of the supporting electrolyte was found to shift the formal standard potential towards more positive values with increasing concentration.

Cr(III) reduction in $NaClO_4$ (0.2-7 M) solution was also investigated by Andreu and his coworkers[15]. In order to distinguish between double layer and bulk effects on the reaction rate, the ionic surface excesses have been determined. The Cr^{3+} reduction rate response to increasing $NaClO_4$ concentration appeared to be similar to that of Zn^{2+}. In both cases, the location of the discharge plane at 0.28 nm from the outer Helmholtz plane (oHp) gave a satisfactory Frumkin correction to Butler-Volmer Kinetics. The assumption underlying the Frumkin correction is that electron transfer between an electrode and a redox species can occur only when the redox species is at the reaction plane. Thus, the use of concentrated solutions offered a direct way of determining the true transfer coefficient. Additionally, the loss of interaction between the reactant and about five water molecules was observed during the electron transfer for Cr(III) reduction in $NaClO_4$ (0.2-7 M) solution.

2.1.5 Chromium(III) Ions Reduction in the Polyammocarboxylate System

EDTA, CyDTA and DTPA are all polyammocarboxylates, which are able to coordinate with various metal ions. As one of the most famous chelating reagents, EDTA is a ligand

capable of up to six coordinations and it forms strong complexes with both Cr(III) and Cr(II). However, within the pH range of 4-7, EDTA acts as a pentadentate ligand with the sixth site of the coordination shell filled by a rather labile water molecule for Cr(III) and Cr(II).

Several papers have reported electrochemical studies of the Cr(III)EDTA/Cr(II)EDTA couple[28-31]. Within the pH range 4-7, the couple is reversible with a standard potential close to -1.23 V vs SCE. In order to obtain a good current efficiency, it is essential to control several parameters which are listed below.

(a) A high concentration of Cr(III)EDTA, typically 0.4 M;

(b) A high and uniform catholyte flow rate, typically 0.4 m/s;

(c) A gauze cathode (steel) and turbulence promoter;

(d) An elevated temperature above 333 K;

(e) A ratio of EDTA/Cr(III) above one;

(f) Maintaining the catholyte completely free of oxygen.

Under these conditions, it was reported that the current efficiency can reach 70% at a Cr(II) conversion of 80%, calculated from the potential of the Cd electrode in the reservoir, with current densities up to 2500 A/m^2[32].

A series of electrolyses at a current density of 640 A/m^2 for the preparation of Cr(II)EDTA, Cr(II)CyDTA, Cr(II)DTPA was also studied and the results are summarized in **Table 2.2**.

Table 2.2 Electrolysis of Cr(III) in EDTA, CyDTA and DTPA systems[32]

Reaction	E^0/ V vs SCE	Conversion/ %	Current Efficiency/%
$Cr(III)EDTA \rightarrow Cr(II)EDTA$	-1.26	93	72
$Cr(III)CyDTA \rightarrow Cr(II)CyDTA$	-1.20	92	66
$Cr(III)DTPA \rightarrow Cr(II)DTPA$	-1.20	91	68

The performance of all three polyammocarboxylate complexes is similar. It is possible to obtain high conversion at a reasonable current efficiency for all these complexes.

Similar to Cr^{2+}, Cr(II) polyammocarboxylate complexes are also strong reducing reagents capable of some interesting transformations, which are summarized in **Table 2.3**. The chemistry of these Cr(II)L complexes also appear to be very similar. However, as these chemical reactions are generally too slow to use the Cr(III)L/Cr(II)L couples as mediators, an indirect electrosynthesis would have to be carried out with a large holding tank.

Table 2.3 Cr(II) polyammocarboxylate complexes reactions with organics[32]

Substrate	Cr(II)EDTA			Cr(II)CyDTA			Cr(II) DTPA		
	Rate	Conversion /%	Product (yield/%)	Rate	Conversion /%	Product (yield/%)	Rate	Conversion /%	Product (yield/%)
PhC≡CH	δ	79	$PhCH=CH_2$ (68)	δ	79	$PhCH=CH_2$ (67)	δ	66	$PhCH=CH_2$ (44)
$HC≡CCH_2OH$	β	78	$H_2C=CHCH_2OH$ (77)	α	90	$H_2C=CHCH_2OH$ (58)	δ	69	$H_2C=CHCH_2OH$ (39)
PhC≡CCOOH	α	60	PhCH=CHCOOH (32)	β	98	PhCH=CHCOOH (52)	α	75	PhCH=CHCOOH (45)
$PhCH_2Br$	δ	78	PhMe (89)	γ	76	PhMe (18)	γ	85	PhMe (47)
			PhCH2CH2Ph (6)			$PhCH_2CH_2Ph$ (1)	γ	85	$PhCH_2CH_2Ph$ (9)
$PhNO_2$	δ	100	$PhNH_2$ (81)	γ	79	$PhNH_2$ (98)	α	82	$PhNH_2$ (89)

***Cr(II)EDTA 90% consumed α< 10 min, β 10-30 min, γ 30-120 min, δ> 120 min**

2.1.6 Chromium(III) Ions Reduction in the Ammine Complex System

The electrochemical reduction kinetics of ammine and ethylenediamine complexes of Cr(III), for example, $Cr(NH_3)_5Br^{2+}$, $Cr(NH_3)_5Cl^{2+}$, $Cr(NH_3)_5NO_3^{2+}$, $Cr(NH_3)_5NCS^{2+}$, have been studied at the mercury-aqueous interface by Weaver and Satterberg. For most of the ammine complexes studied, anomalously large apparent transfer coefficients and rate

responses to anionic specific adsorption were obtained[33]. The greater enhancement of the reduction rate of Cr(III) ammine complexes provides strong evidence that the outer-sphere transition state lies closer to the electrode than for the corresponding aquo reactants (See **Figure 2.3**) .

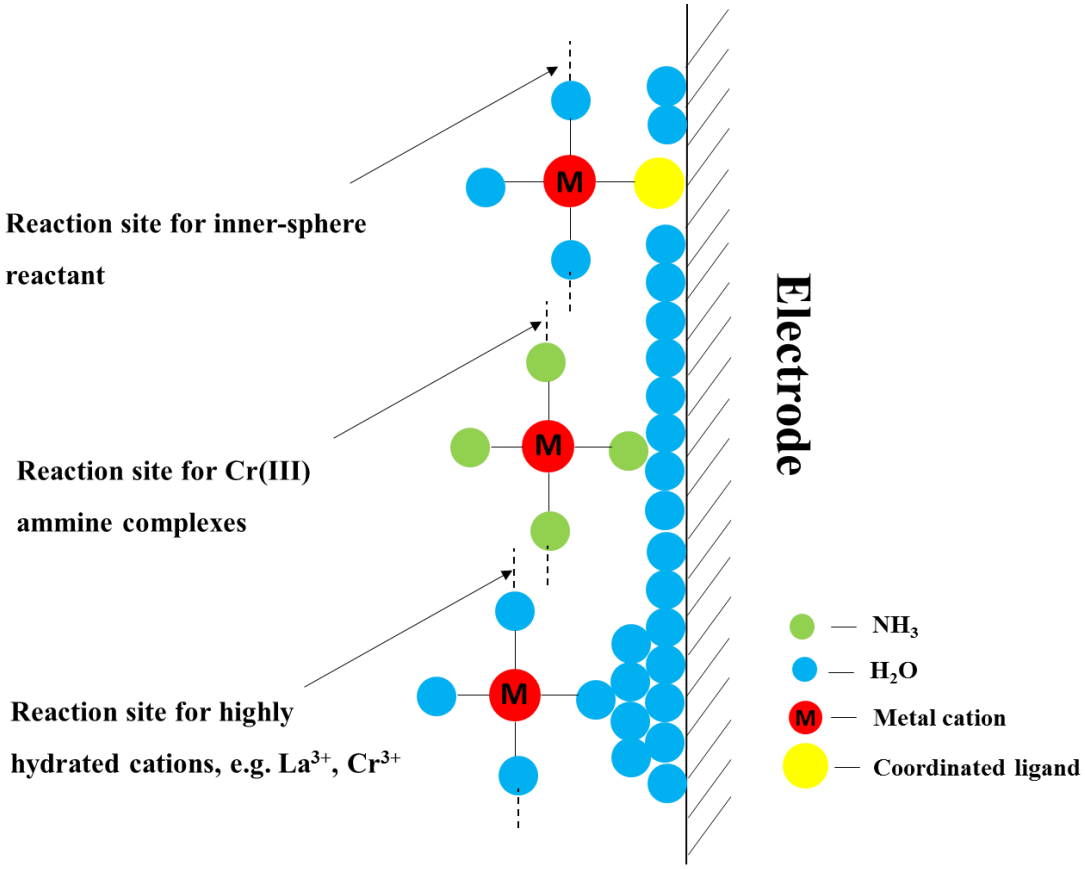

Figure 2.3 Proposed Structure of the mercury-aqueous solution double layer and the reaction sites for aquo and ammine Cr(ll1) complexes [33]

Additionally, larger hydrated radii for some aquo as compared to ammine complexes in bulk solution were also observed. These differences are due to the presence of secondary hydration between the primary hydration layers surrounding the electrode and the aquo cations at their distance of closest approach, which is largely absent for the corresponding ammine cations.

2.1.7 Mechanism of Chromium(III) Ions Reduction

There are two main electrode reaction mechanisms for the simple, one-electron redox reaction of transition metal ions: inner-sphere and outer-sphere mechanism.

The essential differences between inner-sphere and outer-sphere electrode reactions for substitutionally inert metal complexes are illustrated in **Figure 2.4**. During the outer-sphere reactions, electron transfer takes place with the reactant center located at the outer Helmholtz plane (oHp). The coordination spheres of the reactant do not penetrate the layer of solvent molecules that are specifically adsorbed on the electrode surface. However, during electrode reactions that proceed by inner-sphere pathways, one or more of the ligands in the reactant's primary coordination sphere penetrates the Helmholtz plane and is attached to the electrode surface in the transition state[34-36].

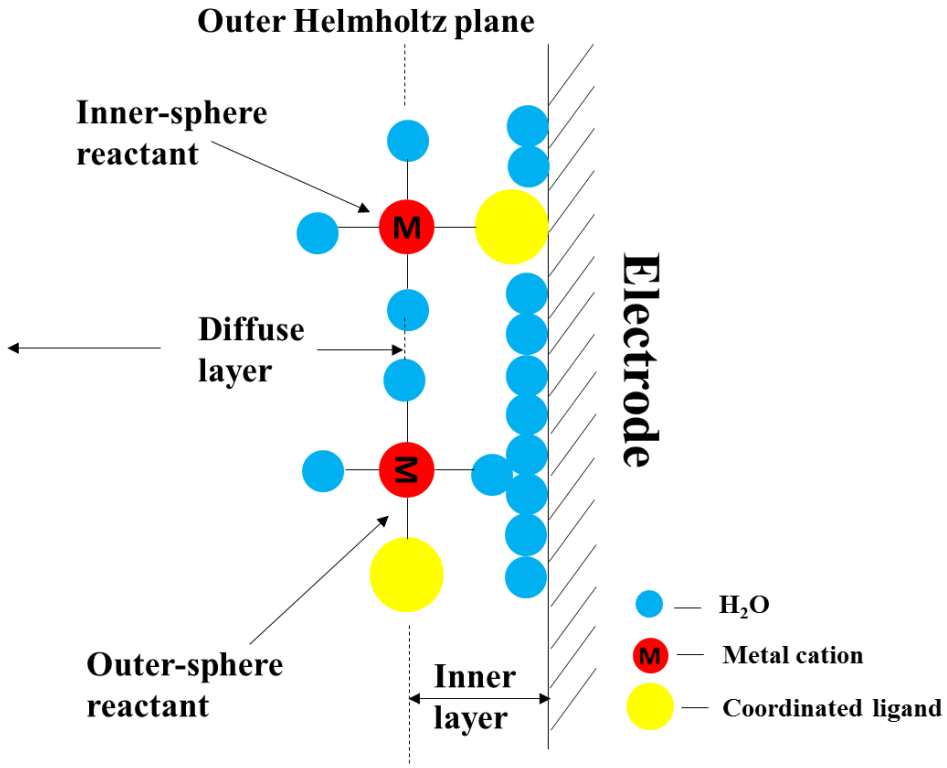

Figure 2.4 Schematic diagram of the double layer at electrode surfaces and the reaction sites of inner-sphere and outer-sphere reactants[37]

Studies of redox reactions involving Cr(III)/Cr(II) couples in homogeneous solution have played a central role in characterizing the nature of inner-sphere and outer-sphere electron transfer reactions. A systematic basis is established to determine whether any particular chromium(III) complex is reduced at the electrode by an inner-sphere or an outer-sphere mechanism. The reactions for the inner-sphere and outer-sphere electrochemical reductions are shown in **Equation 2.8** and **Equation 2.9**, where X^{p-} is a simple anionic ligand (p is the absolute value of charge).

Inner-sphere electrochemical reduction

$$Cr(OH_2)_5X^{(3-p)+}(Hg(e-) \rightleftharpoons Cr(OH_2)_5X^{(3-p)+}\cdots(Hg(e-) \qquad \textbf{Equation 2.8(a)}$$

$$Cr(OH_2)_5X^{(3-p)+}\cdots(Hg(e^-) \xrightarrow{slow} Cr(OH_2)_5X^{(2-p)+}\cdots(Hg \qquad \textbf{Equation 2.8(b)}$$

$$Cr(OH_2)_5X^{(2-p)+}\cdots(Hg \xrightarrow[fast]{H_2O} Cr(OH_2)_6{}^{2+} + X^{p-} + (Hg \qquad \textbf{Equation 2.8(c)}$$

Outer-sphere electrochemical reduction

$$Cr(OH_2)_5X^{(3-p)+}_{bulk} \rightleftharpoons [Cr(OH_2)_5X^{(3-p)+}]_{oHp} \qquad \textbf{Equation 2.9(a)}$$

$$[Cr(OH_2)_5X^{(3-p)+}]_{oHp} \xrightarrow[slow]{+e^-} [Cr(OH_2)_5X^{(2-p)+}]_{oHp} \qquad \textbf{Equation 2.9(b)}$$

$$[Cr(OH_2)_5X^{(2-p)+}]_{oHp} \xrightarrow[fast]{H_2O} Cr(OH_2)_6{}^{2+} + X^{p-} \qquad \textbf{Equation 2.9(c)}$$

Two criteria were proposed by Anson to assign the chromium(III) complex to one of these mechanistic pathways: (1) the response of the reaction rate to additions of iodide anions which are strongly adsorbed on mercury; (2) the dependence of the electrode reaction rate on the electrode potential[37]. Complexes whose reduction rates are increased by adsorbed iodide have a value of apparent transfer coefficient (a_{app}) greater than 0.5 and are likely to follow the outer-sphere mechanism. In contrast, complexes whose reduction rates are decreased by adsorbed iodide have a value of apparent transfer coefficient smaller than 0.5 and are more likely to exhibit the inner-sphere behavior.

Anson examined the behaviors of eight chromium(III) complexes in terms of these two characteristics and the results are summarized in **Table 2.4** [37] . Generally, H_2O, F^- and SO_4^{2-} tend to follow the outer-sphere mechanism, while Cl^-, Br^-, NCS^-, N_3^- and NO_3^- are more likely to exhibit the inner-sphere behavior.

Table 2.4 The reduction of Cr(III) complexes at mercury electrodes[37]

X^{p-} in $Cr(OH_2)_5X^{(3-p)+}$	Potential range -E mV vs SCE	α_{app}	Response to iodide	Likely mechanism
H_2O	750-1100	0.58	+	Outer sphere
F^-	700-1200	0.58	+	Outer sphere
SO_4^{2-}	600-1150	0.56	+	Outer sphere
Cl^-	550-900	0.37	-	Inner sphere
Br^-	200-450	0.43	-	Inner sphere
NCS^-	650-900	0.38	-	Inner sphere
N_3^-	650-1100	0.42	-	Inner sphere
NO_3^-	700-1000	0.41	-	Inner sphere

"+" means rate increase, "-" means rate decrease

A summary of the kinetic data for the reduction of the eight complexes in 1 M $NaClO_4$ is presented in **Table 2.5**.

Table 2.5 Electrochemical reduction kinetics for Cr(III) complexes[37]

X^{p-} in $Cr(OH_2)_5X^{(3-p)+}$	Q_{III} M^{-1}	Q_{II} M^{-1}	-Ex mV	$10^5\ k_{app}$
H_2O	---	---	655	0.75
F^-	2.1×10^4	7.1	859	0.60
SO_4^{2-}	22	3.2	704	0.46
Cl^-	0.11	1.4	589	120
Br^-	2.2×10^{-3}	0.20	539	7×10^4
NCS^-	1.8×10^2	13	722	420
N_3^-	~1000	~70	~723	12
NO_3^-	9.3×10^{-3}	---	---	---

Q_{III} is the equilibrium quotient for $Cr(OH_2)_6^{3+} + X^{p-} \rightleftarrows Cr(OH_2)_5X^{(3-p)+} + H_2O$ **at unit ionic strength, Q_{II} is the equilibrium quotient for** $Cr(OH_2)_6^{2+} + X^{p-} \rightleftarrows Cr(OH_2)_5X^{(2-p)+} + H_2O$ **at unit ionic strength. Ex is the relevant formal potential. k_{app} is the apparent rate constant at Ex**

The various complexes exhibited a very wide range of reactivity toward electrochemical reduction. It can be observed that rate constants for inner sphere reactions are significantly greater than those for outer sphere reactions. The large range of reactivity is caused by the intrinsic difference, such as activated complexes reorganizational energy barrier, and the thermodynamic driving force difference like the average of work required to bring reactant and product to the reaction site. It was suggested that the latter factor is dominant with outer-sphere reactants whereas both factors can contribute significantly to the relative reactivity of inner-sphere reactants [37].

2.2 Previous Studies on Carbon Electrodes

The fundamental reason for the attractiveness of the Cr(III)/Cr(II) electrode is its negative potential with respect to the hydrogen electrode. For the same reason, difficulties are encountered in finding corrosion resistant materials that not only exhibit good

electrocatalytic activity for the Cr(III/Cr(II) electrode reaction, but also show high hydrogen overpotential.

Many metals have been investigated as the electrodes for Cr(III) reduction, such as hanging mercury drop, dropping mercury, mercury amalgam film, lead, titanium, platinum, silver, gold, bismuth and steel mesh. The three metals(Pb, Cd and Hg) with the highest hydrogen overpotentials are highly toxic, which could result in environment problems in practical systems[4].

Carbon electrodes such as vitreous carbon, carbon/graphite felt have a huge surface area, high porosity and adequate electrical conductivity. Over a wide potential range in many aqueous media, carbon electrodes can display an outstanding chemical stability and fairly high hydrogen overpotentials (See **Figure 2.5**). Due to their special properties, carbon electrodes can act as a very promising cathode material for electrochemical reduction of chromium(III) ions in acidic aqueous solutions[11].

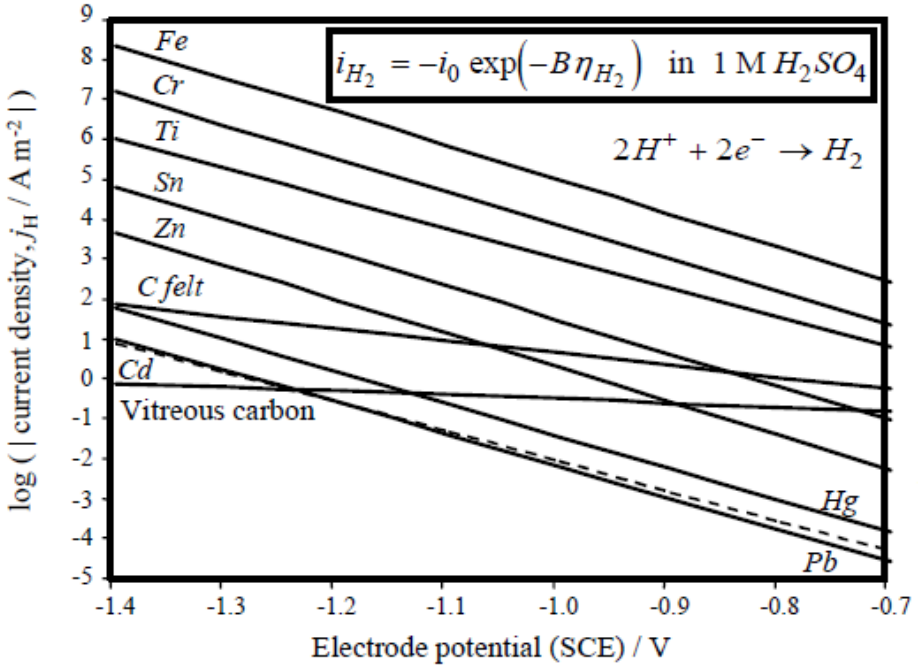

Figure 2.5 Effect of electrode potential on the kinetics of hydrogen evolution on a range of cathode materials in 1 M H_2SO_4[11]

2.2.1 Applications of Reticulated Vitreous Carbon

Reticulated vitreous carbon (RVC) is an open pore material composed of vitreous carbon with a honeycomb structure. Due to its high porosity (97%), high specific surface area (up to 66 $cm^2\,cm^{-3}$ for RVC grade 100), and active electrochemical characteristics, RVC can be used as an electrode material for heavy metal removal from dilute industrial effluents.

Tissot *et al.* electrodeposited PbO_2 on reticulated vitreous carbon and used the electrode for the direct oxidation of CN^-[38]. The removal of Cu(II) from a sulfate system was also performed on reticulated vitreous carbon by Pletcher *et al.*[39, 40]. Leon and Pletcher investigated its applications on the removal of Pb(II) ions from aqueous solution of perchorate, nitrate, tetrafluoroborate, chloride and sulfate[41]. Sparling and his coworkers found that six heavy metals (copper, cadmium, chromium, lead, unanium and zinc) could be successfully deposited on reticulated vitreous carbon[42]. They concluded that for the initial metal concentrations of 50 μmol/L, copper could be deposited with an efficiency of 100% at a flow rate of 0.24 cm/min in a single pass; however, it would require a maximum of 20 passes for 100% chromium deposition at a flow rate of 1.8 cm/min.

2.2.2 Applications of Graphite Felt

In addition to reticulated vitreous carbon, graphite felts have also provided promising results for the recovery of several heavy metal pollutants from dilute solutions due to their favorable physical and chemical characteristics.

The direct electrowinning of copper from dilute cyanide solution was conducted by Lu in a membrane cell with graphite felt (See **Figure 2.6**)[43]**.**

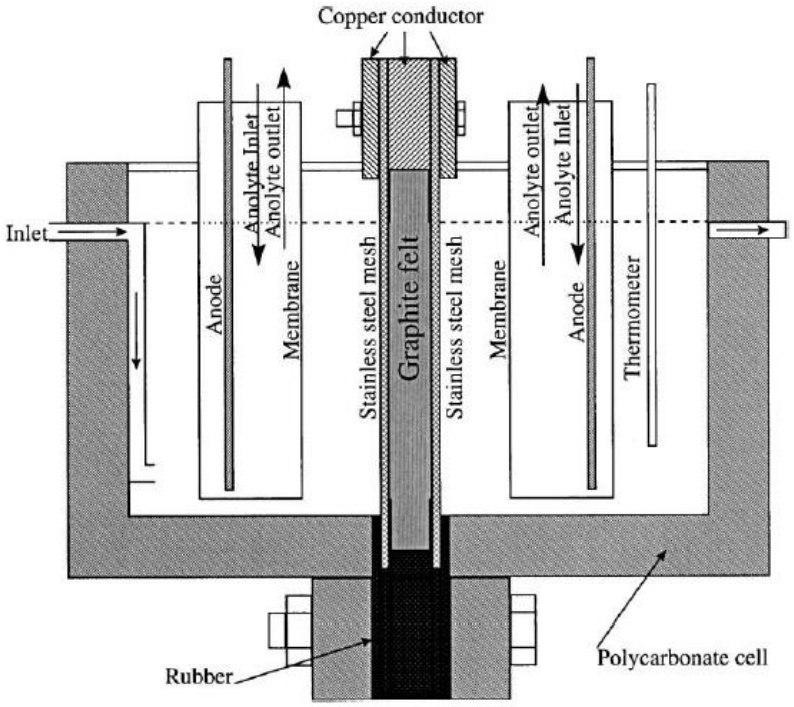

Figure 2.6 Schematic diagram of the electrolytic cell for direct electrowinning of copper from dilute cyanide solution[43]

He reported that copper can be deposited efficiently on the graphite felt from low concentration solutions (1–2 g/L Cu and CN/Cu mole ratio = 3–9) with 50–80% current efficiency and with the removal of around 40% Cu. Additionally, the conductivity of the graphite felt and the specific surface area were found to be significantly increased as the deposition proceeded due to the accumulation of deposited copper on the graphite felt.

Oren also investigated the possibility of removing hexavalent chromium from waste water by electrochemical treatment using a graphite felt electrode[44]. The removal process was found to proceed in two steps: (1) electrochemical reduction of the hexavalent chromium to chromic ion; (2) the formation of an insoluble chromic hydroxide in an electrochemically generated high pH environment.

The removal of mercury(II) from contaminated brines was explored by Astruc *et al.* with the carbon felt flow-through electrodes[45]. It was observed that the mercury

electrodeposition efficiency could be very high with the carbon felts under the mass transfer control, even if low thickness felts were used. The deposition efficiency can be up to 97% at a flow rate of 36 m h^{-1}, which is the most efficient when compared to other three dimensional electrode materials, such as nickel foam, stack of Pt grid and gilt graphite sphere.

Bumroongsakulsawat and Kelsall investigated the possibility of electrochemical reduction of aqueous CO_2 with tin deposited graphite felt[46]. The electrochemical cell is illustrated in **Figure 2.7**. They reported that CO_2 can be reduced electrochemically in the aqueous solution of 1 M $NaClO_4$ + 0.5 M NaOH saturated with CO_2 (pH = 7.8) with an optimal superficial current density and charge yield of 971 A m^{-2} and 0.58, respectively, at 1.62 V (AgCl|Ag) and 99 mL/min solution flow rate.

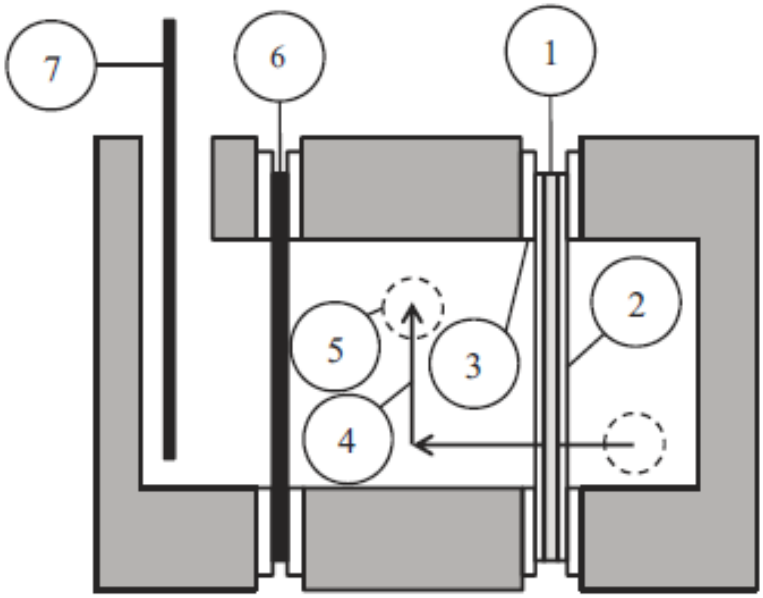

Figure 2.7 Schematic diagram of the electrochemical cell for electrochemical reduction of aqueous CO_2 [46]

(1- Felt Cathode in Gasket, 2-Cu Mesh Holders, 3-Gasket, 4-Electrolyte Solution Flow, 5-Cell Ports, 6-Nafion Membrane, 7-Counter Electrode)

2.2.3 Surface Treatment of Carbon Electrodes

Carbon electrode is hydrophobic and therefore, has inadequate wettability and electrochemical activity in aqueous solutions. The surface modification of graphite or carbon electrode materials has been widely investigated due to the fact that the nature of the surface functional groups of these materials can greatly influence the electrochemical activity.

It has been reported that the oxygen functional groups on the carbon surface can behave as active sites for many electrochemical reactions[47-49]. For example, for the vanadium redox cell reactions, **Equation 2.11** would be strongly influenced by the concentration and nature of the oxygen functional groups on the electrode surface, since oxygen transfer is involved.

$$V^{3+} + e \rightleftharpoons V^{2+} \qquad \textbf{Equation 2.10}$$

$$VO_2^+ + 2H^+ + e \rightleftharpoons VO^{2+} + H_2O \qquad \textbf{Equation 2.11}$$

2.2.3.1 Thermal Treatment

Surface oxide on carbon was first observed by Smith more than 100 years ago[50]. He found that oxygen was chemisorbed by charcoal and could be recovered on heating only as carbon dioxide. When active charcoal reacted with oxygen at a temperature as low as 300 ℃, part of the oxygen consumed remained bound to the surface, being liberated as CO and CO_2 only on subsequent heating[51].

Acid properties can be acquired as well on oxidation. If it is exposed to oxygen at moderate temperatures, e.g. 400 ℃, it shows acidic behavior. On the other hand, if it is heat treated and cooled in a high vacuum on admittance of molecular oxygen at room temperature, it turns basic. By measuring the electrokinetic potential, Kruyt and de Kadt confirmed that the temperature of reaction with oxygen played a great role in determining the basic or acidic properties of the carbon sample[50].

King found that the acidic surface oxides were formed when carbon was treated with oxygen near its ignition point temperature[52]. Smith and his coworkers also studied the reaction of oxygen with carbon between 250 and 450 ℃. From IR spectra, they showed the presence of lactone and carbonyl structures on the surface of carbon after exposure to oxygen[53].

Sun investigated the thermal treatment of graphite felt at various temperatures and treatments. He concluded that the vanadium redox cell resistance values and efficiencies can be significantly improved, when the graphite felt is activated at 400 ℃ for 30 hours. It was found that the time for the untreated graphite felt to show signs of wetting in 2 M $VOSO_4$/2 M H_2SO_4 solution was 52 days. However, the wetting properties of the graphite felt improved after activation of the samples[50]. The reason for this improvement in the hydrophilic property is due to the formation of surface oxides, which provide adsorption sites for water and other polar compounds.

The optimal thermal treatment condition was determined as 400 ℃ for 30 hours. At higher temperatures the cell resistance increased dramatically; for shorter or longer treatment time, the graphite felt exhibited a lower activity in the vanadium redox cell (See **Figure 2.8** and **Figure 2.9**).

Energy efficiencies of over 88% were obtained after treatment compared with only 78% for the untreated felt[50]. The increase in the activity of this material is attributed to the formation of surface active functional groups of C-O-H and C=O. The formation of –C-O-V bond facilitates the electron transfer and oxygen transfer processes and thus reduces the activation overpotential for the V^{IV}/V^{V} redox reactions.

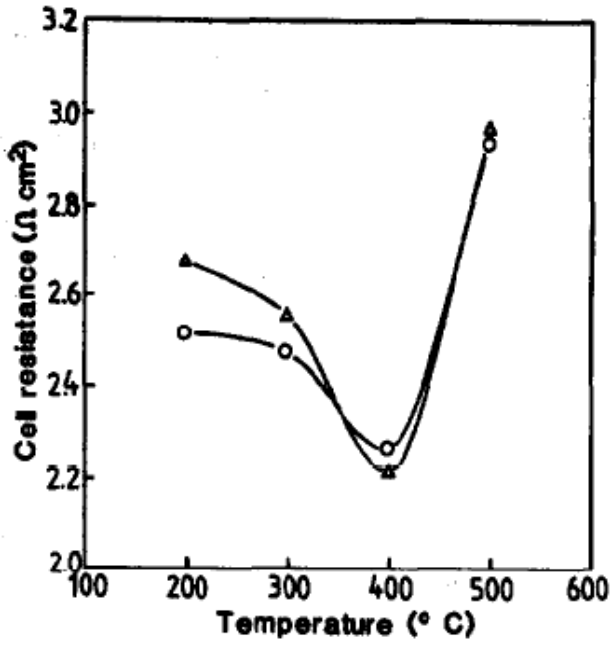

Figure 2.8 Effect of treatment temperature on the cell resistance for activated graphite felt, (O) charge and (Δ) discharge[50]

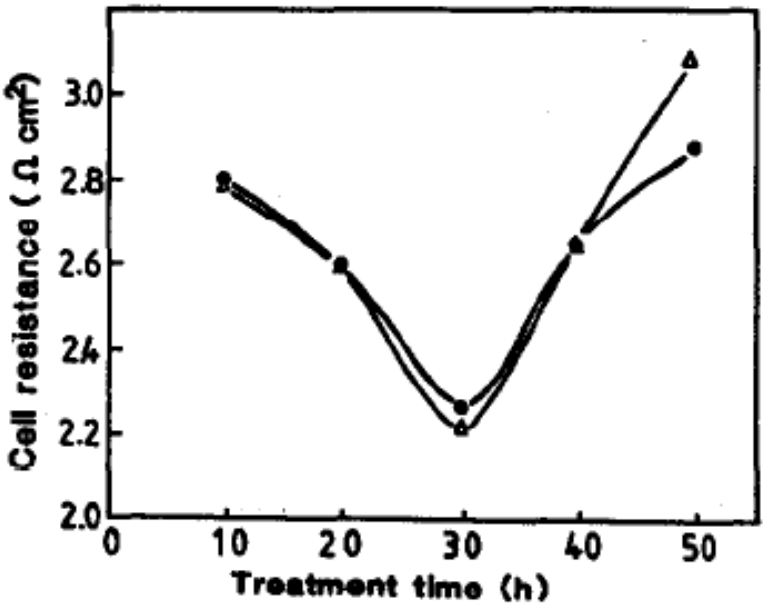

Figure 2.9 Effect of activation time on the cell resistance at constant temperature of 400 ºC for graphite felt, (O) charge (Δ) discharge[50]

2.2.3.2 Acid Treatment

In addition to thermal treatment, a variety of surface treatments in solutions have also been reported to improve the electrochemical activity of carbon and graphite electrodes[54, 55]. Generally, surface oxidation as well as gasification of the carbon are occurring when the carbon electrode is treated with various oxidants in the aqueous solution.

Taylor and Humffray reported that the rate of electrochemical reaction for Fe(III)/Fe(II) redox couple in H_2SO_4 solution was greatly improved when the glassy carbon electrode was polished with 0.3 μm alumina, followed by dipping in concentrated sulfuric acid[55].

Banerjee *et al.* showed that permanganate, whether acidic or alkaline, reacted vigorously with coal even at room temperature until the coal was degraded into water soluble products[54]. An acidic carboxyl group can be formed at room temperature when the carbon is treated with NaOCl, $KMnO_4$ or $(NH_4)_2S_2O_8$ solution.

Bahraman and Gustafson and Puri *et al.* studied the reaction of activated carbon with chlorine water. The first stage of reaction was found to involve conversion of chlorine into hydrochloric acid and chemisorption of a part of the oxygen. After some time when charcoal was not in a position to chemisorb any more oxygen, the reaction involved formation of hydrochloric and chloric acids, with charcoal acting merely as a catalyst. The oxygen content of a sugar charcoal, outgassed at 1200 ℃, could be raised to 25% on repeated treatments with chlorine water at room temperatures[56]. Puri and Donnet found that the reaction of carbon with aqueous potassium persulphate, bromate, periodate and nitrate, lead to the formation of phenolic and carboxylic groups[57].

Sun and Kazacos further investigated the chemical modification of graphite felt in sulfuric acid, nitric acid and mixtures of sulfuric and nitric acids. The optimal acid treatment condition was immersing the graphite felt in the 98% boiling concentrated sulfuric acid for 5 hours[58]. For shorter or longer treatment times, the graphite felt exhibited a lower activity for the vanadium redox cell (See **Figure 2.10** and **Figure 2.11**)

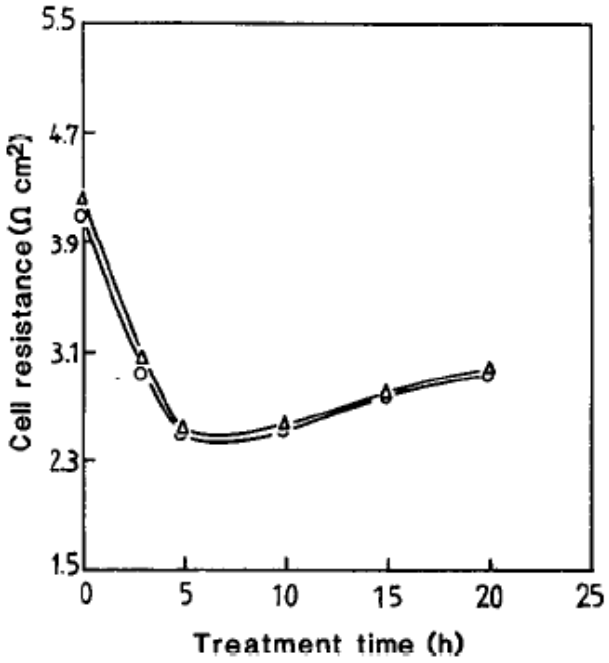

Figure 2.10 Influence of treatment time on the cell resistance of a vanadium redox cell employing graphite felt electrodes activated with 98% H_2SO_4[58]

No improvement in the activity of the graphite felt was observed after the treatment of graphite felt in 98% sulfuric acid at room temperature even after 24 hours immersion time. This is due to the fact that hot concentrated sulfuric acid possesses a stronger oxidizing ability than a dilute solution or a cool concentrated sulfuric acid solution.

After the graphite felt electrode material was treated with boiling concentrated sulfuric acid for 5 hours, an energy efficiency of 91% was obtained in the vanadium cell[58]. Surface analysis of treated and untreated felts using the XPS method showed that the functional groups C-O and C=O increased dramatically compared to untreated samples. The cleaning of graphite felt surface after acid and chemical treatment was also believed to be an important factor which removed the surface contaminants or any inhibitory layer that may hinder electron transfer.

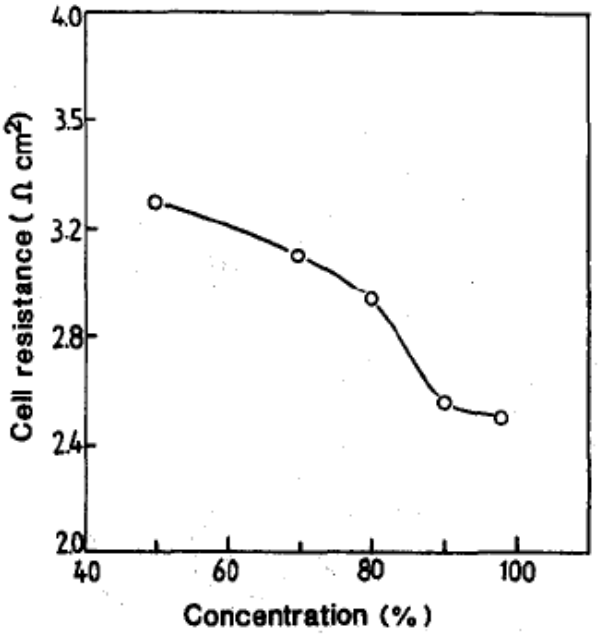

Figure 2.11 Variation of cell resistance with acid concentration for activated graphite felt electrodes treated with H_2SO_4 for constant treatment time (5 h) [58]

Nitric acid and mixtures of sulfuric and nitric acids can also be used to treat the graphite felt. The cell resistance was found to decrease greatly after the treatment, although still higher than those treated by the sulfuric acid; sulfuric acid alone showed the best treatment results[58].

2.3 Tin Background

2.3.1 Productions of Tin

Tin is the 49th most abundant element in Earth`s crust, which contains approximately 2~3 ppm tin. Annual world production in 2014 of tin was approximately 296,000 tons, 70% of which is obtained from the ores and 30% being recovered from the scrap metal. The world`s largest producer of tin in 2014 was China, accounting for 42% of the world production [59].

Tin does not occur as the native element but must be extracted from various ores. Cassiterite (SnO_2) is the only commercially important source of tin. Small quantities of tin are recovered from complex sulfides such as stannite, cylindrite, franckeite, canfieldite, and teallite[2]. Tin minerals are almost always associated with granite rock, usually at a level of 1% tin oxide content.

Cassiterite is dense and hard and thus tends to concentrate by gravity in river sediments. About 80% of mined tin is from secondary deposits found downstream from the primary lodes. The most economical ways of mining tin are through dredging, hydraulic methods or open cast mining. Most of the world's tin is produced from placer deposits, which may contain as little as 0.015% tin[2].

It is reported that about 253,000 tonnes of tin have been mined in 2011, mostly in China (110,000 t), Indonesia (51,000 t), Peru (34,600 t), Bolivia (20,700 t) and Brazil (12,000 t)[1]. **Table 2.6** and **Table 2.7** show the largest tin producing companies and world tin mine reserves. According to the International Tin Institute, the demand of tin is already outstripping supply in 2014. At current consumption rates and technologies, the current reserves of tin will be exhausted in 40 years.

In addition to tin ores, tin scrap is also an important source of the metal. The recovery of tin through recycling of scrap tin, is increasing rapidly. The largest world producers of recycled tin are France and the United States. Approximately 25,000 million food cans are produced in Europe each year and approximately 20% of them have unlacquered tin-coated steel bodies[59].

Table 2.6 Largest tin producing companies(tonnes)[59]

Company	Polity	2006	2007	% change
Yunnan Tin	China	52,339	61,129	16.7
PT Timah	Indonesia	44,689	58325	30.5
Minsur	Peru	40,977	35,940	-12.3
Malay	China	52,339	61,129	16.7
Malaysia Smelting Corp	Malaysia	22,850	25,471	11.5
Thaisarco	Thailand	27,828	19,826	-28.8
Yunnan Chengfeng	China	21,765	18,000	-17.8
Liuzhou China Tin	China	13,499	13,193	-2.3
EM Vinto	Bolivia	11,804	9,448	-20.0
Cold Bell Group	China	4,696	8,000	70.9

Table 2.7 World tin mine reserves (tonnes, 2011)[59]

Country	Reserves
China	1,500,000
Malaysia	250,000
Peru	310,000
Indonesia	800,000
Brazil	590,000
Bolivia	400,000
Russia	350,000
Australia	180,000
Thailand	170,000
Other	180,000
Total	4,800,000

2.3.2 Applications of Tin

Tin is widely used in tin-plated containers, solders, alloys, babbit, pewter, and more specialized alloys such as dental amalgams and the titanium alloys used in aircraft engineering. In 2006, about half of the world`s tin produced was used in solder. The rest was divided between tin plating, tin chemicals, brass and bronze, and glass uses[59].

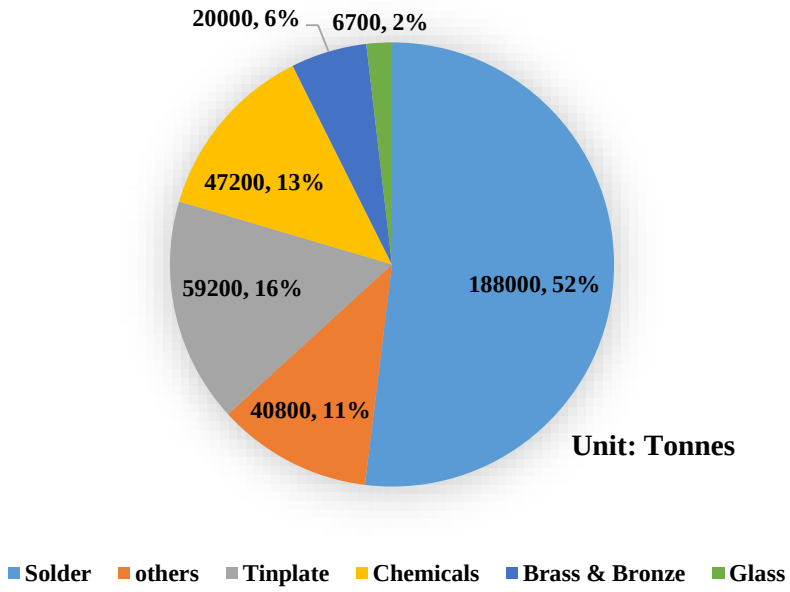

Figure 2.12 World consumption of refined tin by end-use, 2006[59]

Tin has long been used as a solder in the form of an alloy with lead, accounting for 5 to 70% weight percent. Tin has a melting point of 232 ℃ and lead has a melting point of 328 ℃. They can form a eutectic mixture with lead containing 63% tin and 37% lead. For the last few decades, such solders have been widely used for joining pipes or electric circuits[60]. The properties of tin, lead, and eutectic solder are summarized in **Table 2.8**.

Table 2.8 Materials properties of tin, lead, and eutectic solder[60]

Materials Properties	100Sn	63Sn37Pb	100Pb
Melting point, ℃	232	183	328
Electrical conductivity, Ω^{-1} cm^{-1}	9.1	6.9	4.8
Thermal conductivity, W m^{-1} K^{-1}	66	50.9	35
Coefficient of thermal expansion, 10^{-6}/℃	22	24.1	28.9
Surface tension, dyn cm^{-1}	545	490	439
Shear strength, psi	4,000	3,450	2,000
Tensile strength, MPa	21.5	27.5	17.3
Percent elongation	<0.82	40	55

Tin bonds readily to iron and is used for coating lead, zinc and steel to prevent corrosion. Tin-plated steel containers are widely used for food preservation, and this forms a large part of the market for metallic tin.

Tin can combine with other elements to form a wide variety of useful alloys. The most commonly alloyed element is copper. Pewter consists of 85-99% tin, and Bell metal contains 22% tin. Bronze is mostly copper, containing only 12% tin; addition of phosphorus gives phosphor bronze.

2.3.3 Physical Properties of Tin

Tin metal is silver white, soft, ductile and nontoxic, with excellent corrosion resistance in air, lubricity, and ability to form many useful alloys. Tin melts at a low temperature of about 232 ℃ and boils at a high temperature of 2602 ℃. With its low melting point and high boiling point, tin has a liquidus range exceeded by few metals. It readily alloys with many metals, such as copper, nickel, silver, gold, and palladium[59, 60].

There are two allotropic forms of tin: white (β) and gray (α). β-tin is the familiar form, which is stable at and above room temperature. It is malleable and crystallizes in the body-centered tetragonal system (See **Figure 2.13**).

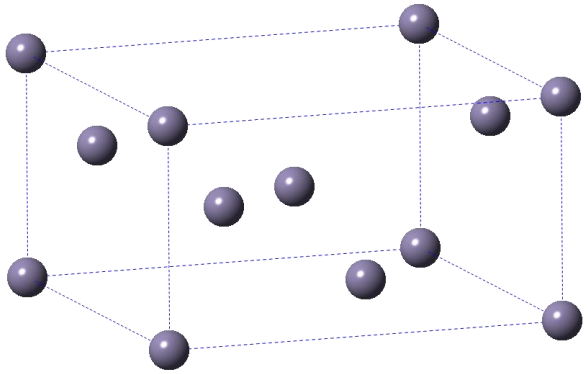

Figure 2.13 Structure of β-tin[59]

However, α-tin, which is stable below 13.2 ℃, has a diamond lattice similar to silicon or germanium (See **Figure 2.14**). It is considerably less dense than β-tin and is nonmetallic in appearance and properties. It is a dull-gray powdery material with no common uses, other than a few specialized semiconductor applications.

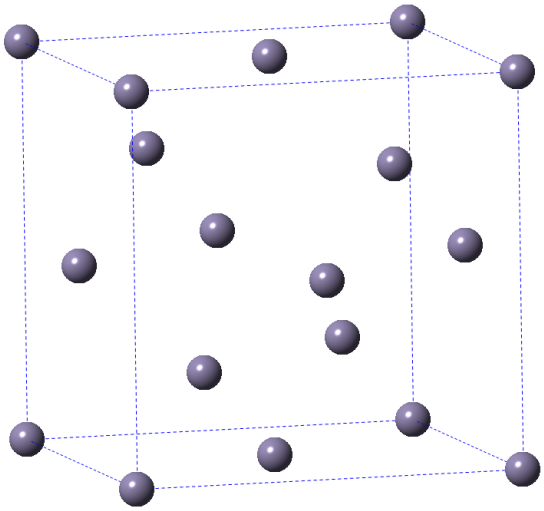

Figure 2.14 Structure of α-tin[59]

The allotropic transformation occurs at 13 ℃ (See **Equation 2.12**). The allotropic change is known as “tin pest”, probably because it appears to spread from the center of initiation. On the addition of antimony, lead, or bismuth, the transformation is inhibited or prevented, increasing the durability of the tin[59].

$$\alpha - \mathrm{Sn} \underset{\longleftarrow}{\overset{13\ ^{\circ}\mathrm{C}}{\longrightarrow}} \beta - \mathrm{Sn} \qquad \textbf{Equation 2.12}$$

2.3.4 Chemical Properties of Tin

Tin has the electronic configuration of $4d^{10}5s^{2}5p^{2}$. Thus there are four electrons available for bonding. Theoretically, solution of Sn(IV) should be readily reduced to Sn(II) by many reducing reagents, especially metals such as antimony and nickel. However, in practice, Sn(IV) does not exist in its simple ion form in water; instead, it most likely forms hydroxyl compounds such as $Sn(OH)_6^{2-}$, which eventually becomes insoluble SnO_2 [59]. Meanwhile, Sn(II) is readily oxidized to Sn(IV) by common oxidants including dissolved oxygen from air. Tin can be used as a protective coat for other metals. The formation of a protective oxide layer is able to prevent further oxidation[60].

Tin resists corrosion from water, but can be attacked by acids and alkalis[60]. This is evident from **Figure 2.15**.

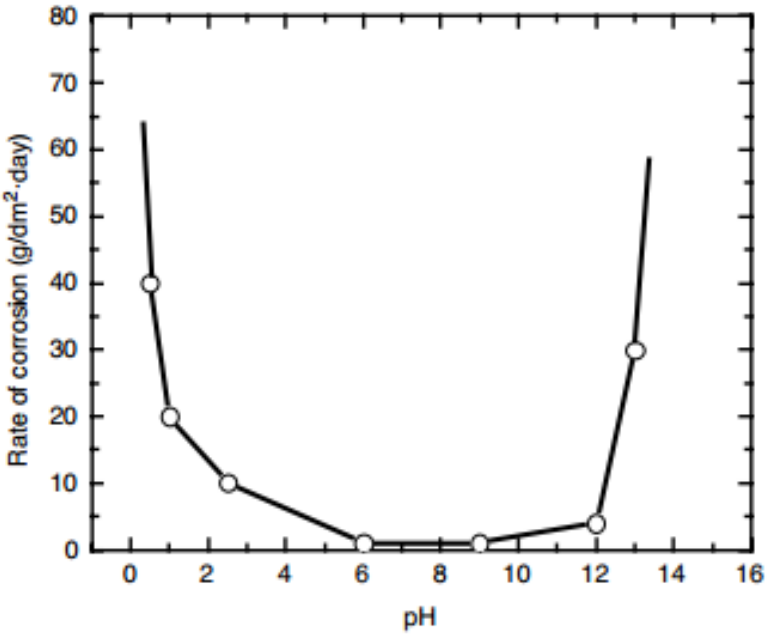

Figure 2.15 Tin corrosion behavior in aqueous media[60]

The overpotential of hydrogen on the tin surface is quite high, about 0.75 V, so that attack by acids and bases is slow unless an oxidizing reagent is present to depolarize the evolution of hydrogen.

In acidic solution, Sn(II) compounds probably exist in the form of Sn^{2+} aquo ions, while Sn^{4+} aquo ions probably do not exist, either being hydrolyzed as previously described or complexed, as in $SnCl_6^{2-}$ and $Sn(OH)_6^{2-}$. In alkaline media, Sn(IV) is the most stable. Alkaline stannite or Sn(II) solution disproportionate according to the **Equation 2.13**.

$$2[Sn(OH)_4]^{2-} \rightarrow [Sn(OH)_6]^{2-} + Sn + 2OH^- \qquad \textbf{Equation 2.13}$$

This reaction is important in plating from alkaline stannate solution. All tin compounds tend to hydrolyze in aqueous solution. Therefore, alkaline solution must be stabilized by the presence of excess alkali, and acid solution must be stabilized by the presence of excess acid[60].

2.3.5 Eh-pH Diagram for the Sn-H_2O System

The thermodynamics of the SnO_2 recovery system can be discussed in terms of the Sn-H_2O diagram (See **Figure 2.16**).

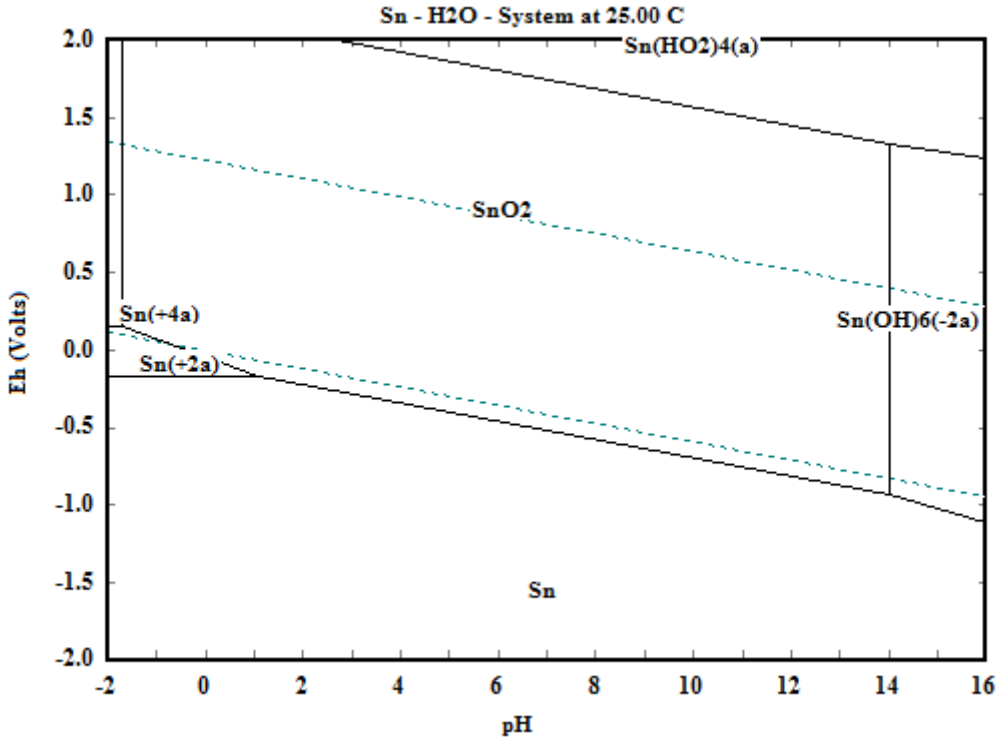

Figure 2.16 The Sn-H_2O Eh-pH diagram at 25 ℃ and 0.1 M Sn species in solution

The diagram shows that the extraction of Sn from SnO_2 could be done by two methods.

(1) A strong acid could be applied to extract Sn as Sn^{4+}.

$$SnO_2 + 4H^+ \rightarrow Sn^{4+} + 2H_2O \qquad \textbf{Equation 2.14}$$

This treatment would likely require a very strong acid to extract Sn. Generally, the kinetics of SnO_2 leaching in dilute sulfuric acid and hydrochloric acid is very slow.

(2) Reductively extract tin at a low pH by reducing tin to the stannous state (Sn^{2+}).

$$SnO_2 + 4H^+ + 2\,Red^- \rightarrow Sn^{2+} + 2H_2O + 2Ox \qquad \textbf{Equation 2.15}$$

The metallic tin can then be produced by electrolysis or reductive precipitation.

Electrolysis $Sn^{2+} + 2e^{-} \rightarrow Sn$ **Equation 2.16**

Precipitation $Sn^{2+} + 2Red^{-} \rightarrow Sn + 2Ox$ **Equation 2.17**

The Eh-pH diagram for the chromium system shown in **Figure 2.1** shows that the Cr^{3+}/Cr^{2+} has a reducing potential of -0.42 V. This is suitable for the reduction requirement for SnO_2 of about 0 V at pH 0.

2.4 Previous Studies on Reactions of Inorganic Solids with Chromium(II) Ions

Chromium(II) ions can capture with ligands during the oxidation process, where the ligands may be derived from the oxidizing reagent or may be picked up from the solution. Additionally, chromium(II) ions have the capacity to form two different species even if they are oxidized to the same oxidation state. Specifically, oxidation by a simple $1e^-$ process yields only mononuclear Cr(III) species; a number of $2e^-$ oxidizing reagents form binuclear Cr(III)[61]. These two properties make the chromium(II) ion an especially useful reducing reagent in the study of mechanisms of oxidation-reduction reactions in aqueous solutions[13].

2.4.1 Reactions of Metal Oxides with Chromium(II) Ions

The reactions of metal oxides with chromium(II) ions were examined by Zabin and Taube[12]. The reduction results are summarized in **Table 2.9**. It was found that Pb_3O_4 shows the best reaction kinetics, while the leaching rates for V_2O_5, SnO_2, TiO_2, CrO_2 and Co_3O_4 are extremely slow.

Table 2.9 A summary of the reactions of Cr^{2+} with metal oxides[12]

(Temp 25 ℃, ClO_4^- system, total volume 50 mL)

Oxide	$[H^+]$, M	$[Cr^{2+}]$, M	Cr(III) product	Rate $Msec^{-1}m^{-2}$
PbO_2	0.45	0.079	$Cr(OH_2)_6^{3+}$,a	$>8 \times 10^{-6}$
Tl_2O_3	0.89	0.080	$Cr(OH_2)_6^{3+}$,a	$>4 \times 10^{-6}$
MnO_2	0.95	0.022	$Cr(OH_2)_6^{3+}$,a	$\sim 2 \times 10^{-5}$
Mn_2O_3	0.25	0.079	$Cr(OH_2)_6^{3+}$,a	$\sim 3 \times 10^{-7}$
Pb_3O_4	0.45	0.079	Dimer, b	$>3 \times 10^{-5}$
Ca_2PbO_4	0.89	0.080	Dimer, b	$\sim 4 \times 10^{-6}$
$PbO_{1.75}$	0.45	0.079	Dimer, b	$>5 \times 10^{-6}$
Fe_2O_3	0.45	0.079	---	$< 8 \times 10^{-9}$
Co_2O_3	0.67	0.039	$Cr(OH_2)_6^{3+}$,a	$\sim 4 \times 10^{-8}$
CeO_2	0.20	0.029	$Cr(OH_2)_6^{3+}$,a	$\sim 2 \times 10^{-8}$
Mn_3O_4	0.45	0.079	---	$\sim 2 \times 10^{-7}$
V_2O_5	0.10	0.016	$Cr(OH_2)_6^{3+}$	$\sim 8 \times 10^{-9}$
SnO_2	0.89	0.080	---	c
TiO_2	0.89	0.080	---	c
CrO_2	0.89	0.080	---	c
Co_3O_4	1.0	0.167	---	c

a. $Cr(OH_2)_6^{3+}$ constitutes more than 95% of the Cr(III) product.

b. $Cr(OH_2)_6^{3+}$ constitutes less than 10%.

c. Less than 5% reaction during a time interval in which PbO_2 reacts completely.

One of the most important observations was that the rate of reduction of the oxides by Cr^{2+} was significantly accelerated by chloride ions. The rate of reaction for a slow oxide such as Fe_2O_3 was more sensitive to Cl^- than it was for an active oxide such as MnO_2. It was reported that the reaction rate of Fe_2O_3 with Cr^{2+} could be accelerated by a factor of more than 100 when the concentration of chloride ions was 0.45 M. It was proposed that

Cr^{2+}-Cl^- bonds are established. When the chloride ion was associated with Cr^{2+}, it lowered the overall positive charge of the Cr(III) species, thus reducing the activation energy necessary for the transfer of Cr^{2+} to the surface layer[12].

2.4.2 Reactions of Metal Sulfides with Chromium(II) Ions

Kelsall and Yin studied the reduction of PbS particles by Cr^{2+} ions. The reaction is described as **Equation 2.18**.

$$PbS + 2H^+ + 2Cr^{2+} \rightarrow Pb + H_2S + 2Cr^{3+} \qquad \textbf{Equation 2.18}$$

The time dependence of the fractional conversion of PbS to Pb is shown in **Figure 2.17**. They reported that it took less than 15 minutes to completely reduce the 100 μm PbS precipitate particles with 0.8 M Cr(II), which corresponded to *ca.* a ninety-fold stoichiometric excess. The apparent rate coefficient for the reaction was determined to be 3.2×10^{-6} m s^{-1}. The magnitude of the apparent rate coefficient suggested that the reaction occurred under mixed mass transport and surface chemical control[11].

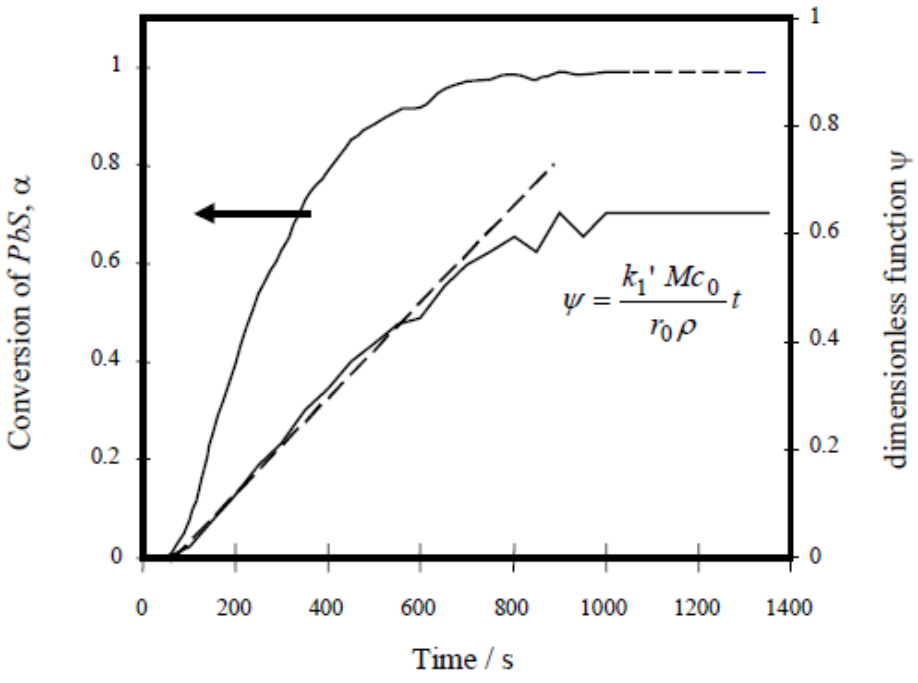

Figure 2.17 Time dependence of PbS conversion to Pb by 0.8 M Cr(II)[11]

(ψ is the integrated kinetic equation, $k_1^{`}$ is the first order rate coefficient (s^{-1}), M is the molar mass of PbS (g/mol), r_0 is the initial mean radius of PbS particles (m), t is the time (s), ρ is the density of PbS (g/cm^3), c_0 is the initial concentration of Cr(II) (mol/m^3))

Kelsall also pointed out that in order to avoid inhibition of the reaction, a significant decrease in molar volume must accompany that phase transition as the metal product is formed by a topochemical reaction on the metal sulfide reactant. For the metal sulfide reactant, the reductant is first oxidized at the metal/solution interface; the electrons flow through the metal product to the metal sulfide/solution interface; hydrogen sulfide product is then transported via the pores resulting from the decrease in molar volume.

2.4.3 Reactions of Nonoxidic Solids with Chromium(II) Ions

Reactions of a number of nonoxidic solids with Cr^{2+} were also investigated by Zabin and Taube [12]. The results are summarized in **Table 2.10**.

Table 2.10 The reactions of Cr^{2+} with solids [12]

Nonoxidic solids	Reactions
$PbCl_2$	$PbCl_2 \rightarrow CrCl^{2+}(95\%) + Pb^0$
AgCl	$AgCl \rightarrow CrCl^{2+}(95\%) + Ag^0$
AgBr	$AgBr \rightarrow CrBr^{2+}(75\%) + Ag^0$
AgI	$AgI \rightarrow Cr(OH_2)_6^{3+}(98\%) + I^- + Ag^0$
AgSCN	$AgSCN \rightarrow CrNCS^{2+}(50\%) + Ag^0$
AgOAc	$AgOAc \rightarrow Cr(OH_2)_6^{3+}(95\%) + Ag^0$
$Fe_2(SO_4)_3$	$Fe_2(SO_4)_3 \rightarrow CrSO_4^+(95\%) + Fe^{2+}$
$FePO_4$	$FePO_4 \rightarrow Cr(III) - PO_4$ complex $(95\%) + Fe^{2+}$

All reactions were found to be over in 15 minutes when 2 equiv of solid was reacted with every equiv of Cr^{2+} ion[12]. Monoiodo Cr(III) may be the primary product for the reaction of AgI with Cr^{2+}. However, due to the catalysis effect of elementary silver, monoiodo Cr(III) eventually dissociated to $Cr(H_2O)_6^{3+}$.

2.4.4 Mechanism of Reactions of Solid Oxides with Chromium(II) Ions

The mechanism of reduction of solid oxides by Cr^{2+} is different from the reduction of oxidizing reagents in homogeneous solution in some important respects. For example, thallium(III) ion is known to oxidize Cr^{2+} to form $(CrOH)_2^{4+}$ as the major product, but when Tl^{3+} is incorporated into the oxide, the product formed on oxidizing Cr^{2+} is $Cr(H_2O)_6^{3+}$. The formation of $(CrOH)_2^{4+}$ may be taken to imply oxidation involving a $2e^-$ change, while the formation of $Cr(H_2O)_6^{3+}$ suggests that oxidation has occurred simply by extracting one electron from $Cr(H_2O)_6^{2+}$[12].

$$Tl^{3+} + Cr^{2+} \rightarrow Cr^{IV} + Tl^{+} \qquad \textbf{Equation 2.19}$$

$$Cr^{IV} + Cr^{2+} \rightarrow (CrOH)_2^{4+} \qquad \textbf{Equation 2.20}$$

An obvious difference between the reduction of an isolated cation in homogeneous solution and the cation as part of a solid is that, in the former case, the electron that is absorbed is localized at the absorbing center, while in the latter case, the electron may be trapped at a point some distance removed from the absorbing center. It was suggested by Zabin that for the heterogeneous process, the primary electron transfer is to a level belonging to the lattice rather than directly to a trapped state on a particular ion for the homogeneous process[12].

Zabin reported that no oxygen transfer was observed when PbO_2 reacted with Cr^{2+}, which is very anomalous[12]. This may due to the fact that although Cr^{2+} can make a bond to O^{2-} in the reduction of the oxide, the damage that results to the lattice may occur at a point remote from the point of attack, so that Cr^{3+} is unable to capture oxide from the lattice[12, 62, 63]. It was found that although PbO_2 showed no transfer, Tl_2O_3 showed one oxygen transfer for each two Cr^{2+} ions oxidized. The difference between these two is

that O^{2-} is not so firmly bound by Tl_2O_3 as it is by PbO_2, and Cr^{3+} is able to remove it from the lattice.

For each oxide, the reducing reagent attacks its surface layer, and transfers negative charge to the oxide, leaving excess positive charge on the surface. With the accumulation of the charge, the transfer rate of Cr^{2+} diminishes. At the steady state, the loss of cations and O^{2-} from the solid is equal to the rate at which Cr^{2+} attacks. Zabin and Taube pointed out that if the lattice of the product is significantly different from the host lattice, the marked change in geometry can result in a strong tendency for the electrons absorbed to be trapped at the surface where the defects are destroyed as H^+ removes O^{2-}. This tendency of electron accumulation can accelerate the release of metal ion. However, if the product ion fits into the host lattice well, the tendency for the damage to localize at the surface is not as great; a large surface concentration of the reducing reagent is needed to drive the reaction and it proceeds at a lower rate[12].

2.5 Previous Studies on Hydrometallurgical Recovery of Tin

2.5.1 Natural Ores

Since the 1960s, research has been focused on the recovery of tin from low grade tin concentrate with hydrometallurgical methods. However, this research is mainly performed in the labs, and few have been applied to the real industry. The main source of tin in nature is cassiterite, which is insoluble in aqueous solutions. Therefore, cassiterite has to be reduced to Sn(II) or metallic Sn first in hydrometallurgy. No work on the direct leaching of tin concentrate has been reported.

Reduction of SnO_2 to Sn -Acid leaching-Electrolysis

The flowsheet for tin recovery in the smelter located in New Brunswick, Canada is illustrated in **Figure 2.18**.

Tin concentrate processed by this smelter consisted of 25% ~ 30% Sn, 0.5% Zn and impurities such as tungsten, tantalum and niobium. Initially, SnO_2 was reductively roasted and most of the tungsten, tantalum and niobium were removed by magnetic separation. The non-magnetic parts were leached by sulfuric acid. After filtration and purification, the tin leachate was processed by electrolysis. Metallic tin could be electrodeposited at the cathode with a purity of up to 99.9% [5]. The anode reaction was oxygen evolution.

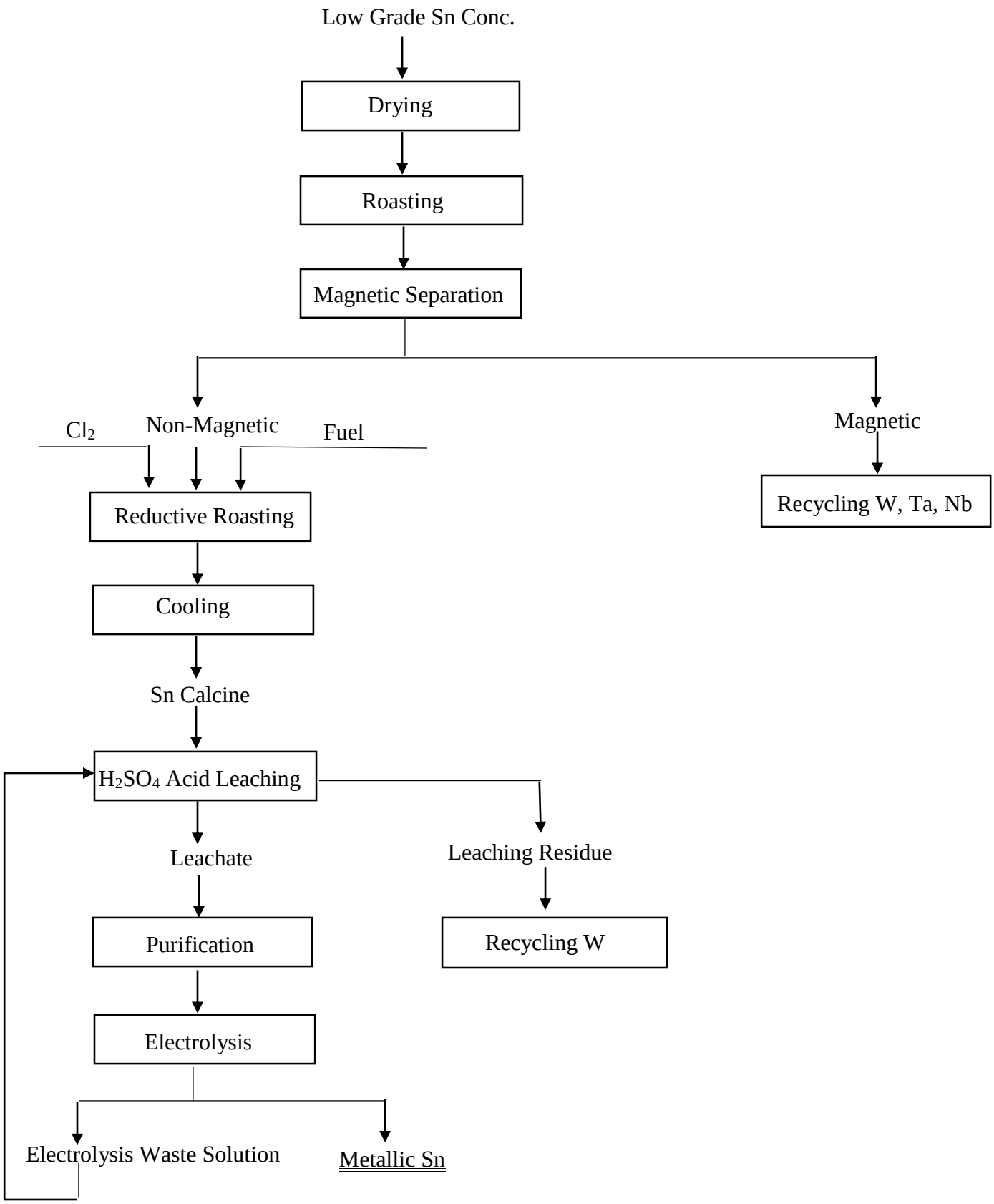

Figure 2.18 Flowsheet for tin recovery in New Brunswick, Canada [5]

Reduction of SnO_2 to Sn-Acid leaching-Displacement Reaction

The "Reduction (Sn)-Acid leaching-Displacement Reaction" method was only applied in research laboratories. The composition of the concentrate treated by this method is shown in **Table 2.11**.

Table 2.11 Tin concentrate composition /%[64]

Concentrate	Sn	Fe	SiO_2	F	S	Ca	Mg	Al
A	14.2	6.5	30.0	8.0	2.8	9.0	0.8	5.8
B	18.8	8.5	34.0	0.98	4.8	0.83		5.6

The first step was to calcine the tin concentrate to remove sulfur, and then SnO_2 was chemically reduced to metallic Sn by hydrogen gas. Hydrochloric acid or sulfuric acid with the addition of $FeCl_3$ (NaCl) was used to extract tin. Finally, metallic tin was produced by displacement reaction with aluminum scraps (See **Equation 2.21**). The recovery efficiency of tin with this method could be at least 99%[64].

$$3Sn^{2+} + 2Al \rightarrow 3Sn + 2Al^{3+} \qquad \textbf{Equation 2.21}$$

Reduction of SnO_2 to SnO-Acid leaching-Electrolysis

The composition of tin concentrate treated by this process is illustrated in **Table 2.12.**

Table 2.12 Composition of the tin concentrate[65]

Name	Composition%					
	Sn	Fe	Al	SiO_2	S	F
I	19.0	7.4		42.0	4.8	1.7
II	15.2	8.0		39.0	3.2	1.2
III	24.9	15.6	7.2	21.0	1.5	
IV	21.8	16.9	2.9	15.6	3.7	
V	30.3	15.2	1.9	9.2	7.3	
VI	14.2	6.5		30.0	2.8	9.0
VII	18.8	8.5	5.8	34.0	4.8	0.98

The tin concentrate was melted together with quartz sand and lime at 1200 ~1450 ℃ to form glassy state. SnO_2 was reduced to SnO and immediately cools in water. This could maintain the stability of SnO in the glassy state. Sulfuric acid was then used to dissolve the formed SnO. There are three requirements for the glassy state: (1) avoid the formation of Sn in the reduction step, as it is insoluble in sulfuric acid; (2) reduce the volatilization loss of SnO_2 or SnS; (3) avoid any anions that can form acid insoluble tin compounds, for example, F^-[65, 66].

The leaching efficiency was the highest when the amount of SiO_2 is about 30% in the glassy state. Excess sulfur, fluorine and CaO would decrease the recovery efficiency. CaO would accelerate the volatilization of SnO. In the flotation step, the amount of CaF_2 must be lowered to less than 1%; otherwise, fluorine could form compounds with Sn(IV), which is only soluble in hydrochloric acid. Sulfur should also be removed by calcining in order to avoid the formation of volatile SnS and insoluble tin sulfides. The overall flowsheet is shown in **Figure 2.19**.

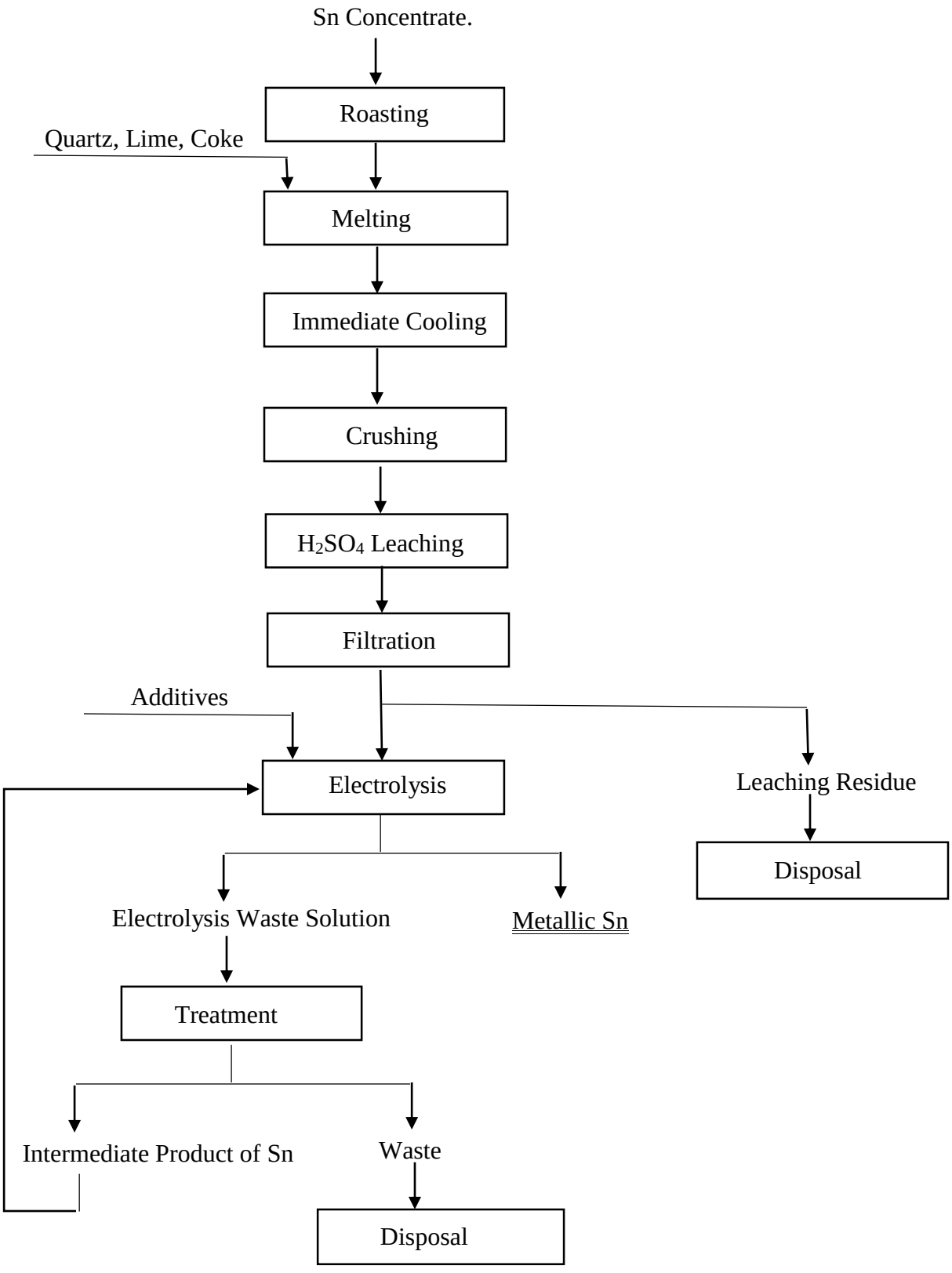

Figure 2.19 Flowsheet for tin recovery with acid leaching [65]

Na_2S+NaOH Pressure leaching-Electrolysis

The composition of the tin concentrate treated by this method is listed in **Table 2.13**

Table 2.13 Composition of the tin concentrate [67]

Element	Sn	Zn	Fe	C	As	Sb	Bi	Pb	SiO_2	S
%	19.78	0.80	26	0.02	0.78	1.32	0.03	1.00	3	13

The minerals were completely dissolved at the temperature of 250 ~ 350 ℃ in the autoclave, with 50~ 200 g/L basic Na_2S solutions. The reaction is shown as **Equation 2.22**.

$$SnO_2 + 3Na_2S + 2H_2O \rightarrow Na_2SnS_3 + 4NaOH \qquad \textbf{Equation 2.22}$$

The leaching solution consisted of 40 g/L Sn, 0.2 g/L Sb, 0.2~0.5 g/L As[67]. The anion exchange resin or zinc powder was used to remove Sb and As in the leachate. Thin steel sheets were used as both anode and cathode to electrodeposit Sn metal from the solution. The cathode and anode reactions are expressed as **Equation 2.23** and **Equation 2.24**.

Cathode $SnS_3^{2-} + 6H^+ + 4e^- \rightarrow Sn + 3H_2S$ **Equation 2.23**

Anode $O_2 + 2H_2O + 4e^- \rightarrow 4OH^-$ **Equation 2.24**

Fuming dust -NaOH+Na_2S leaching-Electrolysis

Tin concentrate first reacted with sulfide species and then it was volatilized to form fuming dust, the composition(%) of which is 35.1 Sn, 2.0 As, 1.9 Sb, 0.2 Bi, 0.1 Cu, 5.4 Pb, 5.6 S, 3.4 Zn. NaOH and Na_2S solutions were used to leach the fuming dust. Due to the presence of SnO and SnS in the fuming dust, oxidizing reagents should be added during the leaching. AAA grade tin could be electrodeposited from the leaching solution under a current density of 200 A/m^2 with a current efficiency at 95%. The electrolyte was the mixture of Na_2SnO_3 and Na_2SnS_3[6]. The flowsheet is illustrated in **Figure 2.20**.

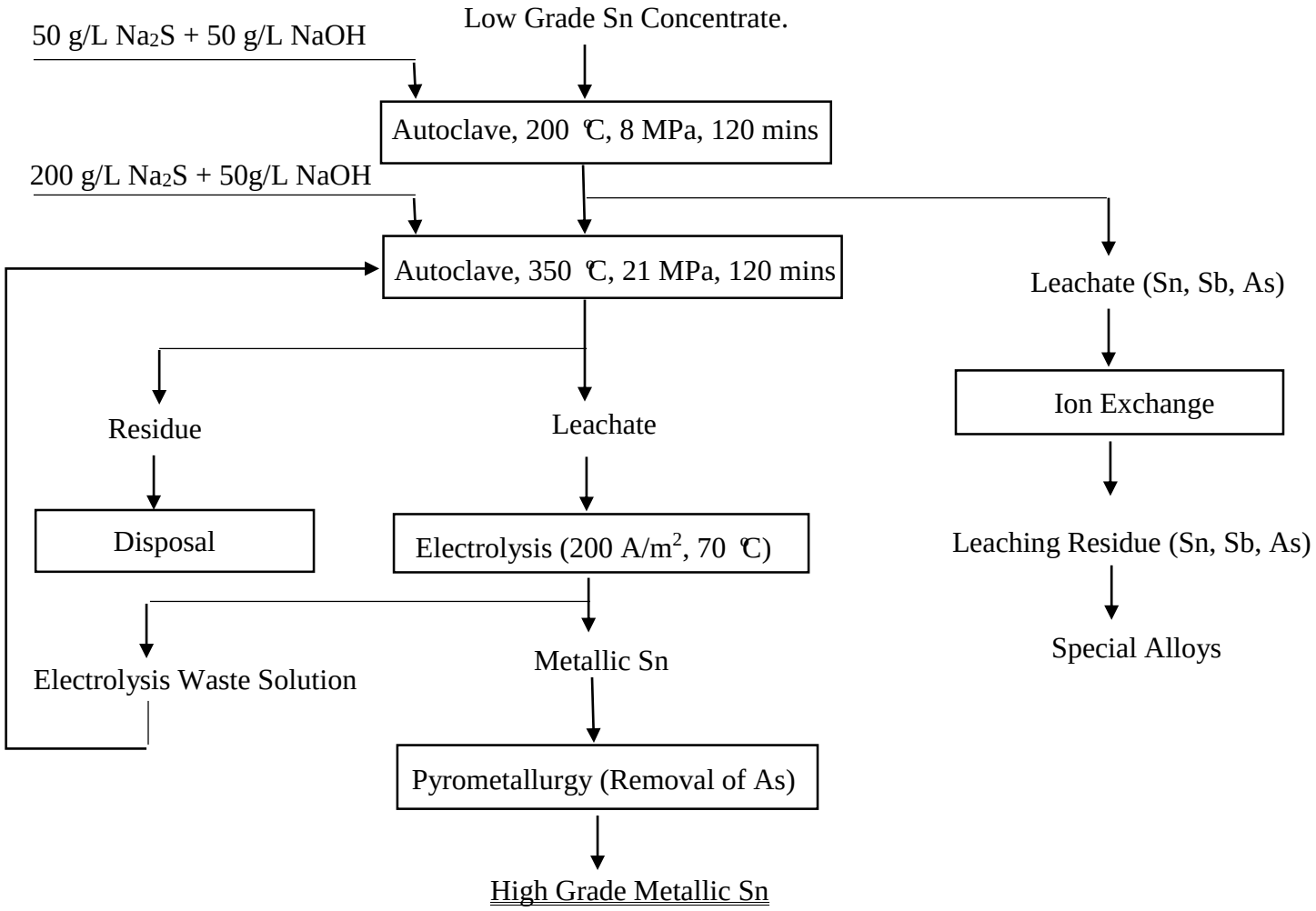

Figure 2.20 Flowsheet for tin recovery with basic leaching [6]

Hydrometallurgy- Electrometallurgy

The following method was conducted using the tin concentrate from Igla, Egypt. The composition is shown in **Table 2.14**.

Table 2.14 Chemical and Spectral Analysis of the Tin Concentrate in Igla[68]

Chemical analysis	Components	SnO_2	SiO_2	TiO_2	Fe_2O_3	Al_2O_3	MgO
	Contents/%	93.01	2.60	0.75	0.40	0.71	0.11
	Components	FeO	MnO	Na_2O	K_2O	$+H_2O$	$-H_2O$
	Contents/%	0.47	0.42	0.14	0.15	1.84	0.02
Spectral Analysis	Components	Sc	Zr	Be	V	Pb	Cu
	Contents/10^{-5}	30	290	4	92	43	56

The flowsheet for this processing method is shown in **Figure 2.21**. Three metallurgy methods (smelting, basic leaching and acid leaching) are described in the flowsheet. Among all these methods, the basic leaching of SnO_2 in the autoclave was the most efficient one, thus having the most advantages.

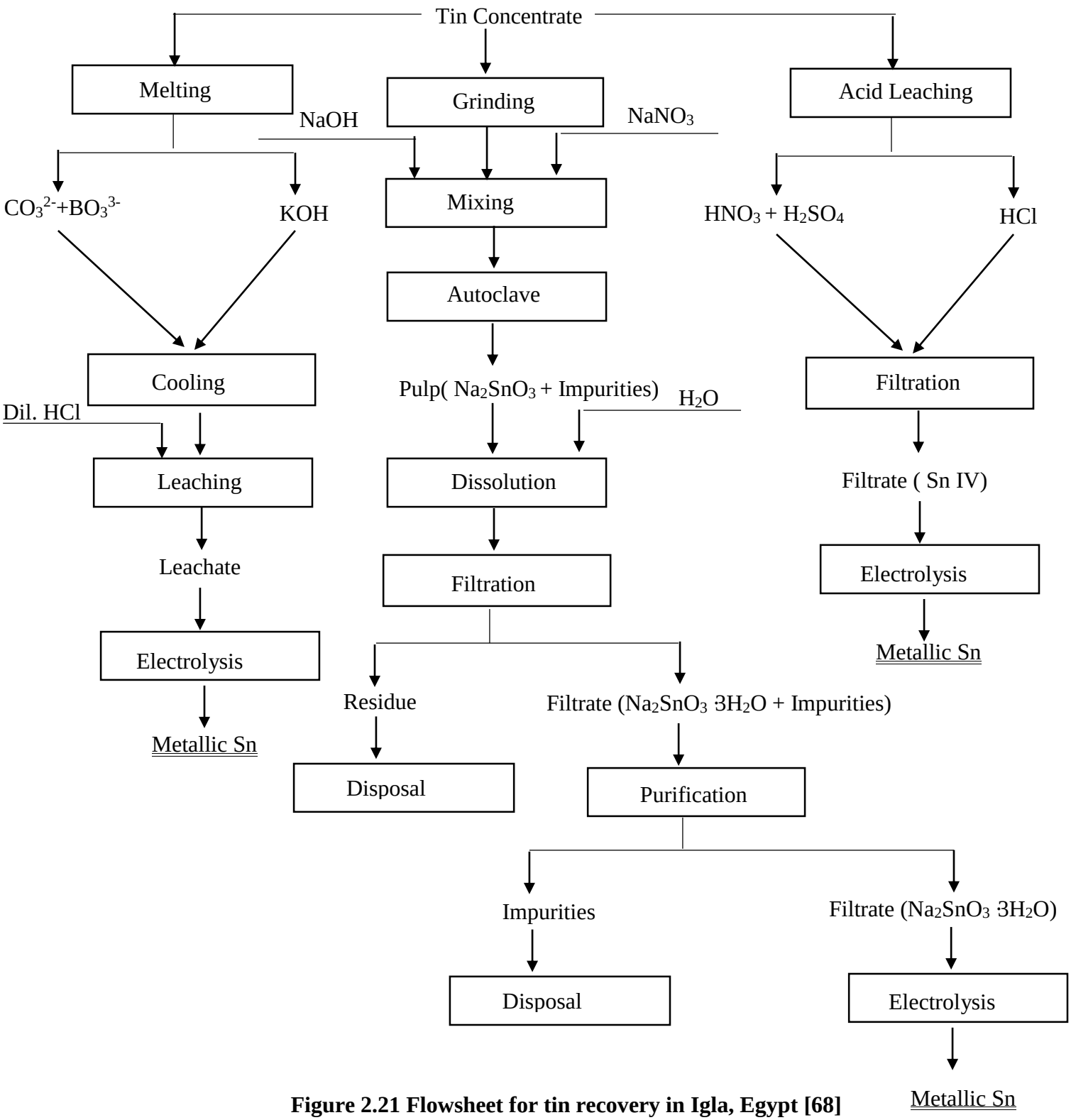

Figure 2.21 Flowsheet for tin recovery in Igla, Egypt [68]

2.5.2 Secondary Sources

The recovery of tin from scrap, dross and sludges is routine practice in pyrometallurgy as well as in hydrometallurgy. The hydrometallurgy method is often preceded by a fire-refining stage, with preparation of tin anodes for electrorefining in acidic or alkaline baths. Tin recovery from tinned cans is usually carried out in heated alkaline leaching solutions by the anodic dissolution of tin and its electrochemical deposition on steel cathodes as a spongy sediment or compact metal[69].

Stefanowicz and his coworkers found that the hydrometallurgical method could be successfully applied for tin recovery from sludge produced in tin fluoroborate electroplating electrolytes[69]. The sludge was leached with concentrated hydrochloric acid at room temperature for one month or by boiling in 10% HCl solution for two hours.

With a current density of 500 A/m^2, 93% efficiency of tin recovery was achieved in the H_2SnCl_6 electrolyte at tin concentrations exceeding 50 g/L with a steel cathode and graphite anode. The flowsheet is illustrated in **Figure 2.22**.

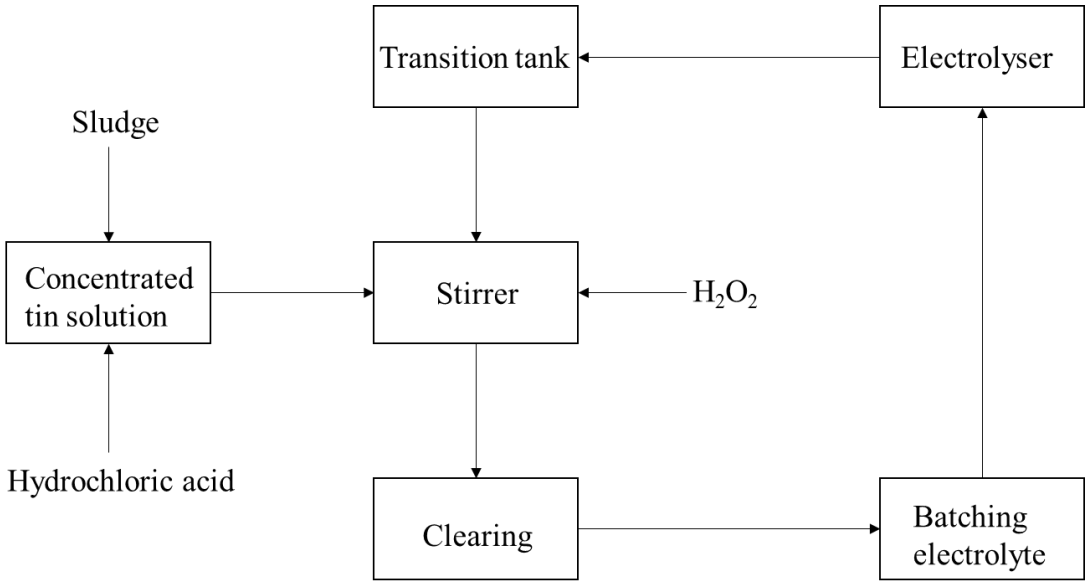

Figure 2.22 Flowsheet of tin recovery by the continuous method[69]

Printed circuit boards (PCBs) are the most essential components of all electrical and electronic equipments, which contain noteworthy quantity of metals. Waste PCBs typically consist of 28% metals, 23% plastics and 49% ceramics[70]. Ample amounts of metallic elements such as Cu (20%), Pb (2%), Sn (4%), Ni (2%), Fe (8%), Zn (1%) and Pd (0.005%) as well as some precious metals like Ag (0.2%) and Au (0.1%) are also a part of these wastes[71]. Therefore, recycling of PCBs is necessary for the safe disposal and utilization of these metals.

Jeong and his coworkers reported that the leaching efficiency of tin from solder was 95.97% using 5.5 M HCl at a pulp density 50 g/L, a temperature of 90 ℃ and a mixing time of 165 minutes. Meanwhile, 97.79% tin was leached out from solder materials of liberated swelled epoxy resin with 4.5 M HCl at 90 ℃ within 60 minutes at a fixed pulp density of 50 g/L. However, in the case of H_2SO_4 and HNO_3, no significant amount of leaching was observed under the same experimental conditions as in HCl[72]. **Figure 2.23** describes the flowsheet for recovery of tin from solder materials of waste PCBs**.**

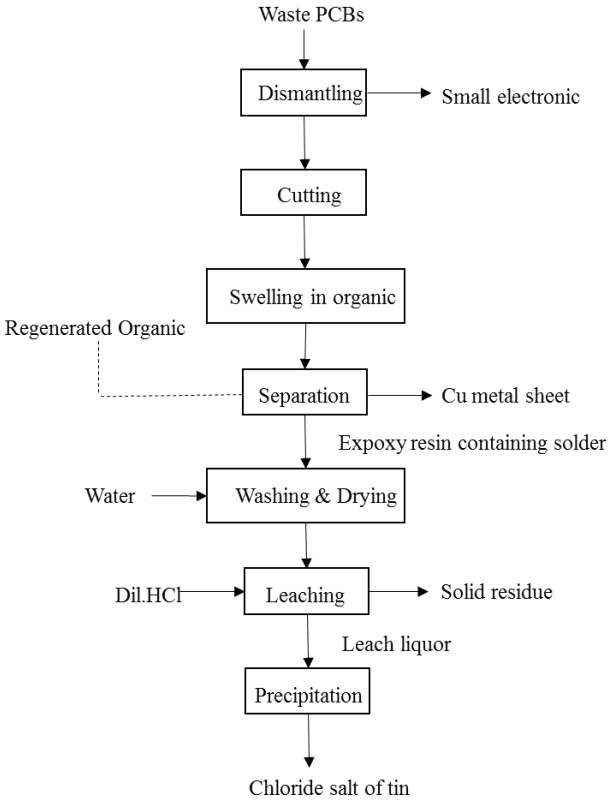

Figure 2.23 Flowsheet for recovery of tin materials from solder of waste PCBs[72].

Chapter 3 Electrochemical Reduction of Chromium(III) Ions

3.1 Introduction

The electrochemical reduction kinetics of chromium(III) in the chloride system has been widely studied. However, there are few published results on the current efficiency of chromium(III) reduction in batch electrochemical reactors in the chloride system. In addition, few works on chromium(III) electrochemical reduction in sulfate and MSA systems have been reported. Therefore, this is the first study on the current efficiency of chromium(III) electrochemical reduction in the batch reactors in acidic aqueous solutions. Three acid systems (hydrochloric acid, sulfuric acid and MSA) were investigated in this thesis.

In this chapter, the effects of several variables on the electrochemical reduction system such as acid concentration, current density, graphite felt thickness, graphite felt surface condition and graphite felt usage frequency were evaluated in chloride, sulfate and MSA systems (See **Section 3.4**); accordingly, the comparison and discussion of these three systems were then undertaken (See **Section 3.5**); finally, some conclusions for this electrochemical study were provided (See **Section 3.6**).

3.2 Experimental

3.2.1 Materials

Chromium(III) electrolytes were prepared from reagent grade or analytical grade chemicals and deionized water without further purification. Chromium(III) chloride hexahydrate was provided by Sigma-Aldrich and potassium chromium(III) sulfate dodecahydrate was supplied by Alfa Aesar. Cr(III)-MSA electrolytes were synthesized from lead(II) oxide, potassium chromium(III) sulfate and methane sulfonic acid (Lutropur® MSA 100)(See **Section 3.2.3.1**)**.** Lead(II) oxide was supplied by Sigma-Aldrich and methane sulfonic acid (Lutropur® MSA 100) was provided by BASF, Germany. Sulfuric acid was shipped from BDH and hydrochloric acid was provided by Fisher Scientific. The anolyte was 0.1 M/0.3 M/0.5 M sulfuric acid, and the catholyte was

0.1 M chromium(III) chloride in 0.2 M/0.6 M/1 M hydrochloric acid, or 0.1 M potassium chromium(III) sulfate in 0.1 M/0.3 M/0.5 M sulfuric acid, or 0.1 M potassium chromium(III) methanesulfonate in 0.2 M/0.6 M/1 M methane sulfonic acid. Nitrogen gas was supplied by Praxair.

3.2.2 Apparatus

The electrochemical reduction apparatus used during this study provided controlled conditions for chromium(III) electrochemical reduction. The apparatus is shown in **Figure 3.1** and **Figure 3.2**. The schematic diagram of the electrochemical cell is shown in **Figure 3.3**.

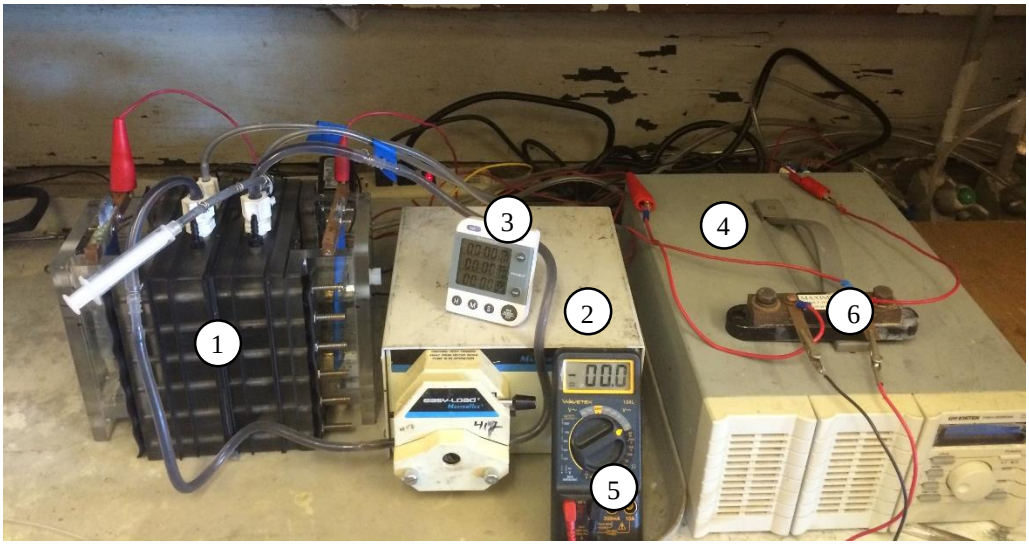

Figure 3.1 Experimental apparatus for Cr(III) electrochemical reduction tests

(1-Electrochemical Reactor, 2-Pump, 3-Timer, 4-DC Power Supply, 5-Multimeter, 6-Standard Resistor)

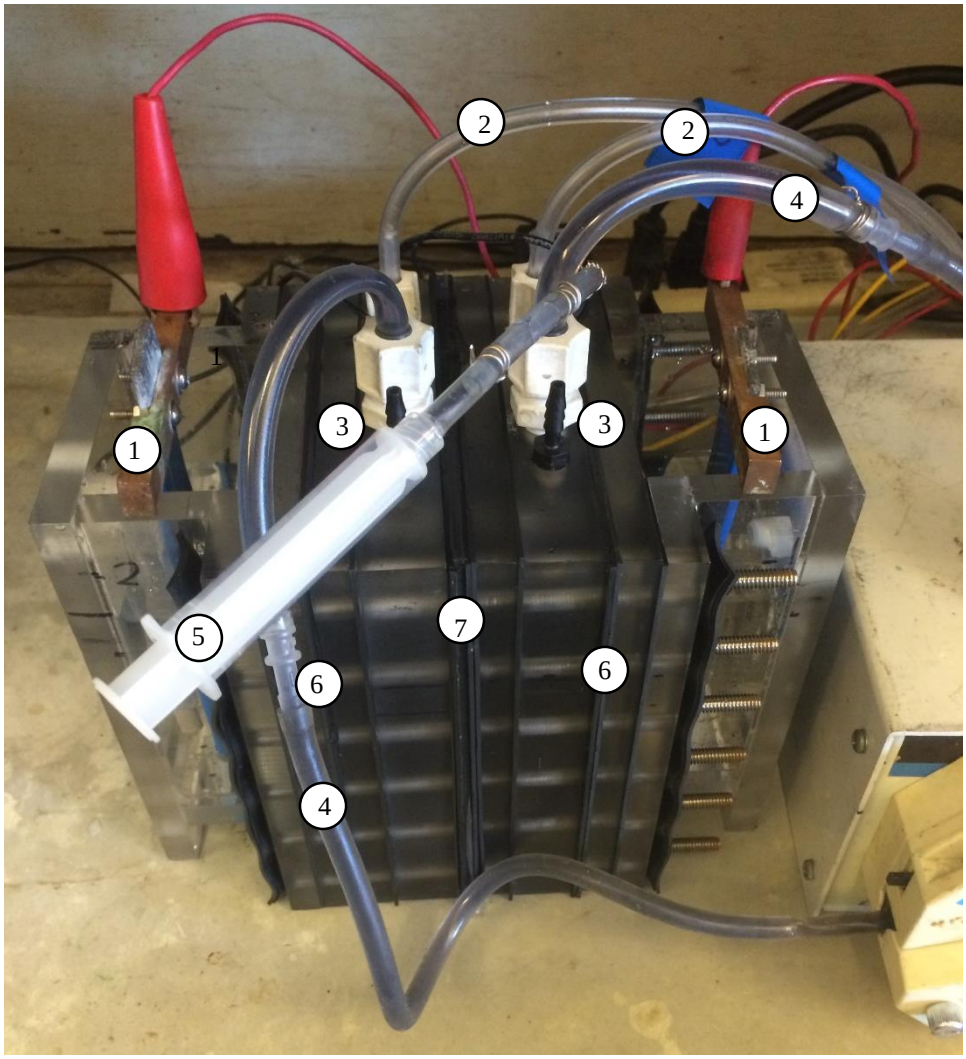

Figure 3.2 Electrochemical reactor for Cr(III) electrochemical reduction tests

(1- Lead-Silver Alloy Anodes, 2-Nitrogen Gas Inlets, 3-Gas Outlets, 4-Ciculation Tubes, 5-Syringe, 6-Ion Exchange Membranes, Nafion N324, 7- Graphite Felt Cathode)

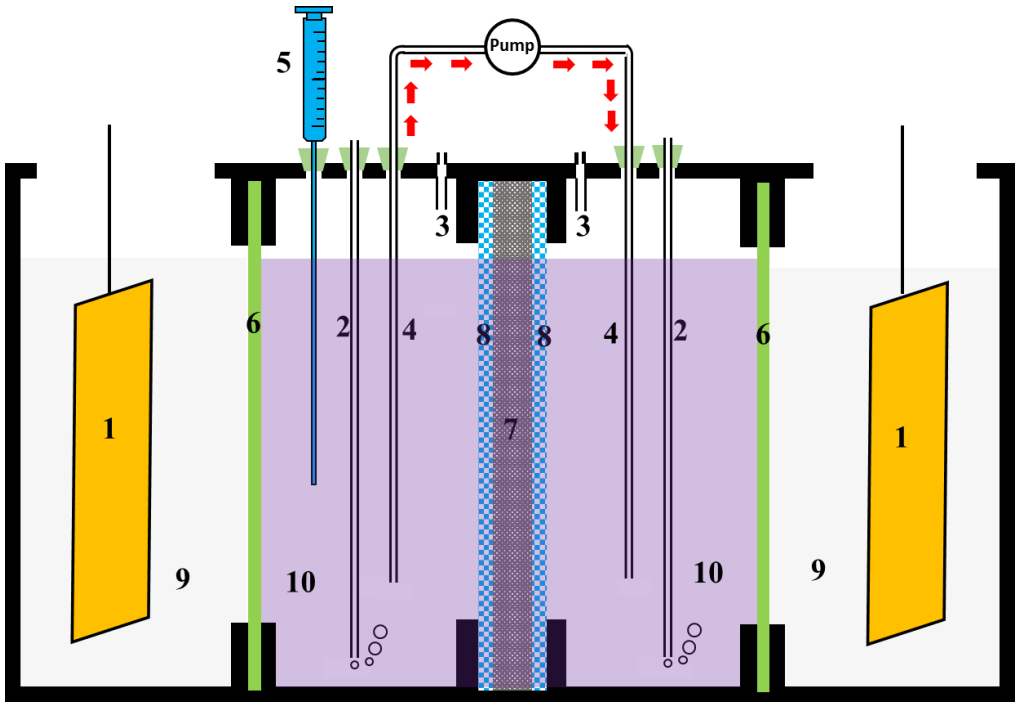

Figure 3.3 Schematic diagram of the electrochemical cell

(1- Lead-Silver Alloy Anodes, 2-Nitrogen Gas Inlets, 3-Gas Outlets, 4-Ciculation Tubes, 5-Syringe, 6-Ion Exchange Membranes, Nafion N324, 7- Graphite Felt Cathode, 8-Tinned SS316 Mesh Holder, 9-Sulfuric Acid Solution, 10- Cr(III) Solution)

The electrochemical experiments were carried out in a three-compartment cell made of acrylic plastics (two anode compartments and one cathode compartment). Nafion N324 cation permeable membrane (DuPont Inc.) was used to separate the catholyte and anolyte. The anode was lead-silver alloy electrode (1% Ag) and the cathode was a stationary graphite felt electrode with a thickness of 6 mm or 12 mm (CeraMaterials, USA).

Stainless steel mesh (SS 316) was used to fix the felt on two sides and conduct electricity to the graphite felt. Tin was electrochemically deposited on the mesh to inhibit the hydrogen evolution reactions; this was due to the low hydrogen overpotential of stainless steel. The tinned-stainless steel mesh surface was further painted except for the electrical contact parts. The working electrode compartment consisted of two blocks with an electrolyte inlet/outlet port on each, between which a graphite felt cathode assembly was

placed, enabling circulation of electrolyte solution through the working electrode to enhance mass transport. The circulation rate of the electrolyte was 170 mL/min controlled by the Masterflex pump. The superficial cathode surface area was 127.5 cm^2. The anode surface area was 22.5 cm^2 for each anode. The current density quoted in this work is referred to the cathode current density, which is based on the apparent geometric area.

3.2.3 Procedures

(1) Preparation of Cr(III)-MSA Electrolytes

Lead(II) oxide was first dissolved in MSA solution to form $Pb(CH_3SO_3)_2$. Calculated potassium chromium sulfate was then added to the $Pb(CH_3SO_3)_2$ solution to precipitate sulfate ions. The $PbSO_4$ precipitates were then filtrated to get Cr(III)-MSA electrolyte. The reactions involved are shown as **Equation 3.1** and **Equation 3.2**.

$$PbO + 2CH_3SO_3H \rightarrow Pb(CH_3SO_3)_2 + H_2O \qquad \textbf{Equation 3.1}$$

$$2Pb(CH_3SO_3)_2 + KCr(SO_4)_2 \rightarrow KCr(CH_3SO_3)_4 + 2PbSO_4 \qquad \textbf{Equation 3.2}$$

(2) Treatment of Graphite Felts

To explore the effect of graphite felt surface condition on the electrochemical reduction, treatment of the graphite felts was needed. There are several ways to treat the felt, which has been described in **Section 2.2.3**. In this research, the graphite felts were treated with 98% concentrated sulfuric acid at 450 ℃ for 5 hours according to Sun`s investigation. This treatment can increase the functional groups and reactive areas on the graphite felt surface[58]. After the acid treatment, the graphite felts were washed thoroughly with deionized water and then dried at 80 ℃ for 24 hours.

(3) Electrochemical Reduction Tests

The experimental procedure consisted of the following steps:

1) 550 mL chromium(III) catholytes and 1200 mL sulfuric acid anolytes were added into the cathode compartment and two anode compartments separately.

2) Before each experiment, the catholyte was purged with nitrogen for at least half an hour to desorb any dissolved oxygen.

3) The current through the electrochemical reduction cell was pre-determined by the desired current density. A multimeter and a standard resistor (5 A, 100 mV) were used to ensure that the value of the current flowing through the two anodes was the same. Same anode current density can maintain the same potentials on the two sides of the graphite felt.

4) Samples of about 4 mL solution were withdrawn with a syringe at predetermined intervals. For the current density of 40 A/m^2, samples were withdrawn at 0 min, 60 min, 120 min, 160 min, 180 min and 210 min. For the current density of 80 A/m^2, samples were withdrawn at 0 min, 30 min, 60 min, 80 min, 90 min and 105 min. For the current density of 160 A/m^2, samples were withdrawn at 0 min, 15 min, 30 min, 40 min, 45 min and 52.5 min. In the 0.3 M H_2SO_4 system, samples were withdrawn at 0 min, 15 min, 30 min, 40 min, 45 min, 52.5 min, 60 mins and 67.5 min. In the 0.5 M H_2SO_4 system, samples were withdrawn at 0 min, 15 min, 30 min, 40 min, 45 min, 60 min, 75 min, 90 min, 105 min and 120 min. Some samples were withdrawn at specific intervals if necessary.

5) The samples were measured with a UV-Vis spectrometer immediately after withdrawal from the reactor to determine the concentration of chromium(III) ions.

3.2.4 Analytical Methods

A Perkin Elmer Lambda 35 UV-Vis spectrometer was used to measure the aqueous chromium(III) absorption, and to determine the concentration of chromium(III) and thus to calculate the current efficiency and chromium(III) conversion. The calibration curves in the chloride, sulfate and MSA systems are shown in **Appendix B**.

3.2.5 Evaluation Factors

Current efficiency and chromium(III) conversion are two key factors to evaluate the electrochemical reduction process. **Equation 3.3** is used to calculate the current efficiency and **Equation 3.4** is used to calculate the chromium(III) conversion.

$$\text{Current Efficiency} = \frac{\left([\text{Cr(III)}]_{\text{Initial}} - [\text{Cr(III)}]_{\text{Final}}\right) \cdot V \cdot F \cdot n}{I \cdot t} \qquad \textbf{Equation 3.3}$$

$$\text{Conversion} = \frac{[\text{Cr(III)}]_{\text{Initial}} - [\text{Cr(III)}]_{\text{Final}}}{[\text{Cr(III)}]_{\text{Initial}}} \qquad \textbf{Equation 3.4}$$

(I is the current (A), t is the reaction time (s), V is the solution volume (L), F is the Faraday constant (96485 C mol^{-1}), n is the number of moles of electrons passed for a half reaction, [ ] is the molarity concentration (mol/L). See **Nomenclature** for detail.)

3.3 UV-vis Spectra for Cr(III) Electrochemical Reduction

3.3.1 UV-vis Spectra for Cr(III) Electrochemical Reduction in the Chloride System

In the chloride system, the cathode and anode reactions are described as **Equation 2.1** and **Equation 2.4**. The total reaction is expressed as **Equation 3.5**.

Cathode	$Cr^{3+} + e^{-} \rightarrow Cr^{2+}$	**Equation 2.1**
Anode	$2H_2O \rightarrow O_2 + 4H^{+} + 4e^{-}$	**Equation 2.4**
Total	$4CrCl_3 + 2H_2O \rightarrow 4CrCl_2 + O_2 + 4HCl$	**Equation 3.5**

The reduction process is illustrated in **Figure 3.4**. The color of the solution was changing from green to blue. Chromium(III) in the chloride system has a maximum absorbance at 428 nm. The peak at around 610 nm was influenced by the absorbance of Cr(II) ions, which has a maximum absorbance at 714 nm[3]. Therefore, the wavelength of 428 nm was used to determine the concentration of Cr(III) and to track the reaction process in the chloride system.

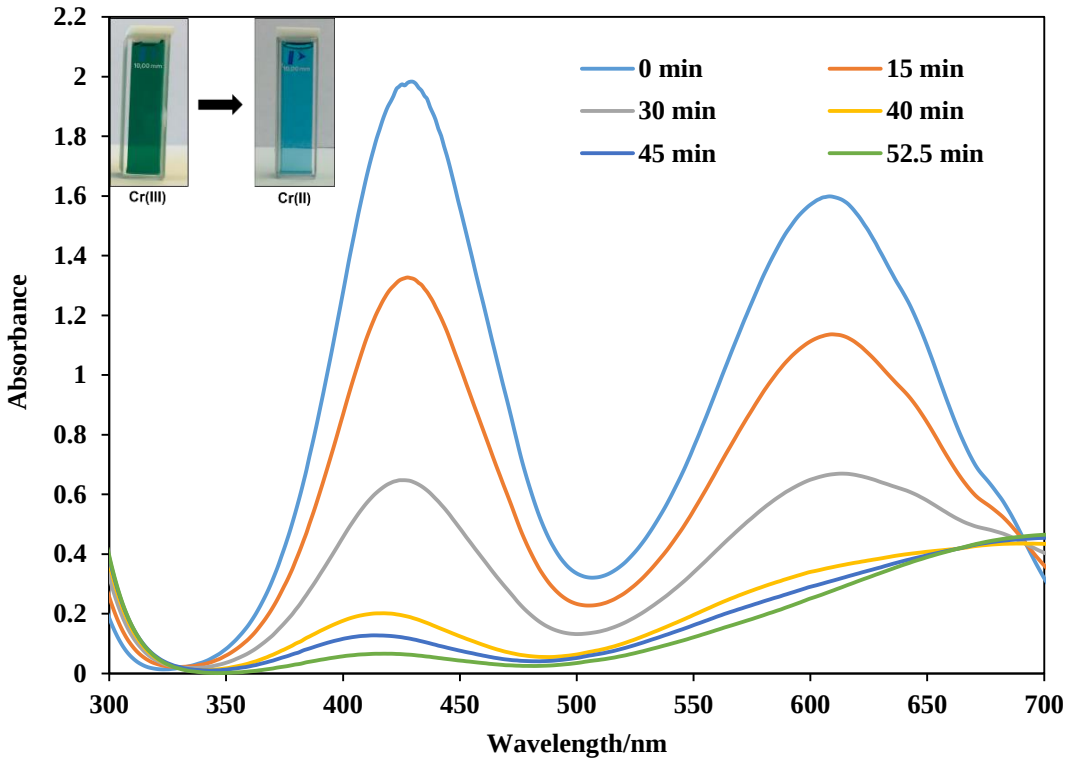

Figure 3.4 UV-vis spectra for Cr(III) reduction in the chloride system

(0.1 M Cr(III), 0.2 M HCl, 6 mm untreated graphite felt, cathode current density=160 A/m^2)

With the ongoing electrochemical reduction, the absorbance at around 428 nm was observed to be decreasing, indicating that Cr(III) ions were being reduced. The other absorbance at around 610 nm was decreasing and the shape was changing with reaction time, which is due to the appearance of Cr(II).

3.3.2 UV-vis Spectra for Cr(III) Electrochemical Reduction in the Sulfate System

In the sulfate system, the cathode and anode reactions are described as **Equation 2.1** and **Equation 2.4**. The total reaction is expressed as **Equation 3.6**.

Cathode $Cr^{3+} + e^{-} \rightarrow Cr^{2+}$ **Equation 2.1**

Anode $2H_2O \rightarrow O_2 + 4H^{+} + 4e^{-}$ **Equation 2.4**

Total $4KCr(SO_4)_2 + 2H_2O \rightarrow 4CrSO_4 + O_2 + 2H_2SO_4 + 2K_2SO_4$ **Equation 3.6**

The reduction process is illustrated in **Figure 3.5**. The color of the solution was changing from purple to blue. Chromium(III) in the sulfate system has a maximum absorbance at 407.5 nm. The peak at around 575 nm was influenced by the absorbance of Cr(II) ions, which has a maximum absorbance at 714 nm[3]. Therefore, the wavelength of 407.5 nm was used to determine the concentration of Cr(III) and to track the reaction process in the sulfate system.

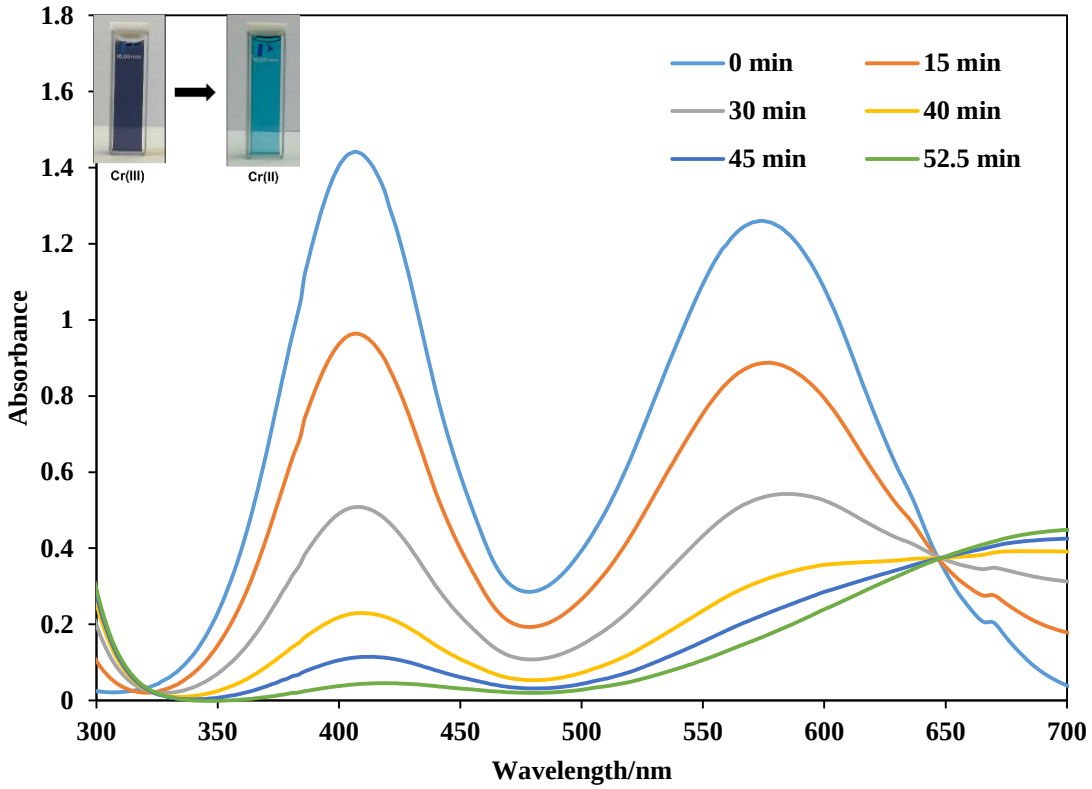

Figure 3.5 UV-vis spectra for Cr(III) reduction in the sulfate system

(0.1 M Cr(III), 0.1 M H_2SO_4, 6 mm untreated graphite felt, cathode current density=160 A/m^2)

The absorbance at around 407.5 nm was seen to be decreasing with the reaction time, which indicated that Cr(III) ions were being electrochemically reduced. Similar to the chloride system, the peak shape at around 575 nm was also changing with reaction time. This is because of the absorbance influence of Cr(II).

3.3.3 UV-vis Spectra for Cr(III) Electrochemical Reduction in the MSA system

In the MSA system, the cathode and anode reaction are described as **Equation 2.1** and **Equation 2.4**. The total reaction is expressed as **Equation 3.7**.

Cathode $Cr^{3+} + e^{-} \rightarrow Cr^{2+}$ **Equation 2.1**

Anode $2H_2O \rightarrow O_2 + 4H^{+} + 4e^{-}$ **Equation 2.4**

Total $4KCr(CH_3SO_3)_4 + 2H_2O \rightarrow 4Cr(CH_3SO_3)_2 + O_2 + 4CH_3SO_3H + 4KCH_3SO_3$

Equation 3.7

The reduction process is presented in **Figure 3.6**. The color of the solution is also changing from purple to blue. Chromium(III) in the MSA system has a maximum absorbance at 407.5 nm; the same as with the sulfate system.

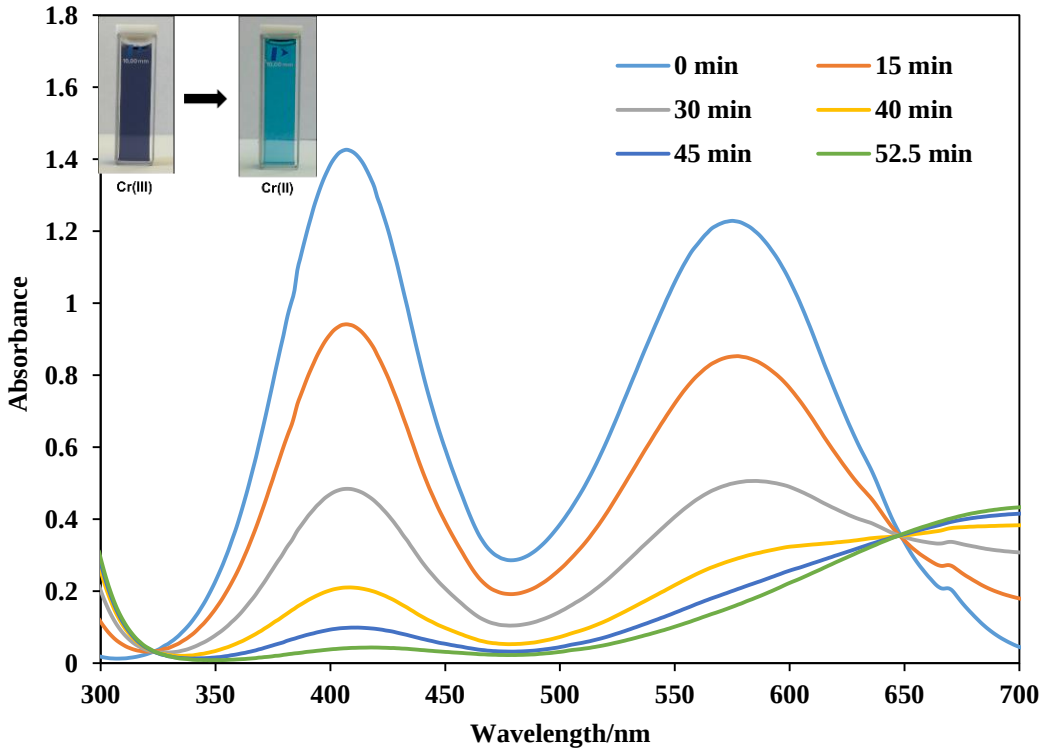

Figure 3.6 UV-vis spectra for Cr(III) reduction in the MSA system

(0.1 M Cr(III), 0.2 M MSA, 6 mm untreated graphite felt, cathode current density=160 A/m^2)

Much like the spectra in the sulfate system, the absorbance at around 407.5 nm was decreasing with the reaction time, indicating that the Cr(III) ions were electrochemically reduced.

3.4 Electrochemical Reduction in Acidic Aqueous Systems

A number of experimental variables were studied in the chloride, sulfate and MSA system. All the experiments were performed under ambient conditions unless otherwise noted. Electrochemical tests were repeated four times for each variable to ensure the reproducibility.

3.4.1 Electrochemical Reduction in the Chloride System

Effect of Acid Concentration

The effect of acid concentration on the current efficiency and conversion in the chloride system was studied under the conditions shown in **Table 3.1**.

Table 3.1 Experimental conditions for the effect of acid concentration in the chloride system

Temperature	Room temperature
Graphite felt	Fresh/ untreated
Graphite felt thickness	6 mm
Cathode current density	160 A/m^2
Catholyte	0.1 M Fresh $CrCl_3$ + 0.2 M/0.6 M/1 M HCl
Anolyte	0.1 M/0.3 M/0.5 M H_2SO_4

It was found that decreasing hydrochloric acid concentration could slightly increase the current efficiency (See **Figure 3.7**). However, the effect of acid concentration on the reduction tests was modest. The current efficiency decreased rapidly after the

chromium(III) conversion reached 0.9. This is probably because the reduction process has reached its completion point and most of the chromium(III) ions are converted to chromium(II) ions; the hydrogen evolution reaction becomes the predominant reaction on the graphite felt, leading to low current efficiency for the chromium(III) reduction.

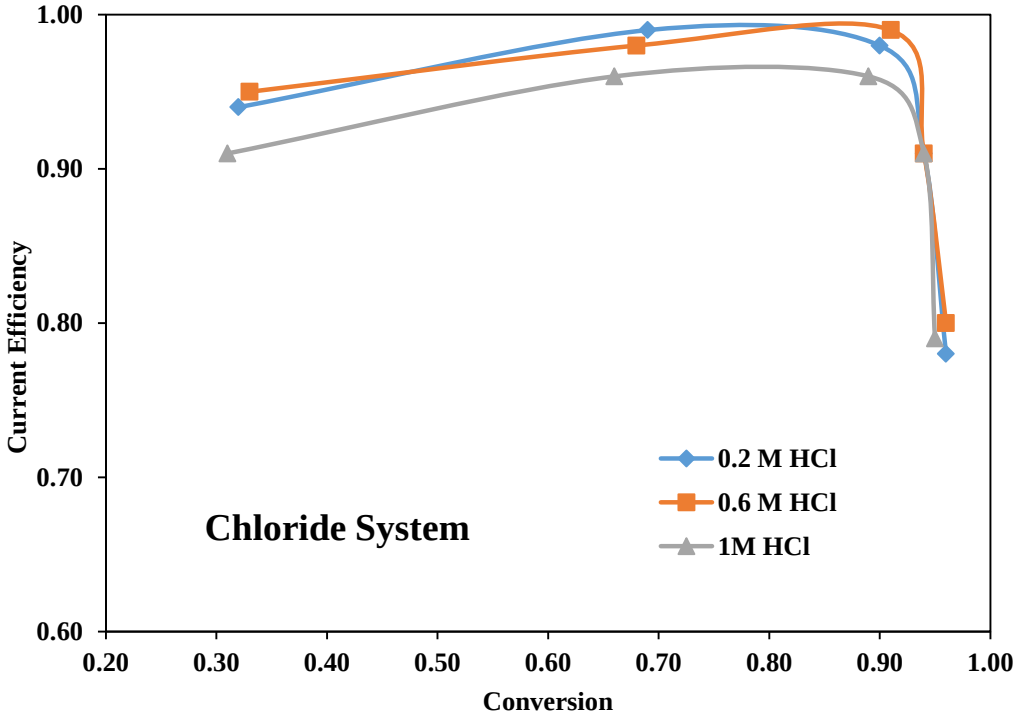

Figure 3.7 The effect of acid concentration in the chloride system

Starting with 0.1 M fresh Cr(III) solution and fresh untreated graphite felt, the current efficiency can reach 0.98, 0.99 and 0.96 with the conversion of 0.90 at the current density of 160 A/m^2 when the hydrochloric acid concentration increases from 0.2 M to 1 M.

Effect of Current Density

The effect of current density on the current efficiency and conversion in the chloride system was studied under the conditions shown in **Table 3.2**.

Table 3.2 Experimental conditions for the effect of current density in the chloride system

Temperature	Room temperature
Graphite felt	Fresh/ untreated
Graphite felt thickness	6 mm
Catholyte	0.1 M Fresh $CrCl_3$ + 0.2 M HCl
Anolyte	0.1 M H_2SO_4
Cathode current density	40/80/160 A/m^2

It was initially found that lower current density could lead to high current efficiency, but due to the ongoing reduction of Cr(III), the effect became less obvious (See **Figure 3.8)**. The current efficiencies were almost the same when the conversions ranged from 0.7 to 0.9.

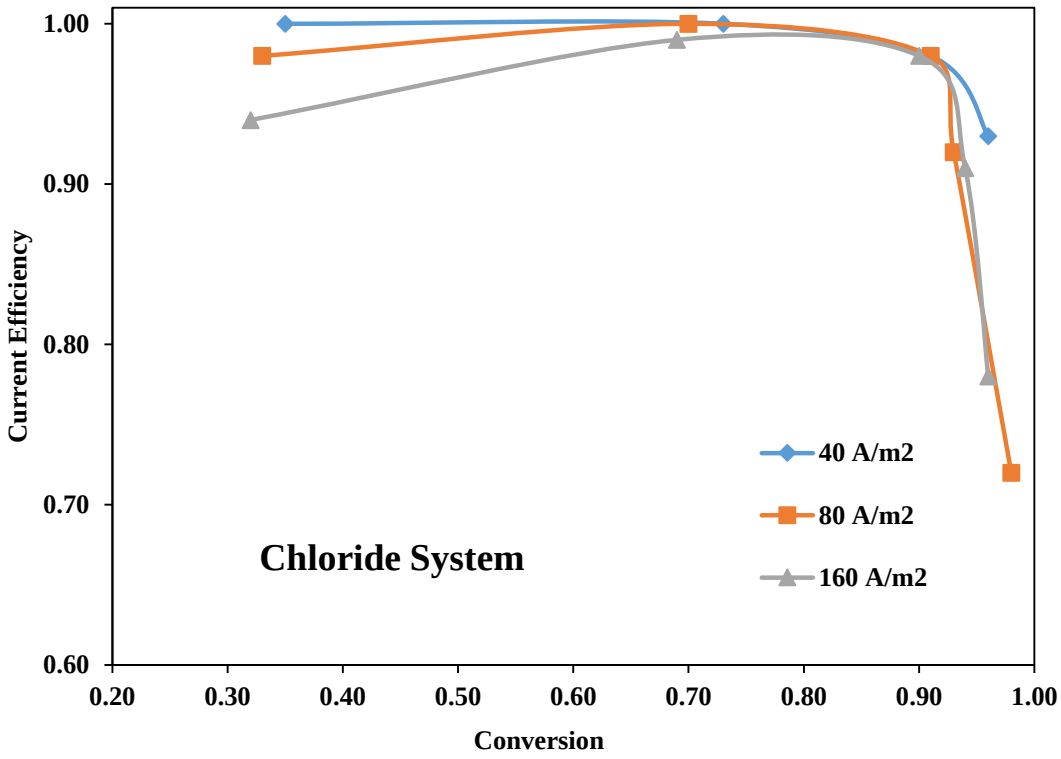

Figure 3.8 The effect of current density in the chloride system

Starting with 0.1 M fresh Cr(III) solution + 0.2 M hydrochloric acid, the current efficiency can reach 0.99, 0.99 and 0.98 with the conversion of 0.90 at the current density of 40 A/m^2, 80 A/m^2 and 160 A/m^2 respectively.

Effect of Graphite Felt Thickness

The effect of graphite felt thickness on the current efficiency and conversion in the chloride system was studied under the conditions shown in **Table 3.3**.

Table 3.3 Experimental conditions for the effect of graphite felt thickness in the chloride system

Temperature	Room temperature
Graphite felt	Fresh/ untreated
Catholyte	0.1 M Fresh $CrCl_3$ + 0.2 M HCl
Anolyte	0.1 M H_2SO_4
Cathode current density	160 A/m^2
Graphite felt thickness	6 mm/12 mm

It was found that increasing graphite felt thickness could increase the current efficiency (See **Figure 3.9)**. This is mainly caused by the fact that thicker graphite felts have larger effective surface areas, and thus chromium(III) ions have more active sites to get electrons to reduce, leading to better current efficiency.

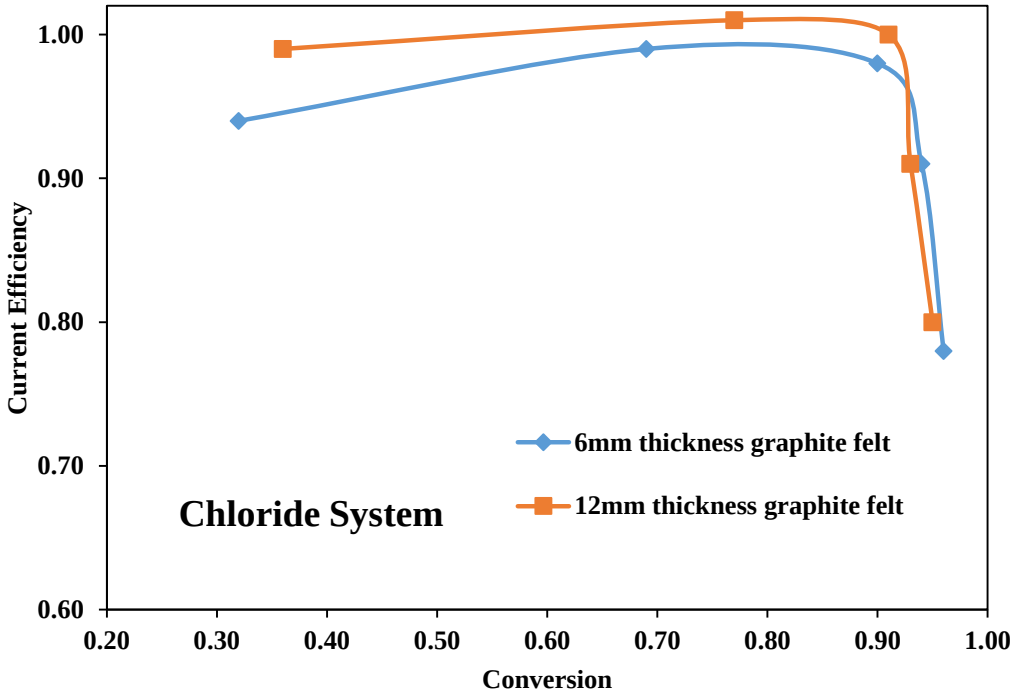

Figure 3.9 The effect of graphite felt thickness in the chloride system

Starting with 0.1 M Fresh Cr(III) solution + 0.2 M hydrochloric acid, the current efficiency can reach 0.98 and 1.00 with the conversion of 0.90 at the current density of 160 A/m^2 for 6 mm and 12 mm thick graphite felt respectively.

Effect of Graphite Felt Surface Condition

The effect of graphite felt surface condition on the current efficiency and conversion in the chloride system was studied under the conditions shown in **Table 3.4**.

Table 3.4 Experimental conditions for the effect of graphite felt surface condition in the chloride system

Temperature	Room temperature
Catholyte	0.1 M Fresh $CrCl_3$ + 0.2 M HCl
Anolyte	0.1 M H_2SO_4
Cathode current density	160 A/m^2
Graphite felt thickness	6 mm
Graphite felt	Fresh untreated/ Acid treated

It was found that graphite felt treated with concentrated sulfuric acid showed better electrochemical reduction results marked by an increase in current efficiency (See **Figure 3.10)**. The main reason for this is that after the mild oxidation of the graphite felt by concentrated sulfuric acid, the effective surface areas of the graphite felt increases. This allows the formation of functional groups in its surface, making the graphite felt more hydrophilic[58]. Therefore, the electrochemical activity of the graphite felt is enhanced.

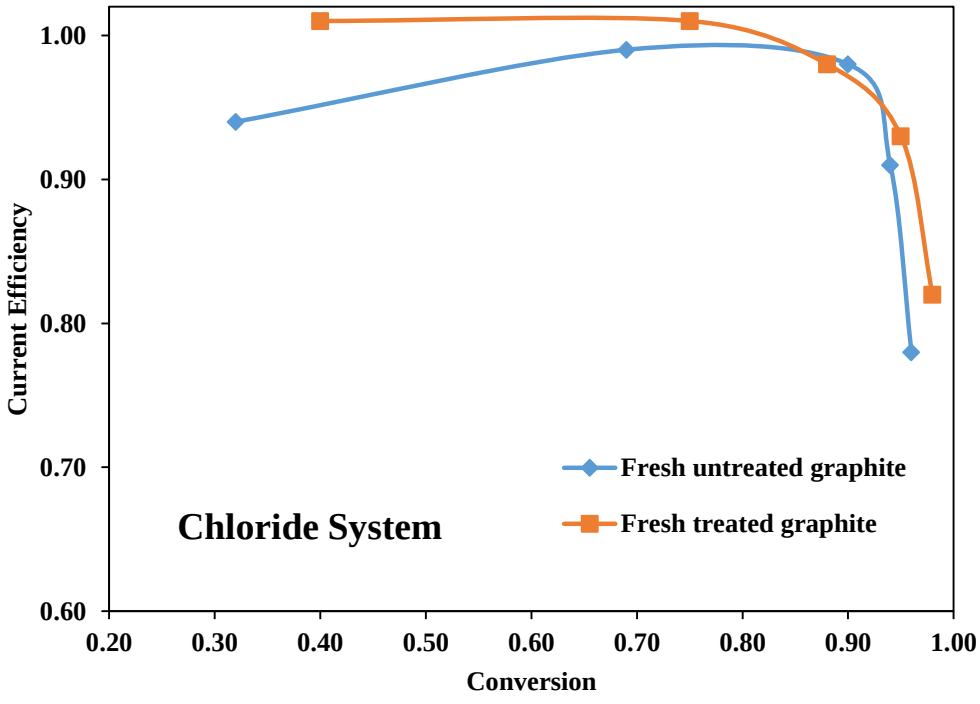

Figure 3.10 The effect of graphite felt surface condition in the chloride system

Starting with 0.1 M fresh Cr(III) solution + 0.2 M hydrochloric acid, the current efficiency can reach 0.98 and 0.97 with the conversion of 0.90 at the current density of 160 A/m^2 for the untreated and treated graphite felt. Generally, treated graphite felt can increase the current efficiency, but the increase is modest in the chloride system.

Effect of Graphite Felt Usage Frequency

The effect of graphite felt usage frequency on the current efficiency and conversion in the chloride system was studied under the conditions shown in **Table 3.5**.

Table 3.5 Experimental conditions for the effect of graphite felt usage frequency in the chloride system

Temperature	Room temperature
Catholyte	0.1 M Fresh $CrCl_3$ + 0.2 M HCl
Anolyte	0.1 M H_2SO_4
Cathode current density	160 A/m^2
Graphite felt thickness	6 mm
Graphite felt	Untreated

It was found that in the chloride system, the electrochemical reduction current efficiency decreased very slightly with an increase in the number of times the graphite felt was used (See **Figure 3.11**). However, generally speaking, the current efficiency remained almost the same (the decrease is significantly small) even if the graphite felt was used several times.

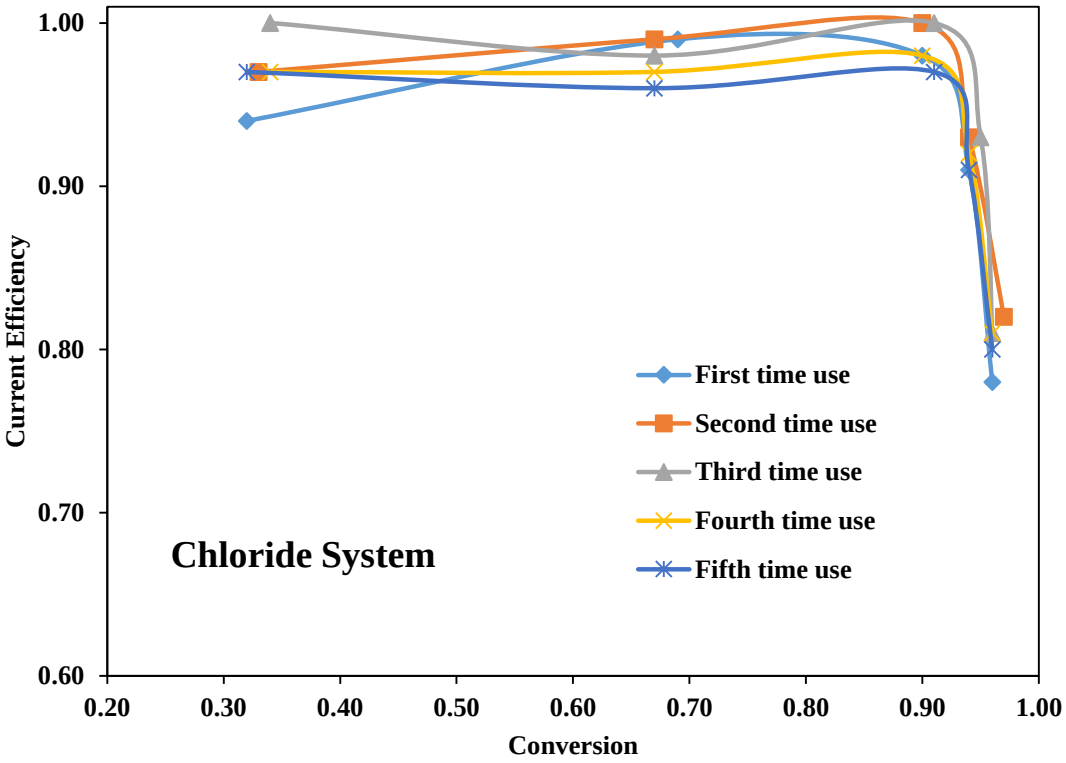

Figure 3.11 The effect of graphite felt usage frequency in the chloride system

3.4.2 Electrochemical Reduction in the Sulfate System

Effect of Acid Concentration

The effect of acid concentration on the current efficiency and conversion in the sulfate system was studied under the conditions shown in **Table 3.6**.

Table 3.6 Experimental conditions for the effect of acid concentration in the sulfate system

Temperature	Room temperature
Graphite felt	Fresh/untreated
Graphite felt thickness	6 mm
Cathode current density	160 A/m^2
Catholyte	0.1 M Fresh $KCr(SO_4)_2$ + 0.1 M/0.3 M/0.5 M H_2SO_4
Anolyte	0.1 M/0.3 M/0.5 M H_2SO_4

It was observed that decreasing sulfuric acid concentration could increase the current efficiency significantly (See **Figure 3.12)**. Unlike in the chloride system, acid concentration had an obvious influence on the current efficiency. Additionally, with the ongoing reduction process, the current efficiencies decreased faster in high acidity systems than that in low acidity systems.

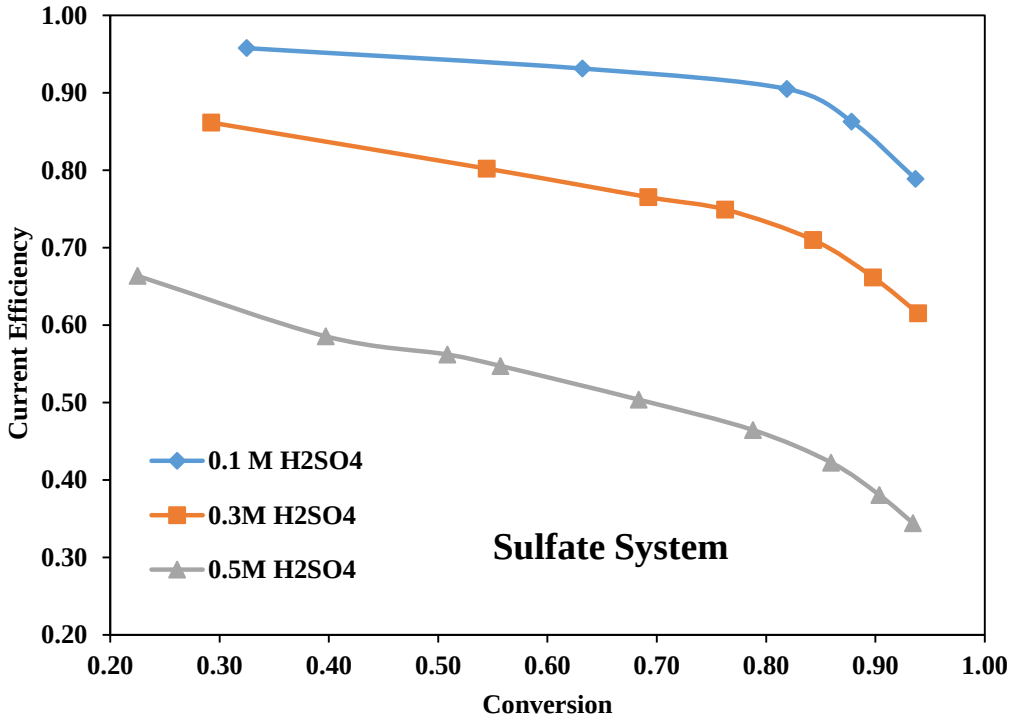

Figure 3.12 The effect of acid concentration in the sulfate system

Starting with 0.1 M fresh Cr(III) solution and fresh untreated graphite felt, the current efficiency can reach 0.84, 0.66 and 0.38 with the conversion of 0.90 at the current density of 160 A/m^2 when the sulfuric acid concentration increases from 0.1 M to 0.5 M.

Effect of Current Density

The effect of current density on the current efficiency and conversion in the sulfate system was studied under the conditions shown in **Table 3.7**.

Table 3.7 Experimental conditions for the effect of current density in the sulfate system

Temperature	Room temperature
Graphite felt	Fresh/untreated
Graphite felt thickness	6 mm
Catholyte	0.1 M Fresh $KCr(SO_4)_2$ + 0.1 M H_2SO_4
Anolyte	0.1 M H_2SO_4
Cathode current density	40/80/160 A/m^2

It was found that higher current density could lead to lower current efficiency (See **Figure 3.13)**. This effect was not very obvious at low conversions, but was more apparent when the conversion increased.

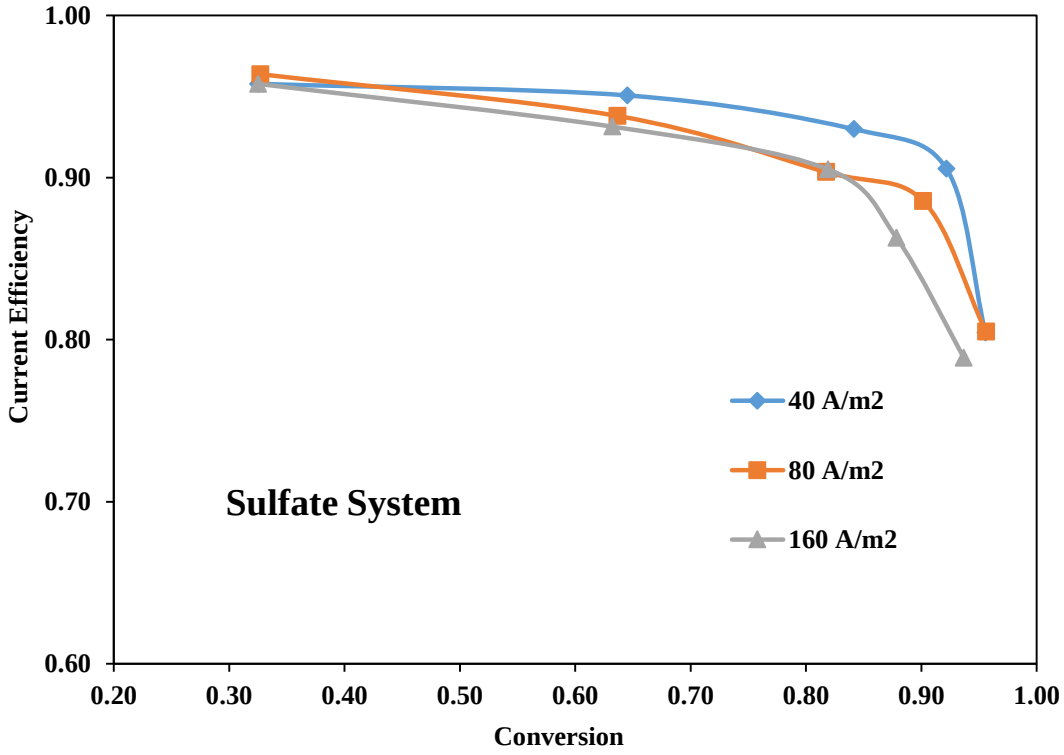

Figure 3.13 The effect of current density in the sulfate system

Starting with 0.1 M fresh Cr(III) solution + 0.1 M sulfuric acid, the current efficiency can reach 0.92, 0.89 and 0.84 with the conversion of 0.90 at the current density of 40 A/m^2, 80 A/m^2 and 160 A/m^2 respectively.

Effect of Graphite Felt Thickness

The effect of graphite felt thickness on the current efficiency and conversion in the sulfate system was studied under the conditions shown in **Table 3.8**.

Table 3.8 Experimental conditions for the effect of graphite felt thickness in the sulfate system

Temperature	Room temperature
Graphite felt	Fresh/untreated
Catholyte	0.1 M Fresh $KCr(SO_4)_2$ + 0.1 M H_2SO_4
Anolyte	0.1 M H_2SO_4
Cathode current density	160 A/m^2
Graphite felt thickness	6 mm/12 mm

Much like in the chloride system, it was observed that increasing graphite felt thickness could increase the current efficiency. The increase of the current efficiency due to the increased thickness of the graphite felt in the sulfate system was more obvious than that of the chloride system (See **Figure 3.14)**.

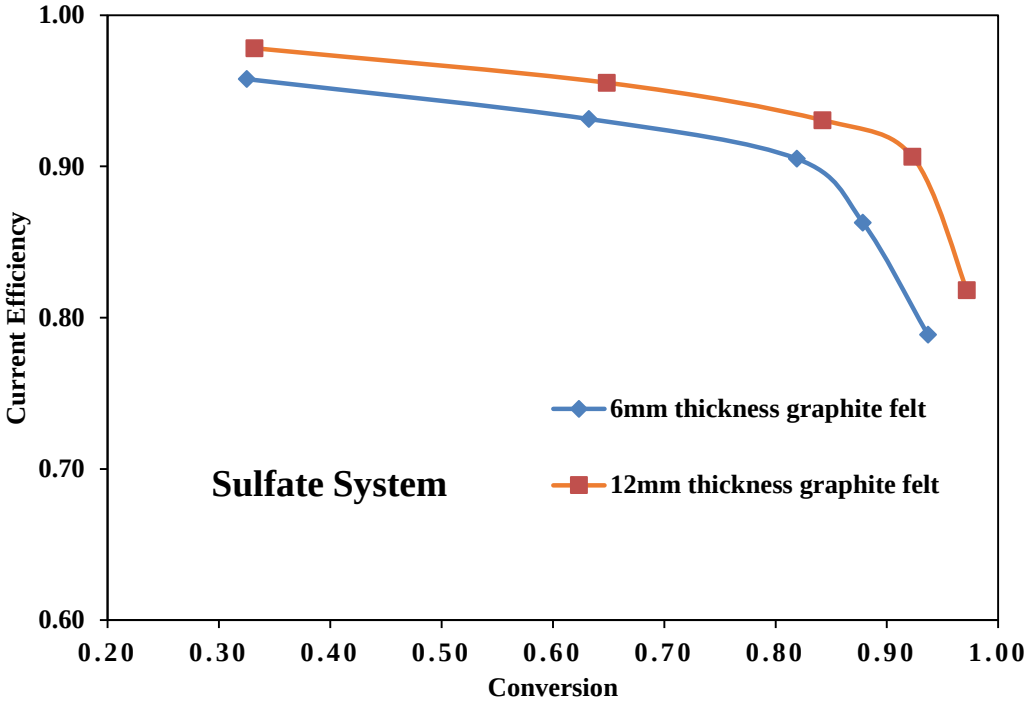

Figure 3.14 The effect of graphite felt thickness in the sulfate system

Starting with 0.1 M fresh Cr(III) solution + 0.1 M sulfuric acid, the current efficiency can reach 0.84 and 0.92 with the conversion of 0.90 at the current density of 160 A/m^2 for 6 mm and 12 mm thick graphite felt respectively.

Effect of Graphite Felt Surface Condition

The effect of graphite felt surface condition on the current efficiency and conversion in the sulfate system was studied under the conditions shown in **Table 3.9**.

Table 3.9 Experimental conditions for the effect of graphite felt surface condition in the sulfate system

Temperature	Room temperature
Catholyte	0.1 M Fresh $KCr(SO_4)_2$ + 0.1 M H_2SO_4
Anolyte	0.1 M H_2SO_4
Cathode current density	160 A/m^2
Graphite felt thickness	6 mm
Graphite felt	Fresh untreated/ Acid treated

Similar to the chloride system, it was found that the felt treated with concentrated sulfuric acid displayed better electrochemical reduction results, especially in the region of high conversions (See **Figure 3.15**).

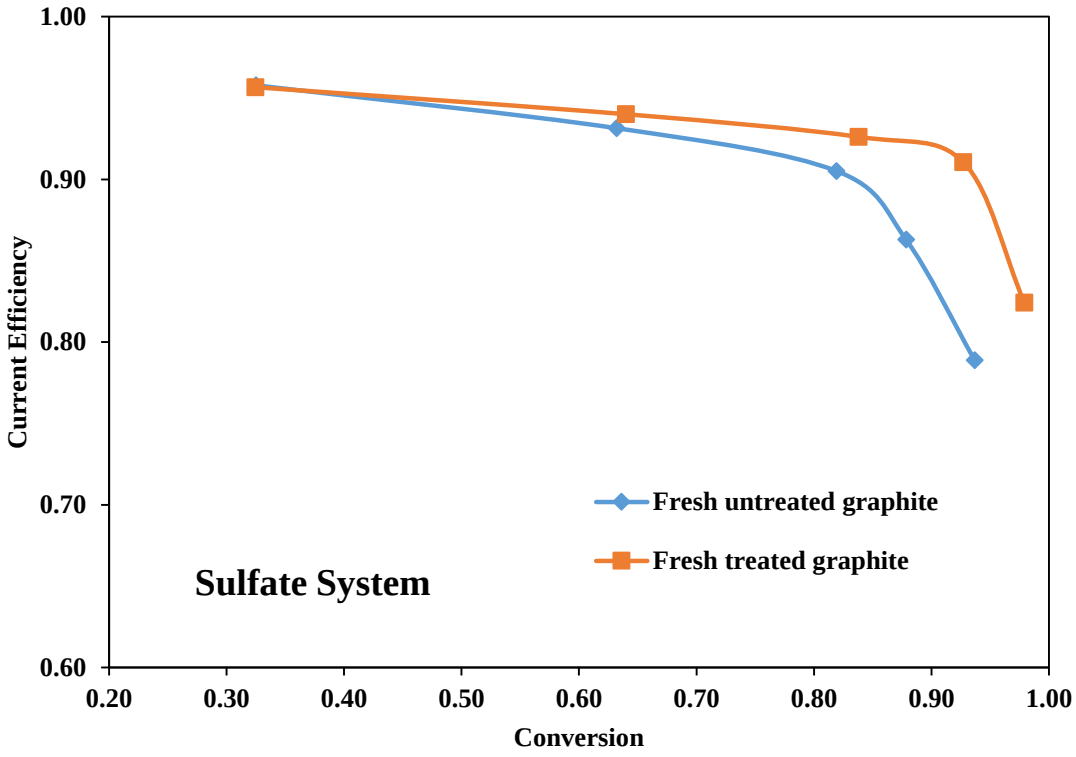

Figure 3.15 The effect of graphite felt surface condition in the sulfate system

Starting with 0.1 M fresh Cr(III) solution + 0.1 M sulfuric acid, the current efficiency can reach 0.84 and 0.92 with the conversion of 0.90 at the current density of 160 A/m^2 for the untreated and acid treated graphite felt.

Effect of Graphite Felt Usage Frequency

The effect of graphite felt usage frequency on the current efficiency and conversion in the sulfate system was studied under the conditions shown in **Table 3.10**.

Table 3.10 Experimental conditions for the effect of graphite felt usage frequency in the sulfate system

Temperature	Room temperature
Catholyte	0.1 M Fresh $KCr(SO_4)_2$ + 0.1 M H_2SO_4
Anolyte	0.1 M H_2SO_4
Cathode current density	160 A/m^2
Graphite felt thickness	6 mm
Graphite felt	Untreated

It was found that in the sulfate system, the electrochemical reduction current efficiency decreased rapidly with an increase in the number of times the graphite felt used. This is significantly different from the chloride system (See **Figure 3.16**). The more times the graphite felt used, the lower the current efficiency, which indicates that the lifetime of the graphite felt for chromium(III) reduction in the sulfate system is short.

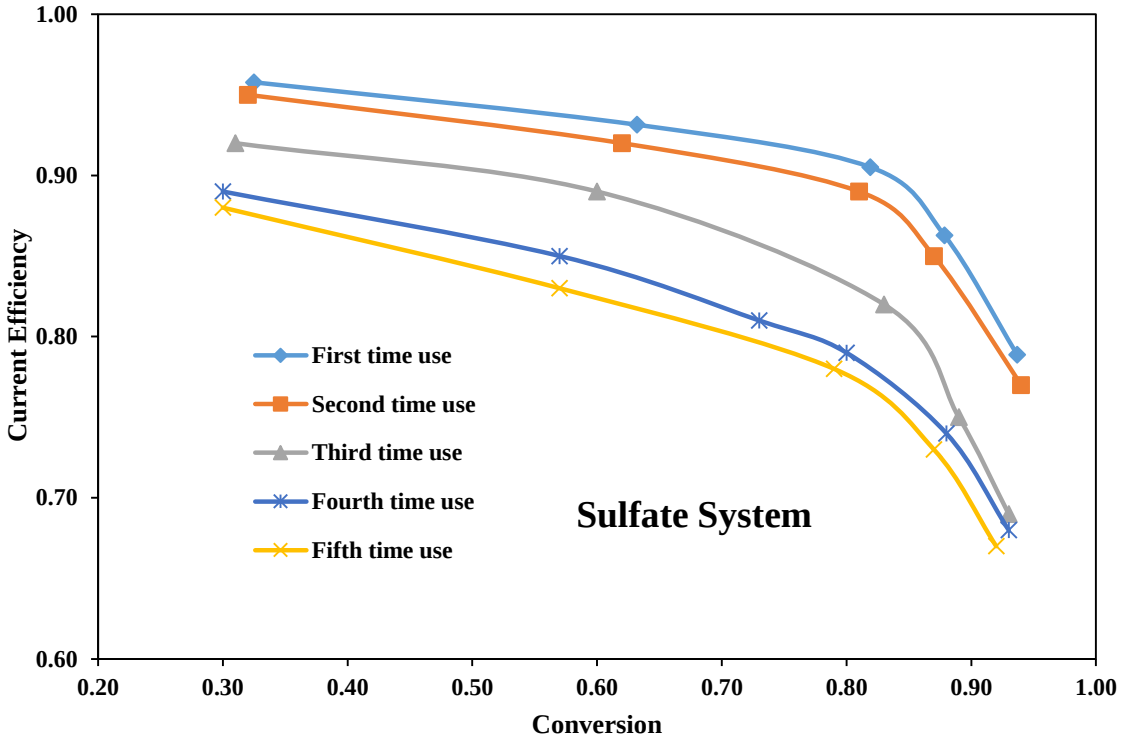

Figure 3.16 The effect of graphite felt usage frequency in the sulfate system

3.4.3 Electrochemical Reduction in the MSA System

Effect of Acid Concentration

The effect of acid concentration on the current efficiency and conversion in the MSA system was studied under the conditions shown in **Table 3.11**.

Table 3.11 Experimental conditions for the effect of acid concentration in the MSA system

Temperature	Room temperature
Graphite felt	Fresh/untreated
Graphite felt thickness	6 mm
Cathode current density	160 A/m^2
Catholyte	0.1 M Fresh $KCr(CH_3SO_3)_4$ + 0.2 M/0.6 M/1 M MSA
Anolyte	0.1 M/0.3 M/0.5 M H_2SO_4

It was found that acid concentration had a slight effect on the current efficiency (See **Figure 3.17**). Decreasing MSA concentration could increase the current efficiency, but the increase was smaller than that of the sulfate system. Generally, the effect of acid concentration on the MSA system was in between the sulfate and the chloride system.

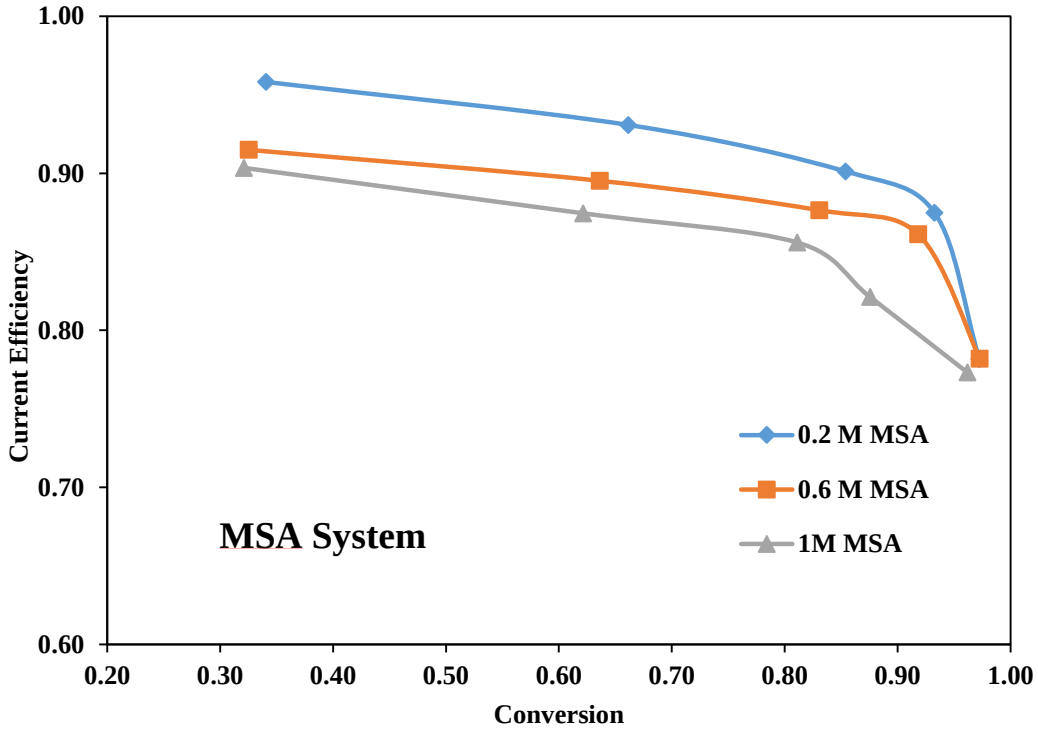

Figure 3.17 The effect of acid concentration effect in the MSA system

Starting with 0.1 M fresh Cr(III) solution and fresh untreated graphite felt, the current efficiency can reach 0.89, 0.87 and 0.81 with the conversion of 0.90 at the current density of 160 A/m^2 when the MSA concentrations increases from 0.2 M to 1 M.

Effect of Current Density

The effect of current density on the current efficiency and conversion in the MSA system was studied under the conditions shown in **Table 3.12**.

Table 3.12 Experimental conditions for the effect of current density in the MSA system

Temperature	Room temperature
Graphite felt	Fresh/untreated
Graphite felt thickness	6 mm
Catholyte	0.1 M Fresh $KCr(CH_3SO_3)_4$ + 0.2 M MSA
Anolyte	0.1 M H_2SO_4
Cathode current density	40/80/160 A/m^2

It was found that the current efficiency at 160 A/m^2 was slightly higher than that at 40 A/m^2 and 80 A/m^2. As the conversion increased, the differences between the current efficiencies at different current densities diminished (See **Figure 3.18**). This is probably due to the increase of reaction kinetics of hydrogen evolution and Cr(III) reduction at current density of 160 A/m^2. However, with an increase of current density, kinetics of Cr(III) reduction increases at a greater rate than that of hydrogen evolution. Therefore, hydrogen evolution becomes kinetically inhibited by Cr(III) reduction.

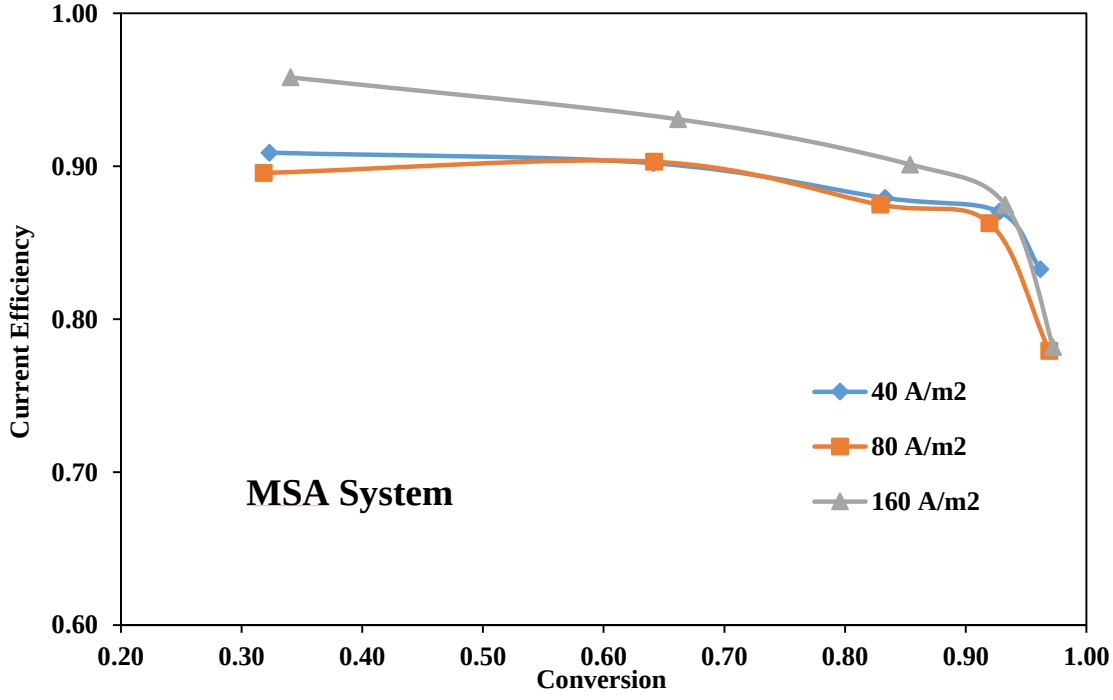

Figure 3.18 The effect of current density in the MSA system

Starting with 0.1 M fresh Cr(III) solution + 0.2 M MSA, the current efficiency can reach 0.88, 0.87 and 0.89 with the conversion of 0.90 at the current density of 40 A/m^2, 80 A/m^2 and 160 A/m^2 respectively.

Effect of Graphite Felt Thickness

The effect of graphite felt thickness on the current efficiency and conversion in the MSA system was studied under the conditions shown in **Table 3.13**.

Table 3.13 Experimental conditions for the effect of graphite felt thickness in the MSA system

Temperature	Room temperature
Graphite felt	Fresh/ untreated
Catholyte	0.1 M Fresh $KCr(CH_3SO_3)_4$ + 0.2 M MSA
Anolyte	0.1 M H_2SO_4
Cathode current density	160 A/m^2
Graphite felt thickness	6 mm/12 mm

Similar to the chloride system and the sulfate system, it was found that increasing graphite felt thickness could increase the current efficiency (See **Figure 3.19**).

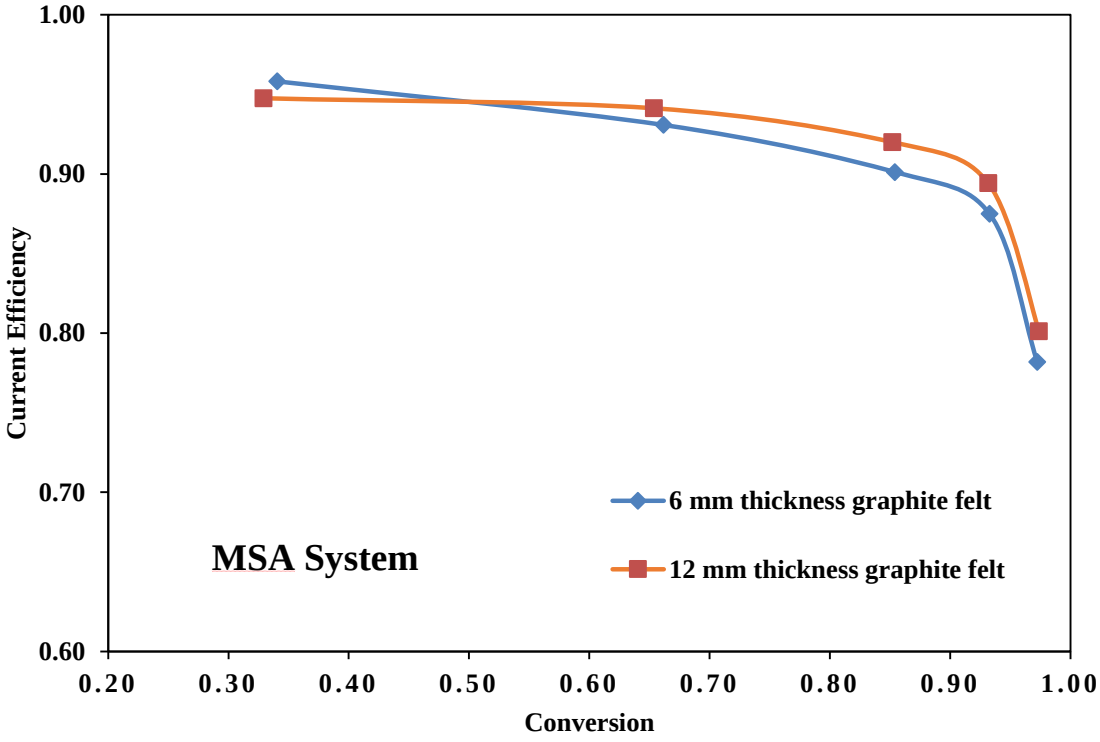

Figure 3.19 The effect of graphite felt thickness in the MSA system

Starting with 0.1 M Cr(III) solution + 0.2 M MSA, the current efficiency can reach 0.89 and 0.91 with the conversion of 0.90 at the current density of 160 A/m^2 for 6 mm and 12 mm thick graphite felt respectively.

Effect of Graphite Felt Surface Condition

The effect of graphite felt surface condition on the current efficiency and conversion in the MSA system was studied under the conditions shown in **Table 3.14**.

Table 3.14 Experimental conditions for the effect of graphite felt surface condition in the MSA system

Temperature	Room temperature
Catholyte	0.1 M Fresh $KCr(CH_3SO_3)_4$ + 0.2 M MSA
Anolyte	0.1 M H_2SO_4
Cathode current density	160 A/m^2
Graphite felt thickness	6 mm
Graphite felt	Fresh untreated/ Acid treated

It was found that graphite felt treated with concentrated sulfuric acid could increase the current efficiency, but the increase was less obvious in the MSA as compared to sulfate and chloride systems (See **Figure 3.20**).

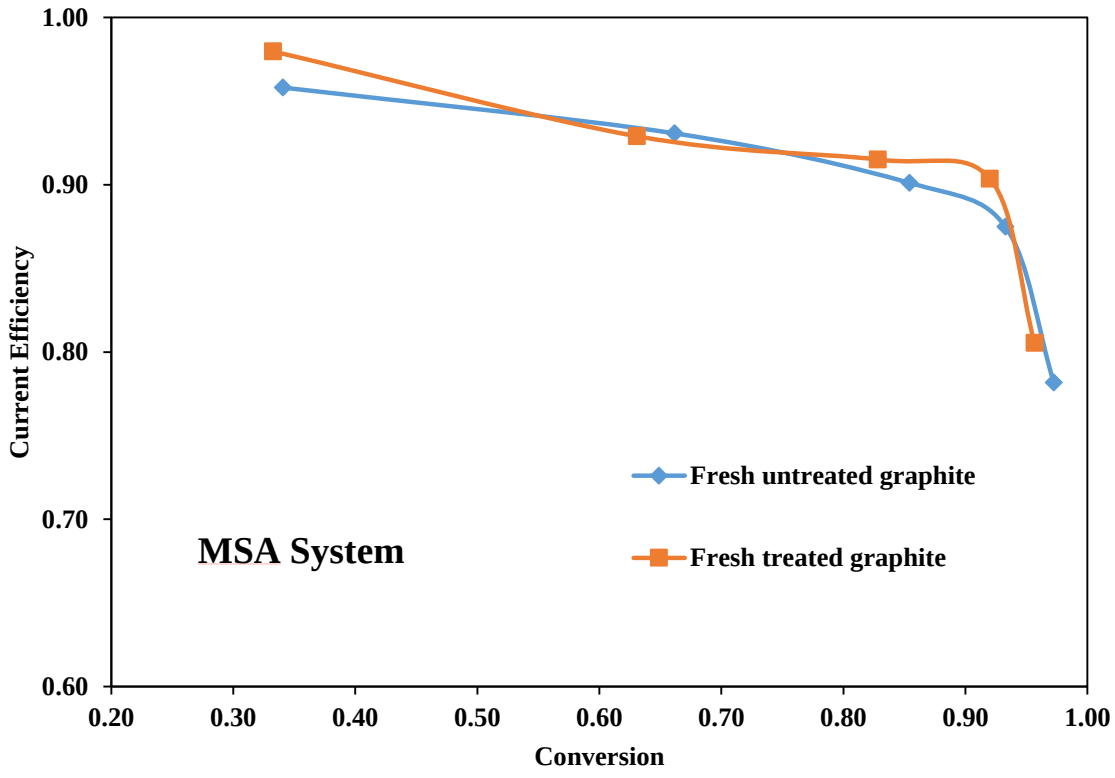

Figure 3.20 The effect of graphite felt surface condition in the MSA system

Starting with 0.1 M fresh Cr(III) solution + 0.2 M MSA acid, the current efficiency can reach 0.89 and 0.91 with the conversion of 0.90 at the current density of 160 A/m^2 for untreated and acid treated graphite felt.

Effect of Graphite Felt Usage Frequency

The effect of graphite felt usage frequency on the current efficiency and conversion in the MSA system was studied under the conditions shown in **Table 3.15**.

Table 3.15 Experimental conditions for the effect of graphite felt usage frequency in the MSA system

Temperature	Room temperature
Catholyte	0.1 M Fresh $KCr(CH_3SO_3)_4$ + 0.2 M MSA
Anolyte	0.1 M H_2SO_4
Cathode current density	160 A/m^2
Graphite felt thickness	6 mm
Graphite felt	Untreated

Similar to the sulfate system, it was found that in the MSA system, the electrochemical reduction current efficiency decreased gradually after every use, but the decrease was less rapid than that of the sulfate system (See **Figure 3.21**).

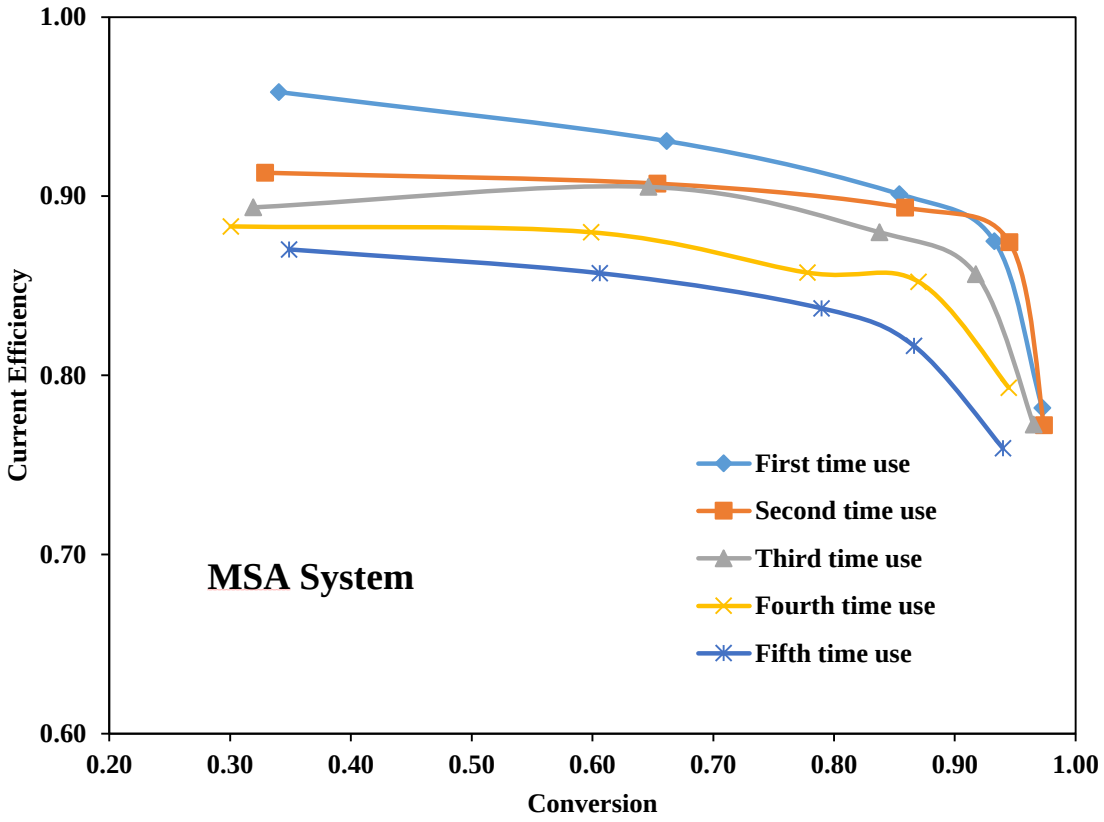

Figure 3.21 The effect of graphite felt usage frequency in the MSA system

3.5 Comparison and Discussion

(1) It was found that the current efficiency in the chloride system was the highest among all three acid systems. Sulfate systems yielded the lowest current efficiencies, while MSA systems were in between. However, the effect of acid concentration was more pronounced in the sulfate system, followed by the MSA system and the chloride system.

The reason for this difference is that chromium(III) in the chloride system is in the form of chromium chloride complex, $CrCl^{2+}$ and $CrCl_2^{+}$, while chromium(III) in the sulfate and MSA system is in the form of water complex ,$Cr(H_2O)_6^{3+}$ [3, 4]. The reduction of complex $CrCl^{2+}$ and $CrCl_2^{+}$ is via an inner-sphere pathway, while $Cr(H_2O)_6^{3+}$ is via an outer-sphere pathway[4]. With the inner-sphere pathway mechanism, the chloride ions are able to penetrate the outer Helmholtz plane and attach to the electrode, acting as a bridge between the electrode and the Cr(III) ions to enhance electron transfer. The more chloride ions complexed, the faster the kinetics[3]. It was reported that the rate constants for Cr(III) /Cr(II) couples decreased with increased aquation in the order $CrCl_3(aq) > CrCl_2^{+} > CrCl^{2+} > Cr(H_2O)_6^{3+}$[3]. Therefore, the chloride system shows better reduction kinetics and current efficiency than those in the sulfate and MSA system.

Although Cr(III) in the sulfate and MSA system is both in the form of $Cr(H_2O)_6^{3+}$, the reduction results in the MSA system were better than those in the sulfate system. This may be due to that the $–CH_3$ group in the MSA is larger than the –OH group in the H_2SO_4. The large methyl group may have an impediment effect on the hydrogen evolution reaction on the cathode, which probably increases the overpotential for the hydrogen generation.

(2) In all three systems, current density has a slight influence on the electrochemical reduction process. In both chloride and sulfate systems, lower current densities lead to better current efficiencies; however, for the MSA system, current density at 160 A/m^2 yielded higher current efficiencies than those at 40 A/m^2 and 80 A/m^2 which can be explained by the different reaction kinetics(See **Section 3.4.3.2**). In this research, the

theoretical reaction time to finish the electrochemical reduction was 2.95 hours for 40 A/m^2, 1.47 hours for 80 A/m^2 and 0.74 hours for 160 A/m^2 respectively. Therefore, although lower current density can achieve higher current efficiency in chloride and sulfate systems, current density of 160 A/m^2 is chosen for all three acid systems considering the reaction time in this research.

(3) It was observed that in all three acid systems, thicker graphite felt and acid treated graphite felt can provide better electrochemical reduction current efficiencies. The reason is provided in **Section 3.4.1.3** and **Section 3.4.1.4**. In consideration of the graphite felt costs and acid treatment costs/time, 6 mm untreated graphite felt is recommended for the electrochemical reduction in this research.

(4) In some tests, the current efficiency raised with conversion. This is probably due to the fact that when the graphite felt is freshly used, the graphite felt surface is not sufficiently activated or wetted. With the ongoing electrochemical reduction, the graphite felt is being gradually activated, becoming more hydrophilic. The change of surface condition from hydrophobic to hydrophilic can provide more reactive areas for Cr(III), and thus increase the current efficiency. This can also explain why the rise of current efficiency with conversion was not observed for the graphite felt treated by the concentrated sulfuric acid (See **Figure 3.10**).

(5) Graphite felts were observed to display a worse reduction result in the sulfate system and MSA system after initial and repeated use; however, no obvious change was found in the chloride system. The more the graphite felt was used, the worse the reduction results. This is probably due to the fact that after the graphite felt was used, the surface condition of the felt was changed. This is visually observed in **Figure 3.22**.

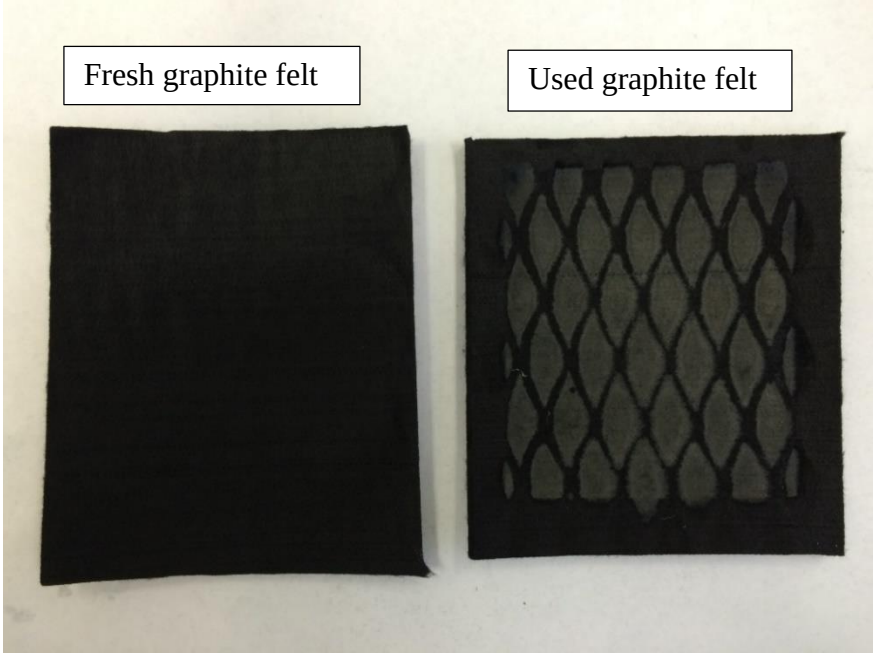

Figure 3.22 Graphite felt before and after use

As indicated above, the reduction of chromium(III) in the sulfate and MSA system is via an outer-sphere pathway, which is strongly influenced by the electrode surface activity. If the surface conditions were significantly changed, the electrochemical reduction process would also be greatly influenced. However, the reduction of $CrCl^{2+}$ and $CrCl_2^{+}$ is via an inner-sphere pathway. The chloride ions are acting as a bridge between the electrode and chromium(III) ions to enhance electron transfer; thus chromium(III) reduction in the chloride system is less influenced by the surface condition of the graphite felt.

If the used graphite felts were retreated again by concentrated sulfuric acid as described in **Section 3.4.3.2**, the outstanding electrochemical activity for chromium(III) reduction would be recovered (See **Figure 3.23**).

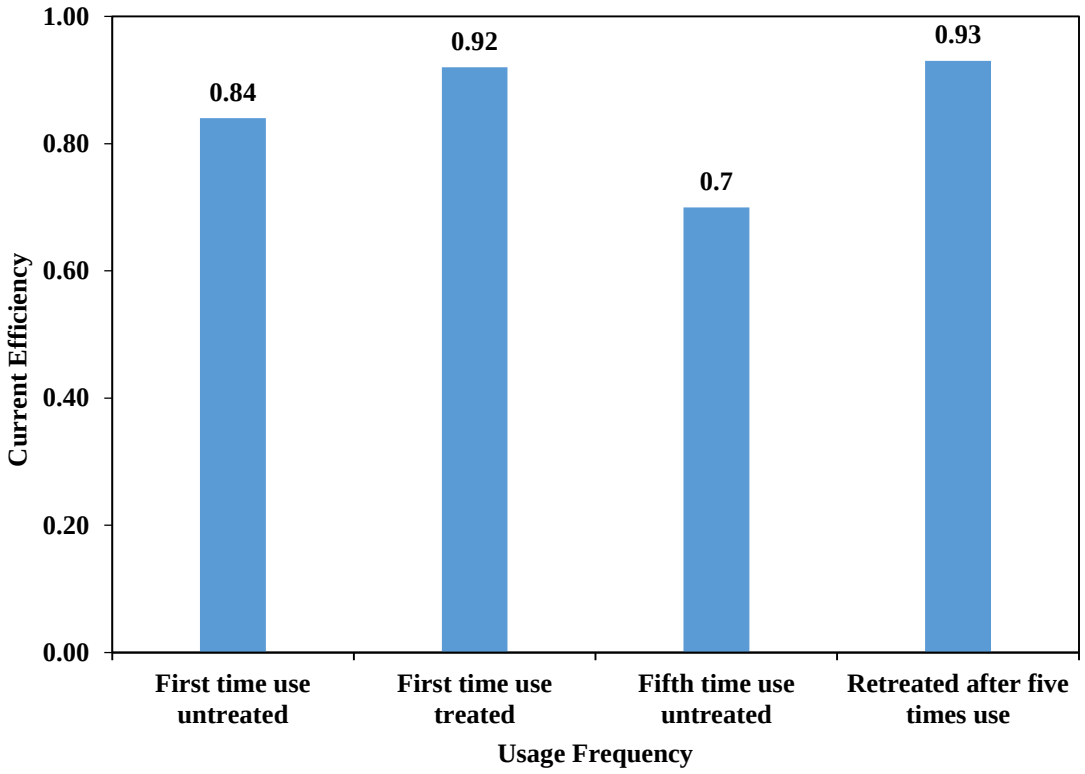

Figure 3.23 The effect of graphite felt retreatment in the sulfate system

3.6 Summary

The following conclusions can be summarized from this electrochemical reduction work:

(1) Chromium(III) ions can be electrochemically reduced to synthesize chromium(II) ions in acidic aqueous solutions, such as hydrochloric acid, sulfuric acid and MSA with a high current efficiency and conversion.

(2) Acid concentration, current density, graphite felt thickness and graphite felt surface condition can all affect the electrochemical reduction results. Acid concentration has a more significant influence on the electrochemical reduction current efficiency in sulfate and MSA systems than that in the chloride system.

(3) Generally, the chloride system shows the best electrochemical reduction results, and the sulfate system displays the worst; the MSA system is in between. Additionally, in sulfate and MSA systems, the graphite felt displays a worse electrochemical activity after repeated use, but no obvious change in the chloride system. This is mainly due to the pathway difference in the electron transfer between the electrode and the Cr(III) ions.

Chapter 4 Tin Recovery in Acidic Aqueous Systems

4.1 Introduction

Due to the large demand of tin in industry and the limitations of traditional pyrometallurgical route for tin recovery, hydrometallurgical technology is urgently needed to treat low grade tin materials. Several studies on the hydrometallurgical recovery of tin has been reported; however, roasting or calcine with a carbon source (such as coke) is always the first step to treat tin concentrate in these recovery processes. No work on direct reductive extraction of tin in acidic aqueous systems has been reported.

Due to the strong reducing ability of Cr(II) ions, SnO_2 can be reduced to Sn(II) ions or/and Sn metal dependent on recovery conditions. Two possible reactions involved are described as below:

Reaction 1: $SnO_2 + 4H^+ + 2Cr^{2+} \longrightarrow Sn^{2+} + 2Cr^{3+} + 2H_2O$ **Equation 1.1**

Reaction 2: $SnO_2 + 4H^+ + 4Cr^{2+} \longrightarrow Sn + 4Cr^{3+} + 2H_2O$ **Equation 1.2**

It was hoped that **Reaction 1** would be the predominant reaction. The advantage of producing Sn(II) is that it may be possible to use electrolysis to recover metallic tin at the cathode (See **Equation 2.16**) or to reductively precipitate metallic tin with a suitable reducing reagent (See **Equation 2.17**).

Electrolysis: $Sn^{2+} + 2e^- \rightarrow Sn$ **Equation 2.16**

Precipitation: $Sn^{2+} + 2Red^- \rightarrow Sn + 2Ox$ **Equation 2.17**

In order to determine whether Sn(II) ions can be the predominant recovery product, two methods has been taken:

(1) Addition of excess SnO_2 to the recovery system

(2) Addition of the Cr(II) solution dropwise to the Cr(III) solution

The purpose of the addition of excess SnO_2 is to minimize the further reaction of Sn(II) with Cr(II). The slow addition of Cr(II) is because that low concentration of Cr(II) can increase the reduction potential of Cr(III)/Cr(II) system based on the Nernst Equation (See **Equation 4.1**). The purpose of these two methods are both to increase the possibility to maintain Sn as the soluble state.

$$Cr^{3+} + e^- \rightarrow Cr^{2+} \qquad E = E^\circ - \frac{RT}{nF} \ln \frac{[Cr^{2+}]}{[Cr^{3+}]} \qquad \textbf{Equation 4.1}$$

(E is the potential, E° is the standard potential, R is the universal gas constant, T is the absolute temperature, F is the Faraday constant, n is the number of moles of electrons passed for a half reaction. See **Nomenclature** for detail)

In this chapter, the temperature effect on the tin recovery test in the chloride, sulfate and MSA system was first investigated (See **Section 4.3**); the comparison and discussion of these three acid systems for tin recovery were then performed (See **Section 4.4**); finally, some conclusions in this recovery study were provided (See **Section 4.5**).

4.2 Experimental

4.2.1 Materials

Tests were conducted on synthetic cassiterite minerals. The synthetic cassiterite was 99.9% tin(IV) oxide (<10 micron powder), supplied by Alfa Aesar. Chromium(III) chloride hexahydrate was shipped from Sigma-Aldrich and potassium chromium(III) sulfate

dodecahydrate was supplied by Alfa Aesar. Cr(III)-MSA electrolytes were synthesized from lead(II) oxide, potassium chromium sulfate and methane sulfonic acid (Lutropur® MSA 100) as described in **Section 3.2.3.1**. Lead(II) oxide was supplied by Sigma-Aldrich and methane sulfonic acid (Lutropur® MSA 100) was provided by BASF, Germany. Chromium(II) solutions in chloride, sulfate and MSA systems were electrochemically synthesized with the procedures described in **Section 3.2.3.3**. The solution used in each test was made from deionized water and all of the other chemicals used in this study were certified analytical grade or reagent grade chemicals.

4.2.2 Apparatus

The recovery apparatus used in this research provided controlled conditions for studies of recovery of tin from synthetic cassiterite minerals in acidic aqueous solutions. The experimental set-up is shown in **Figure 4.1** and **Figure 4.2**. The schematic of the recovery study experimental set-up is shown in **Figure 4.3**.

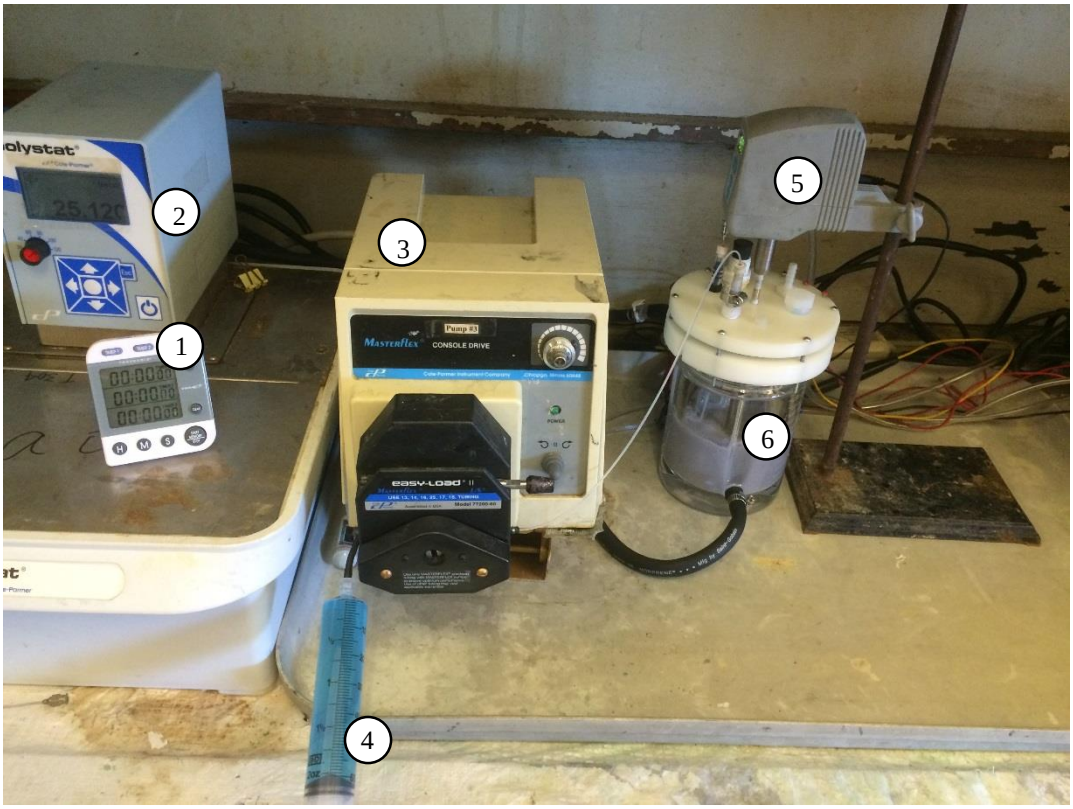

Figure 4.1 Experimental apparatus for tin recovery tests

(1- Timer, 2-Water Bath, 3 -Pump, 4-Syringe, 5- Motor, 6-Recovery Reactor)

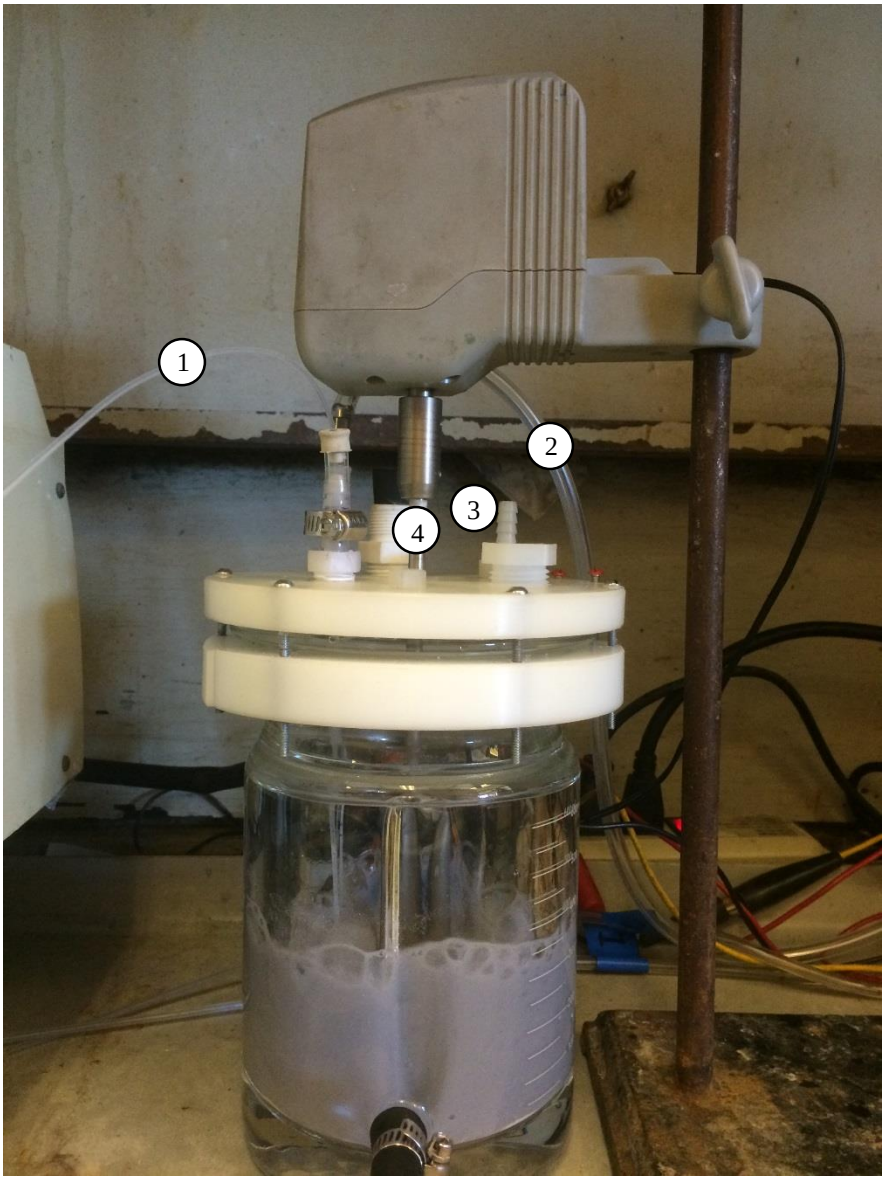

Figure 4.2 Recovery reactor for tin recovery tests

(1-Chromium(II) Inlet, 2-Nitrogen Gas Inlet, 3-Gas Outlet, 4- Stirring Rod)

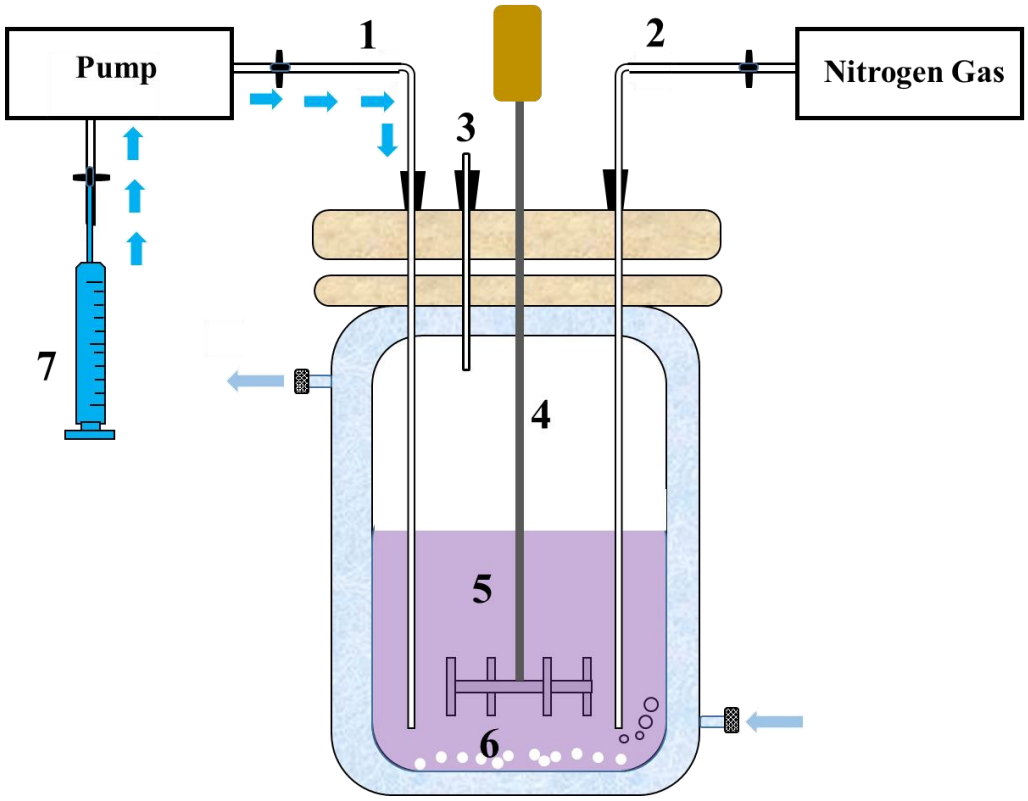

Figure 4.3 Schematic of tin recovery study experimental set-up

(*1-Chromium(II) Inlet, 2-Nitrogen Gas Inlet, 3-Gas Outlet, 4- Stirring Rod, 5-Cr(III) Solution, 6-SnO_2, 7-Cr(II) Solution)*

The 600 mL three-baffled glass reactor was manufactured by CanSci Glass Products Ltd. As chromium(II) solution was easy to oxidize, a high-density polyethylene lid manufactured by the machine shop in Materials Engineering, UBC, was used to seal the reactor. There were several openings on the lid which were used for insertion of a 316 stainless steel stirring rod connected with a motor, nitrogen inlet and outlet, and injection of the chromium(II) solution. The Cr(II) solution was stored in the 60 mL syringe as shown in **Figure 4.1**. In order to add the 300 mL chromium(II) solution dropwise over 90 minutes, a Masterflex pump was used to control the flow rate. The water bath purchased from Cole-Parmer was used to control the recovery temperature.

4.2.3 Procedures

Two cases were investigated in this research: (a) excess SnO_2 (b) excess Cr(II) ions. The experimental procedures consisted of the following steps:

(1) a. Excess SnO_2: Initially, 6 gram SnO_2 powder was added into the three baffled recovery reactor.

b. Excess Cr(II) ions: Initially, 0.5 gram SnO_2 powder was added into the three baffled recovery reactor.

(2) 300 mL 0.1 M Cr(III) + 0.6 M HCl/0.3 M H_2SO_4/0.6 M MSA solution was then added to the reactor with SnO_2.

(3) The reactor was covered with the HDPE lid. The tubes on the reactor were then connected with the water bath in order to control the recovery temperature. The rate of stirring rod was controlled at 500 rpm.

(4) The chromium(III) solution mixed with SnO_2 in the recovery reactor was purged with nitrogen gas for two hours to desorb any oxygen in the reactor.

(5) Five 60 mL capacity syringes were used to withdraw the chromium(II) solution from the electrochemical cell described in **Section 3.2.2**. The syringes were then sealed to protect any exposure to oxygen.

(6) The syringe filled with the chromium(II) solution was connected with the pump tube. Over a period of 90 minute, 300 mL of chromium(II) solution was injected into the recovery reactor drop by drop.

(7) The reaction was stopped 15 minutes later after all the chromium(II) solution was added. The total reaction time is 105 minutes.

(8) The recovery solution was then filtrated by 0.2 μm membrane filter to separate residues and leachates.

(9) The residues were subsequently dried and weighted.

(10) The filtered solution was accurately diluted to 800 mL and then analyzed for dissolved tin content with Atomic Absorption Spectrometer (AAS).

4.2.4 Analytical Methods

The Varian 240 Atomic Absorption Spectrometer (AAS) instrument was used to measure the concentration of tin content in the filtrated solution. The flame was air-acetylene-nitrous oxide.

The X-ray diffraction (XRD) analysis for the recovery residues were performed with a Bruker D8-Advance X-ray diffractometer (Copper $K\alpha_1$ & $K\alpha_2$, 40 kV, 40 mA).

The amounts of metallic Sn and SnO_2 in the recovery residues were calculated based on the mass balance principle which is demonstrated in **Appendix C.**

4.2.5 Evaluation Factors

Conversion of **Reaction 1** and **Reaction 2** is a key factor to evaluate the tin recovery process. In **Section 4.3.1**, **Section 4.3.2** and **Section 4.3.3**, when SnO_2 is in excess, the conversion of **Reaction 1** is the conversion of Cr(II) to make Sn(II) and the conversion of **Reaction 2** is the conversion of Cr(II) to make Sn metal. In **Section 4.3.4**, when Cr(II) is in excess, the conversion of **Reaction 1** is the conversion of SnO_2 to make Sn(II) and the conversion of **Reaction 2** is the conversion of SnO_2 to make Sn metal.

When SnO_2 is in excess, **Equation 4.2** is used to calculate the conversion of Cr(II) to make Sn(II) (**Reaction 1**, see **Equation 1.1**) and **Equation 4.3** is used to calculate the conversion of Cr(II) to make Sn metal (**Reaction 2**, see **Equation 1.2**)

$$CR_1 = \frac{\text{Moles of Cr(II) used to produce Sn(II)}}{\text{Moles of total Cr(II) in the system}} \times 100\% \qquad \textbf{Equation 4.2}$$

$$CR_2 = \frac{\text{Moles of Cr(II) used to produce Sn metal}}{\text{Moles of total Cr(II) in the system}} \times 100\% \qquad \textbf{Equation 4.3}$$

(CR_1 is the conversion of **Reaction 1**, and CR_2 is the conversion of **Reaction 2**)

When Cr(II) is in excess, **Equation 4.4** is used to calculate the conversion of SnO_2 to Sn(II) (**Reaction 1**, see **Equation 1.1**) and **Equation 4.5** is used to calculate the conversion of SnO_2 to Sn metal (**Reaction 2**, see **Equation 1.2**).

$$CR_1 = \frac{\text{Moles of Sn(II) produced}}{\text{Moles of initial Sn element in } SnO_2} \times 100\% \qquad \textbf{Equation 4.4}$$

$$CR_2 = \frac{\text{Moles of Sn metal produced}}{\text{Moles of initial Sn element in } SnO_2} \times 100\% \qquad \textbf{Equation 4.5}$$

(CR_1 is the conversion of **Reaction 1**, and CR_2 is the conversion of **Reaction 2**)

4.3 Reductive Extraction of Tin in Acidic Aqueous Systems

In this thesis, three acidic aqueous systems (chloride, sulfate and MSA system) were studied to investigate the tin recovery results. The effect of temperature was carried out in the temperature range between 25 ℃ and 55 ℃ in all three acid systems.

4.3.1 Reductive Extraction of Tin in the Chloride System

The recovery conditions in the chloride system are described in **Table 4.1.**

Table 4.1 Recovery conditions in the chloride system

Solid	~ 6 g Tin(IV) oxide powder, <10 micron
Rotation speed	500 rpm
Atmosphere	Nitrogen atmosphere
Initial volume of chromium(III) solutions in the reactor	300 mL
Initial composition of chromium(III) solutions in the reactor	0.1 M Chromium(III) chloride 0.6 M Hydrochloric acid
Volume of chromium(II) solutions dropwise added to the reactor	300 mL
Composition of chromium(II) solutions dropwise added to the reactor	~ 0.1 M Chromium(II) chloride 0.2 M Hydrochloric acid
Reaction time	105 minutes
Temperatures	25 ℃, 35 ℃, 45 ℃, 55 ℃

The experimental results are summarized as following:

(1) From **Figure 4.4**, it was found that in the chloride system, the total conversion of Cr(II) to make Sn(II) and Sn metal was significantly high at high temperature. With the increase of temperature, the total conversion of Cr(II) to make Sn(II) and Sn metal was increasing from 10.7% to 99.6%. Almost all of the Cr(II) in the chloride system reacted with SnO_2 at 55 ℃.

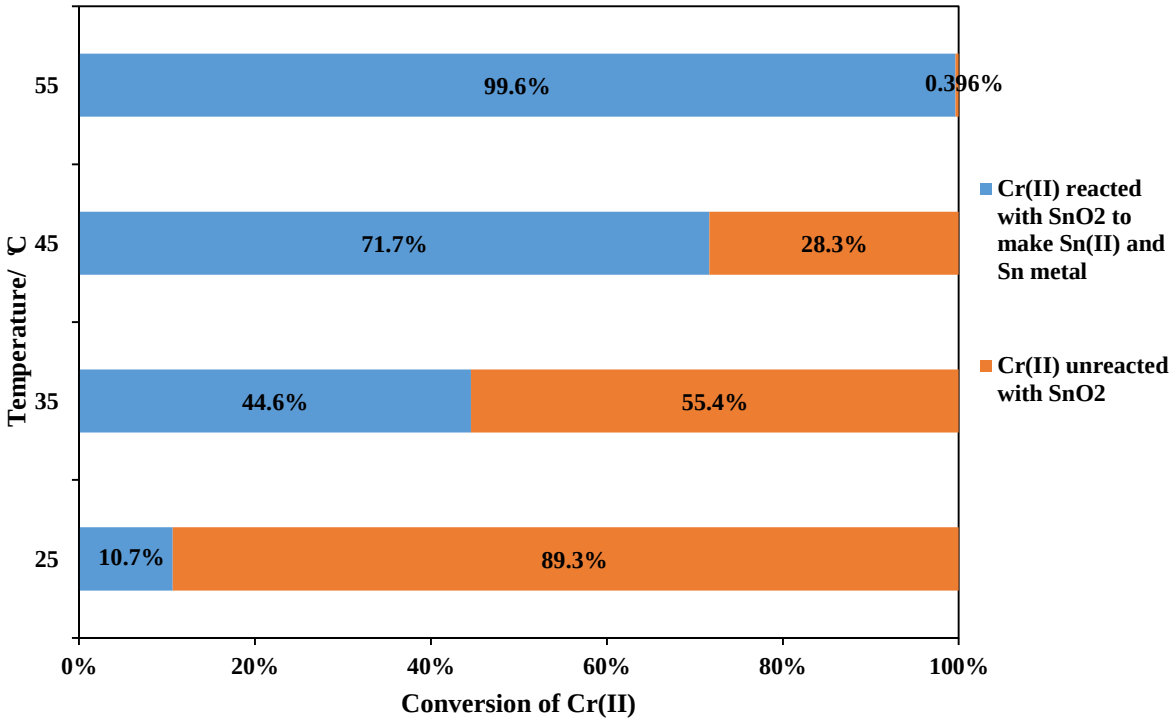

Figure 4.4 Total conversion of Cr(II) in the chloride system

(2) From **Figure 4.5**, it was found that the conversion of Cr(II) to make Sn metal was increasing with temperature. The conversion of Cr(II) to make Sn metal at 55 ℃ was 9.7 times larger than that at 25 ℃. This is reasonable as higher temperature can accelerate the recovery process; more metallic Sn can be produced at a constant reaction time.

Additionally, the conversion of Cr(II) to make Sn(II) was observed to increase from 25 ℃ to 55 ℃ due to the positive temperature effect. The conversion of Cr(II) to produce Sn(II) at 55 ℃ was 3.7 times larger than that at 25 ℃. This conversion increase is smaller than that for Sn metal.

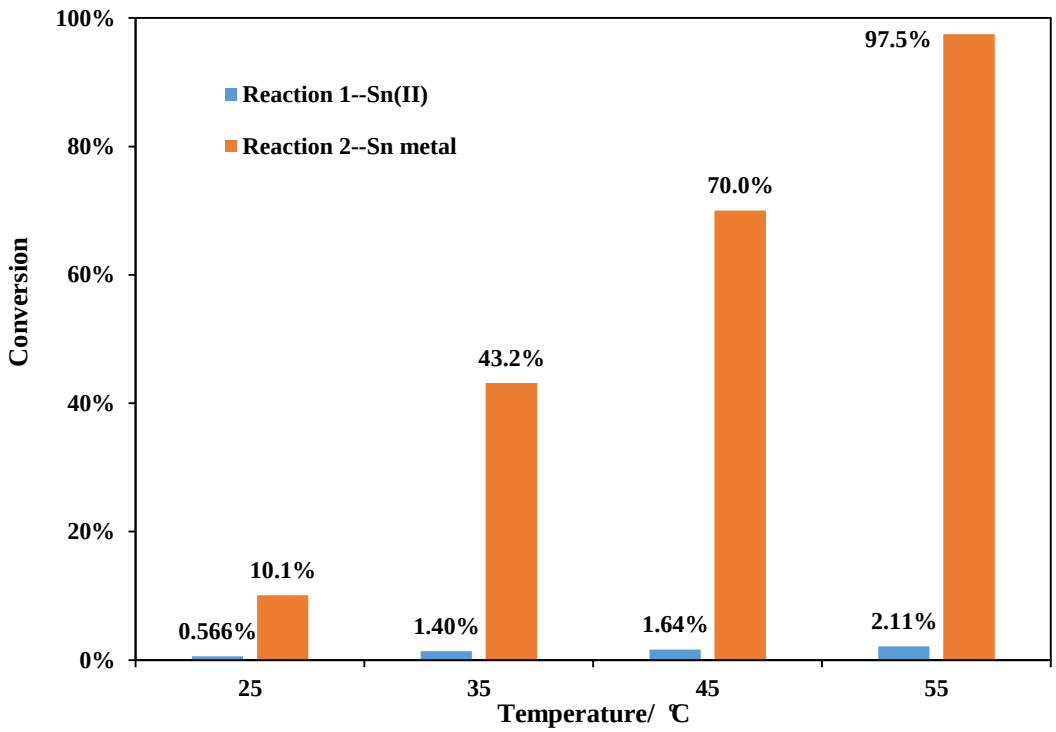

Figure 4.5 Conversion of Cr(II) to make Sn(II) and Sn metal in the chloride system

In the chloride system, the conversion of Cr(II) to make Sn(II) was significantly smaller than that to make Sn metal. The conversion of Cr(II) to make Sn metal was 17.8, 30.9, 42.7 and 46.2 times larger than that to make Sn(II) at 25 ℃, 35 ℃, 45 ℃ and 55 ℃ respectively.

The main product of the recovery test was Sn metal, and the Cr(II) conversion of **Reaction 2** was much higher than that of **Reaction 1**. It can be concluded that in the chloride system, most of the reacted SnO_2 was reduced to Sn metal instead of Sn(II) ions under these experimental conditions.

(3) The residues were confirmed to contain both Sn metal and SnO_2 from the XRD patterns (See **Figure 4.6**). The metallic Sn produced was β-Sn. The four characteristic peaks of β-Sn, specifically, (2,0,0), (1,0,1), (2,2,0) and (2,1,1), are very small at 25 ℃,

but are becoming increasingly obvious when the temperature is increasing from 25 ℃ to 55 ℃ (See **Figure 4.6 (b)**). This increase is the direct evidence of more Sn metal produced.

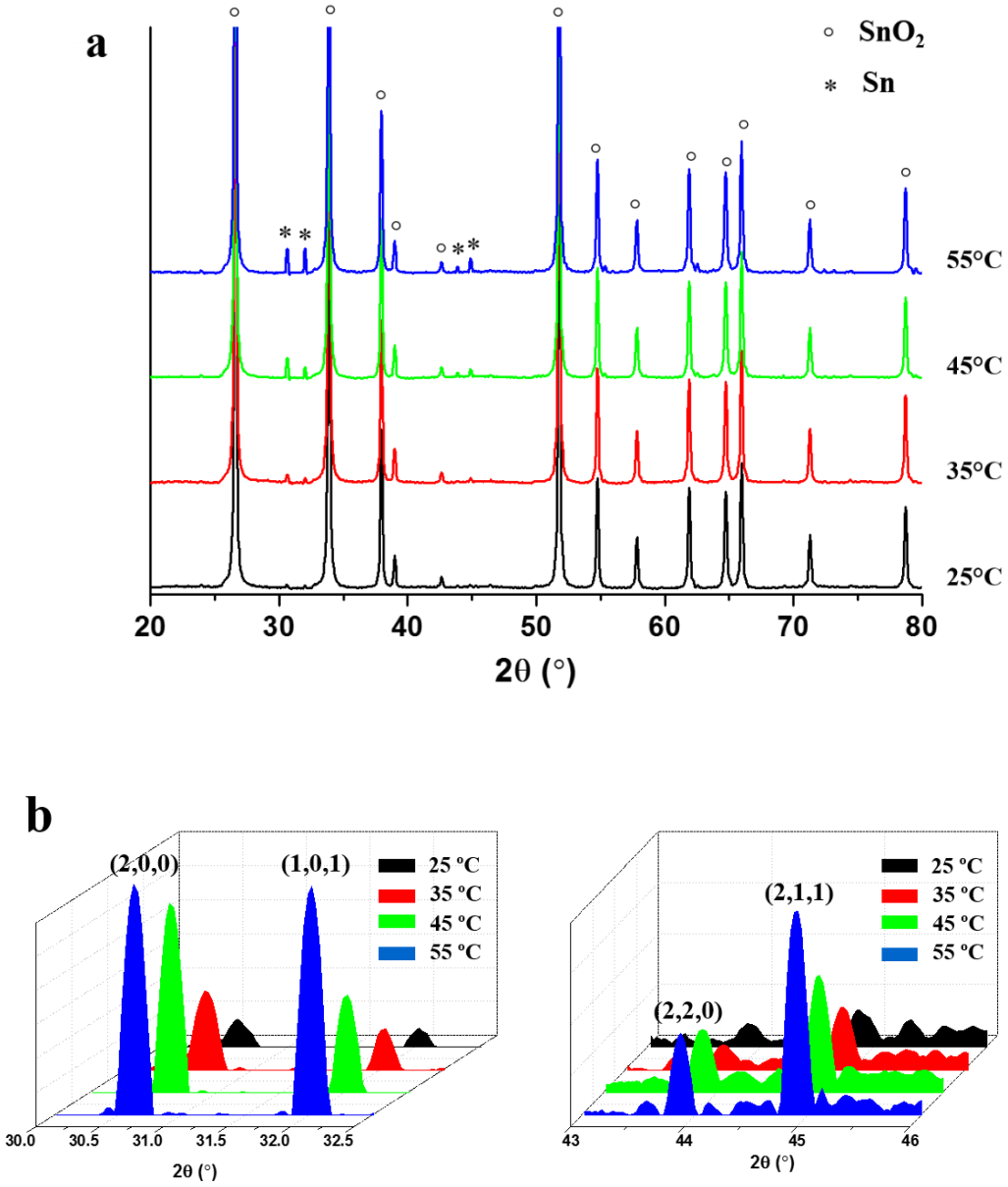

Figure 4.6 (a) XRD patterns for recovery residues in the chloride system (b) XRD patterns including (h,k,l) for Sn product in the chloride system

4.3.2 Reductive Extraction of Tin in the Sulfate System

The recovery conditions in the sulfate system are described in **Table 4.2**.

Table 4.2 Recovery conditions in the sulfate system

Solid	~ 6 g Tin(IV) oxide powder, <10 micron
Rotation speed	500 rpm
Atmosphere	Nitrogen atmosphere
Initial volume of chromium(III) solutions in the reactor	300 mL
Initial composition of chromium(III) solutions in the reactor	0.1 M Potassium chromium(III) sulfate 0.3 M Sulfuric acid
Volume of chromium(II) solutions dropwise added to the reactor	300 mL
Composition of chromium(II) solutions dropwise added to the reactor	~ 0.1 M Potassium chromium(II) sulfate 0.1 M Sulfuric acid
Reaction time	105 minutes
Temperatures	25 ℃, 35 ℃, 45 ℃, 55 ℃

The experimental results are summarized as following:

(1) From **Figure 4.7**, it was found that in the sulfate system, the total conversion of Cr(II) to make Sn(II) and Sn metal was significantly smaller than that in the chloride system. Most of the Cr(II) in the sulfate system didn`t react with SnO_2. Additionally, with the increase of temperature, the total conversion of Cr(II) to make Sn(II) and Sn metal was increasing from 2.60% to 13.0%.

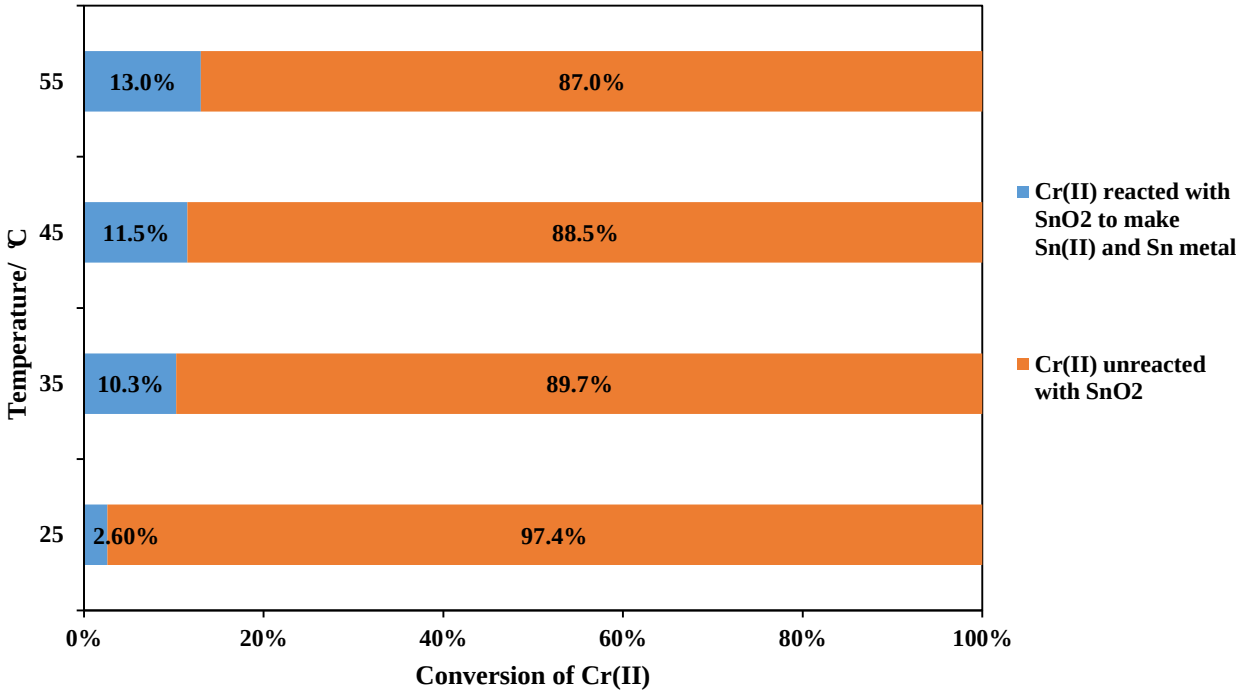

Figure 4.7 Total conversion of Cr(II) in the sulfate system

(2) Similar to the chloride system, the conversion of Cr(II) to make Sn metal increased with temperature. The conversion of Cr(II) to make Sn metal at 55 ℃ was 5.5 times larger than that at 25 ℃ (See **Figure 4.8**).

Additionally, the conversion of Cr(II) to make Sn(II) was significantly small. It decreased from 25 ℃ to 35 ℃, but increased from 35 ℃ to 55 ℃. Higher temperature can lead to higher reaction rate. This is the reason why the conversion of Cr(II) to make Sn(II) increased from 35 ℃ to 55 ℃. The decrease from 25 ℃ to 35 ℃ may be due to the different temperature influence on the kinetics of **Reaction 1** and **Reaction 2**. When increasing temperature, the kinetics increase of **Reaction 2** is more dominant than that of **Reaction 1**. More SnO_2 is reduced to metallic Sn instead of Sn(II) by Cr(II), resulting in smaller Cr(II) conversion of **Reaction 1**.

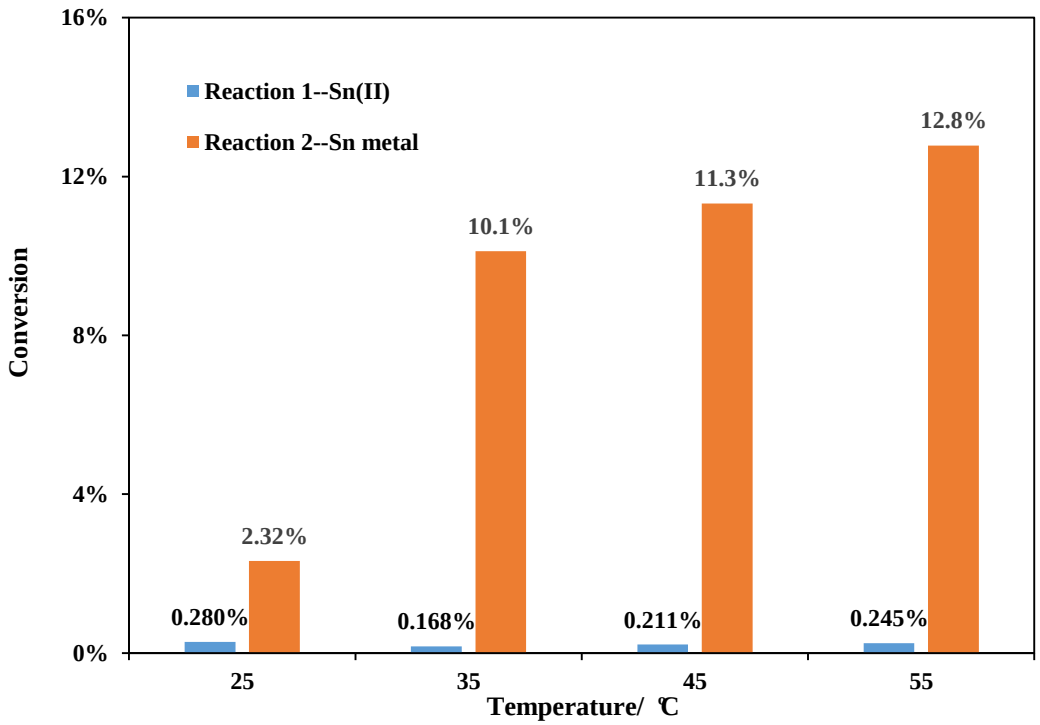

Figure 4.8 Conversion of Cr(II) to make Sn(II) and Sn metal in the sulfate system

In the sulfate system, the conversion of Cr(II) to make Sn(II) was significantly smaller compared to the conversion of Cr(II) to make Sn(II) metal. The main product of the recovery test was Sn metal, and the Cr(II) conversion of **Reaction 2** was much higher than that of **Reaction 1**. This indicates that in the sulfate system, **Reaction 2** is the dominant tin recovery reaction, rather than **Reaction 1**.

(3) The XRD patterns confirmed the formation of β-Sn metal during the recovery process (See **Figure 4.9**).

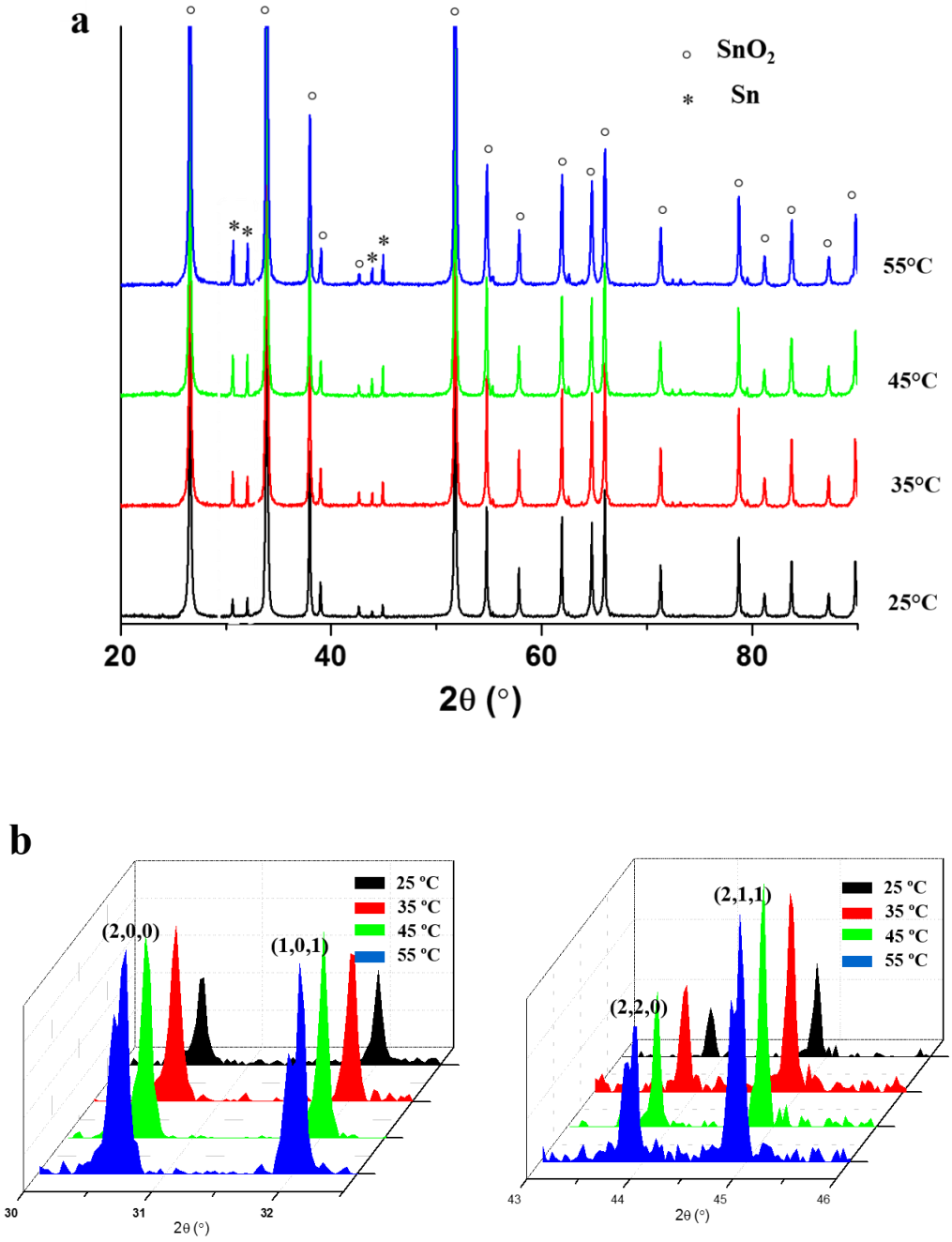

Figure 4.9 (a) XRD patterns for recovery residues in the sulfate system (b) XRD patterns including (h,k,l) for Sn product in the sulfate system

4.3.3 Reductive Extraction of Tin in the MSA System

The recovery conditions in the MSA system are described in **Table 4.3**.

Table 4.3 Recovery conditions in the MSA system

Solid	~ 6 g Tin(IV) oxide powder, <10 micron
Rotation speed	500 rpm
Atmosphere	Nitrogen atmosphere
Initial volume of chromium(III) solutions in the reactor	300 mL
Initial composition of chromium(III) solutions in the reactor	0.1 M Potassium chromium(III) methanesulfonate 0.6 M Methane sulfonic acid (MSA)
Volume of chromium(II) solutions dropwise added to the reactor	300mL
Composition of chromium(II) solutions dropwise added to the reactor	0.1 M Potassium chromium(II) methanesulfonate 0.2 M Methane sulfonic acid (MSA)
Reaction time	105 minutes
Temperatures	25 ℃, 35 ℃, 45 ℃, 55 ℃

The experimental results are summarized as following:

(1) From **Figure 4.10**, it was found that in the MSA system, the total conversion of Cr(II) to make Sn(II) and Sn metal was also significantly smaller than that in the chloride system. Most of the Cr(II) in the system didn`t react with SnO_2. This is consistent with the sulfate system. With the increase of temperature, the total conversion of Cr(II) to make Sn(II) and Sn metal was increasing from 1.69% to 9.50%, which is smaller than the sulfate system.

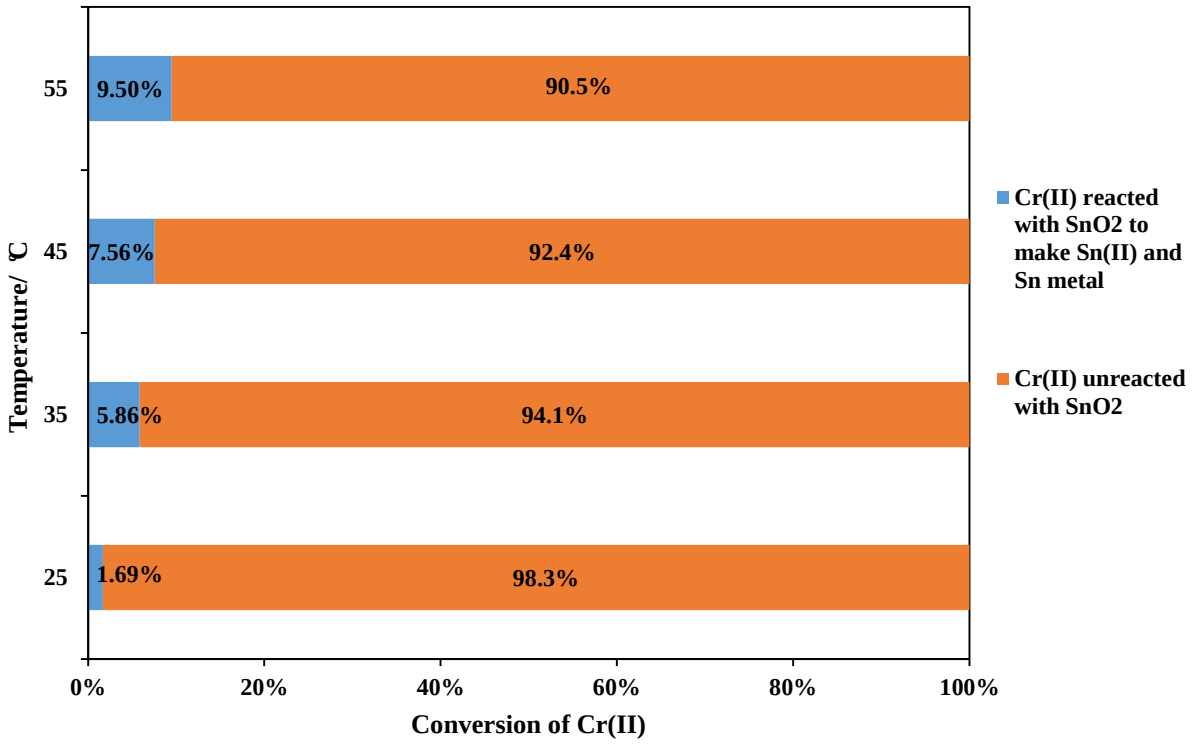

Figure 4.10 Total conversion of Cr(II) in the MSA system

(2) From **Figure 4.11**, it was found that the conversion of Cr(II) to form Sn metal increased with temperature. This is consistent with the results observed in the chloride and sulfate system. The conversion of Cr(II) to make Sn metal at 55 ℃ was 5.8 times higher than that at 25 ℃.

The conversion of Cr(II) to make Sn(II) was significantly smaller as compared to the chloride and sulfate system. Like the sulfate system, the conversion of **Reaction 1** decreased from 25 ℃ to 35 ℃, but increased from 35 ℃ to 55 ℃.

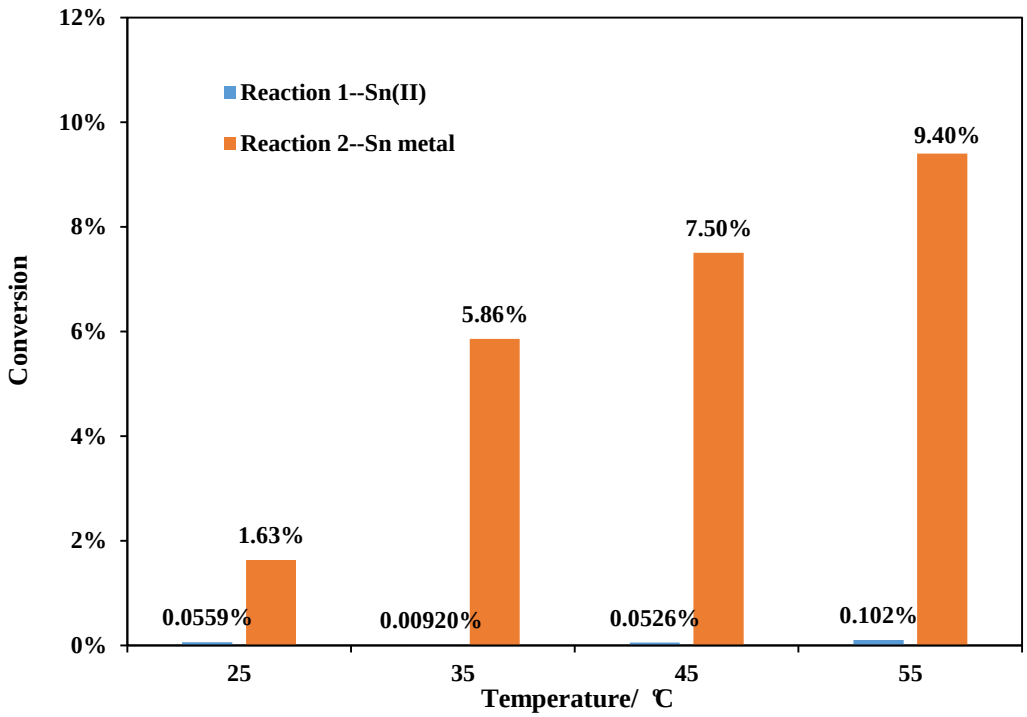

Figure 4.11 Conversion of Cr(II) to make Sn(II) and Sn metal in the MSA system

It was observed that the main product of the recovery test was Sn metal, and the Cr(II) conversion of **Reaction 2** was much higher than that of **Reaction 1**. Similar to the chloride and sulfate system, most of the reacted SnO_2 was reduced to Sn metal instead of Sn(II) in the MSA system under these experiment conditions.

(3) **Figure 4.12** indicates that the residues contained both β-Sn metal and unreacted SnO_2. The characteristic peaks for β-tin metal, specifically, (2,0,0), (1,0,1), (2,2,0) and (2,1,1) were significantly small at 25 ℃, but became more apparent when the temperature increased from 25 ℃ to 55 ℃ (See **Figure 4.12(b)**).

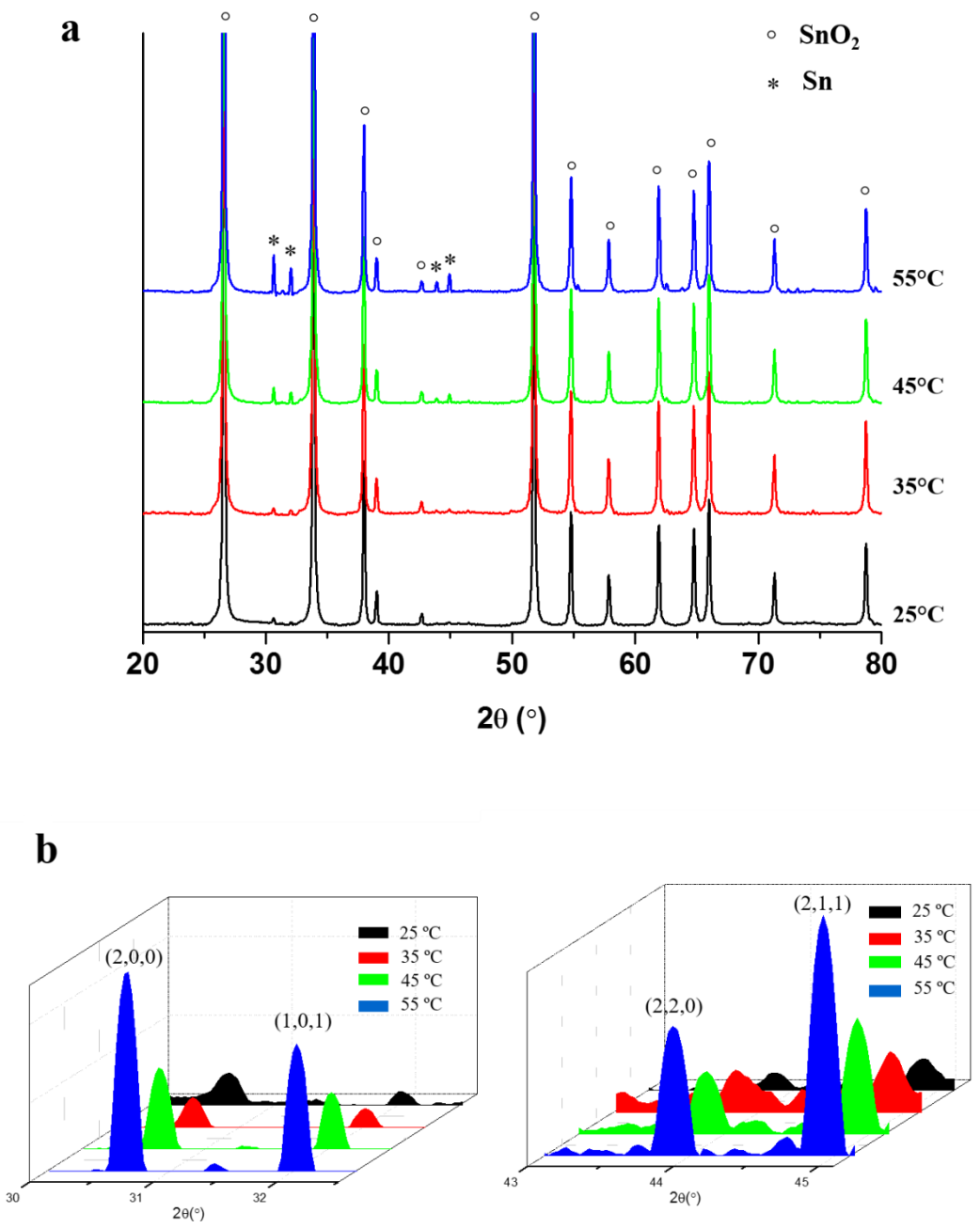

Figure 4.12 (a) XRD patterns for recovery residues in the MSA system (b) XRD patterns including (h,k,l) for Sn product in the MSA system

4.3.4 Reductive Extraction of Tin in the Chloride System with Excess Chromium(II) Ions

The recovery process was also investigated with excess Cr(II) in the chloride system at the temperature of 55 ℃. The experimental conditions are described in **Table 4.4**.

Table 4.4 Recovery conditions in the chloride system with excess Cr(II)

Rotation speed	500 rpm
Atmosphere	Nitrogen atmosphere
Initial volume of chromium(III) solutions in the reactor	300 mL
Initial composition of chromium(III) solutions in the reactor	0.1 M Chromium(III) chloride 0.6 M Hydrochloric acid
Volume of chromium(II) solutions dropwise added to the reactor	300 mL
Composition of chromium(II) solutions dropwise added to the reactor	~ 0.1 M Chromium(II) chloride 0.2 M Hydrochloric acid
Reaction time	105 minutes
Temperatures	55 ℃
Solid	~0.5 g/ ~6 g Tin(IV) oxide powder, <10 micron

The experimental results are summarized as following:

(1) In **Figure 4.13**, when Cr(II) is in the excess, the blue bar means the total conversion of SnO_2 to Sn(II) and Sn metal; the orange bar indicates the percentage of unreacted SnO_2 in the system. When SnO_2 is in excess, the blue bar describes the total conversion of Cr(II) to make Sn(II) and Sn metal; the orange bar illustrates the percentage of Cr(II) unreacted with SnO_2.

It was found that despite the presence of excess Cr(II) ions, SnO_2 was not completely consumed (See **Figure 4.13**). More than half of the SnO_2 in the system didn`t react with Cr(II).

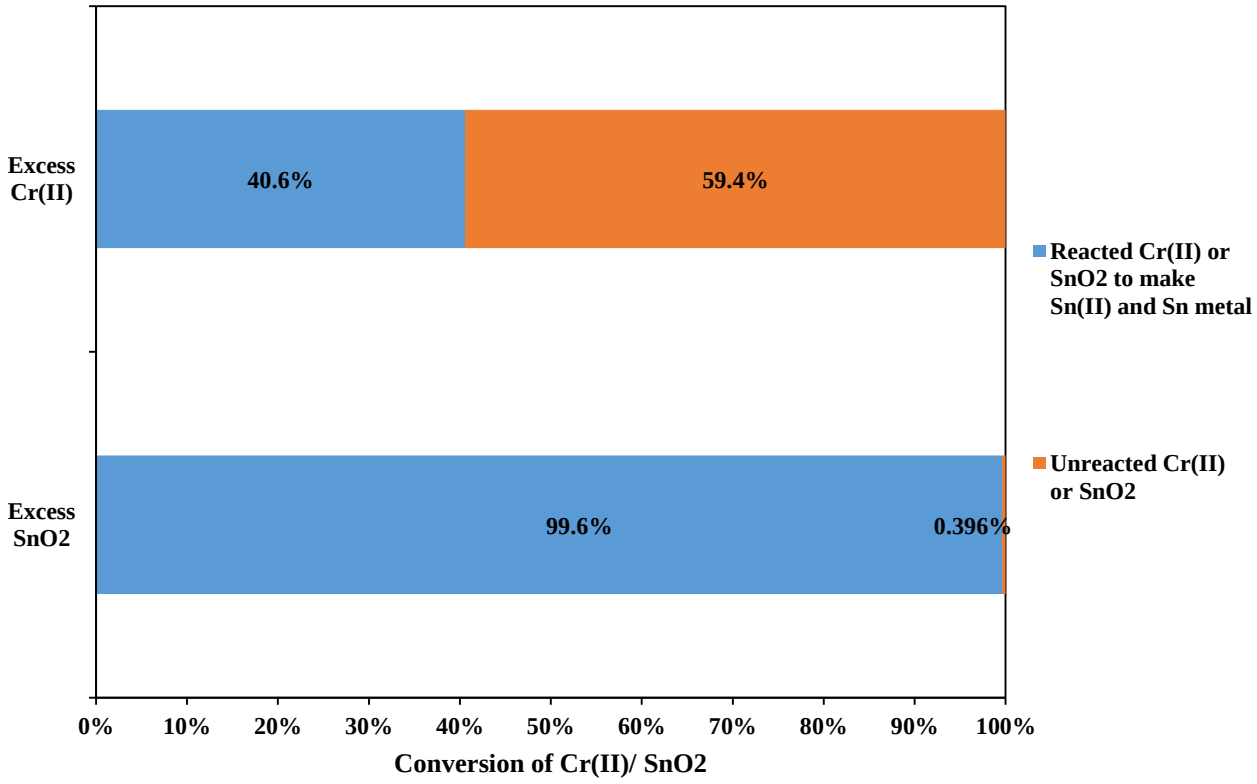

Figure 4.13 Total conversion of Cr(II) or SnO_2 in the chloride system, T=55 ℃

(2) In **Figure 4.14**, when Cr(II) is in excess, the blue bar means the conversion of SnO_2 to Sn(II); the orange bar indicates the conversion of SnO_2 to Sn metal. When SnO_2 is in excess, the blue bar describes the conversion of Cr(II) to make Sn(II); the orange bar illustrates the conversion of Cr(II) to make Sn metal.

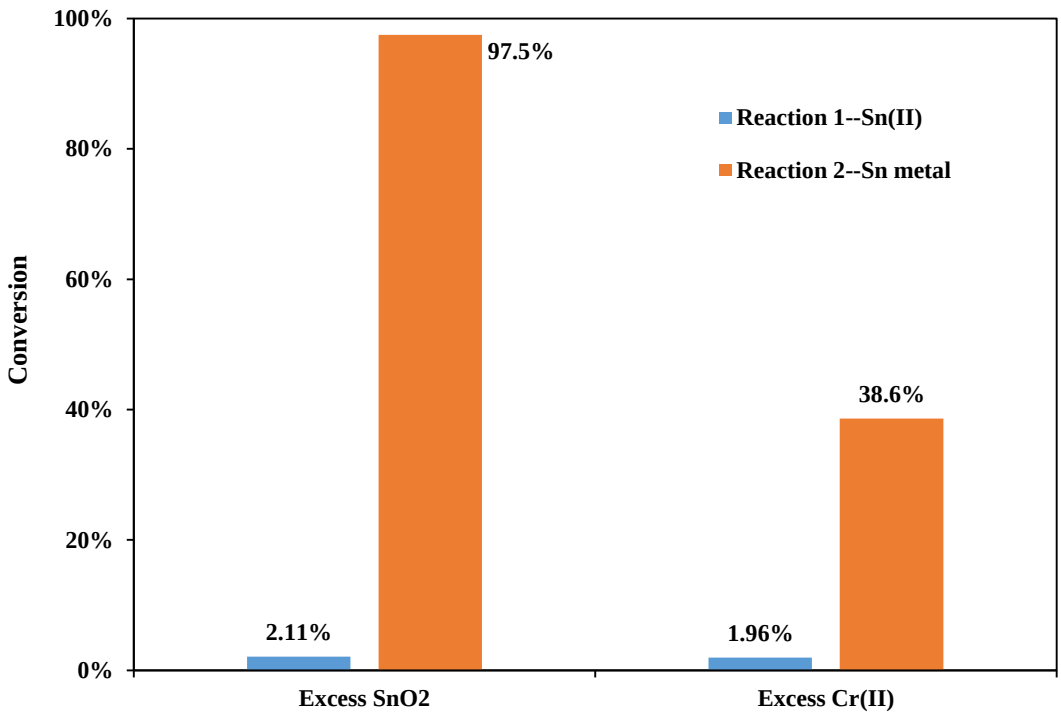

Figure 4.14 Conversion of Cr(II) or SnO_2 to make Sn(II) and Sn metal in the chloride system, T=55 ℃

It was observed that when Cr(II) was in excess, the main product of the recovery test was also Sn metal; the conversion of SnO_2 to Sn metal (**Reaction 2**) was much higher than the conversion of SnO_2 to Sn(II) (**Reaction 1**). This is consistent with the results when SnO_2 was in excess as described in **Section 4.3.1** (See **Figure 4.5**).

However, the conversion of **Reaction 1** and **Reaction 2** was smaller when Cr(II) was in excess than that when SnO_2 was in excess. The possible reasons are discussed in **Section 4.4**.

(3) The XRD patterns shown in **Figure 4.15** indicate that despite the presence of excess Cr(II) ions, both β-Sn metal and SnO_2 existed in the residue after reaction. SnO_2 was not completely consumed during the reaction.

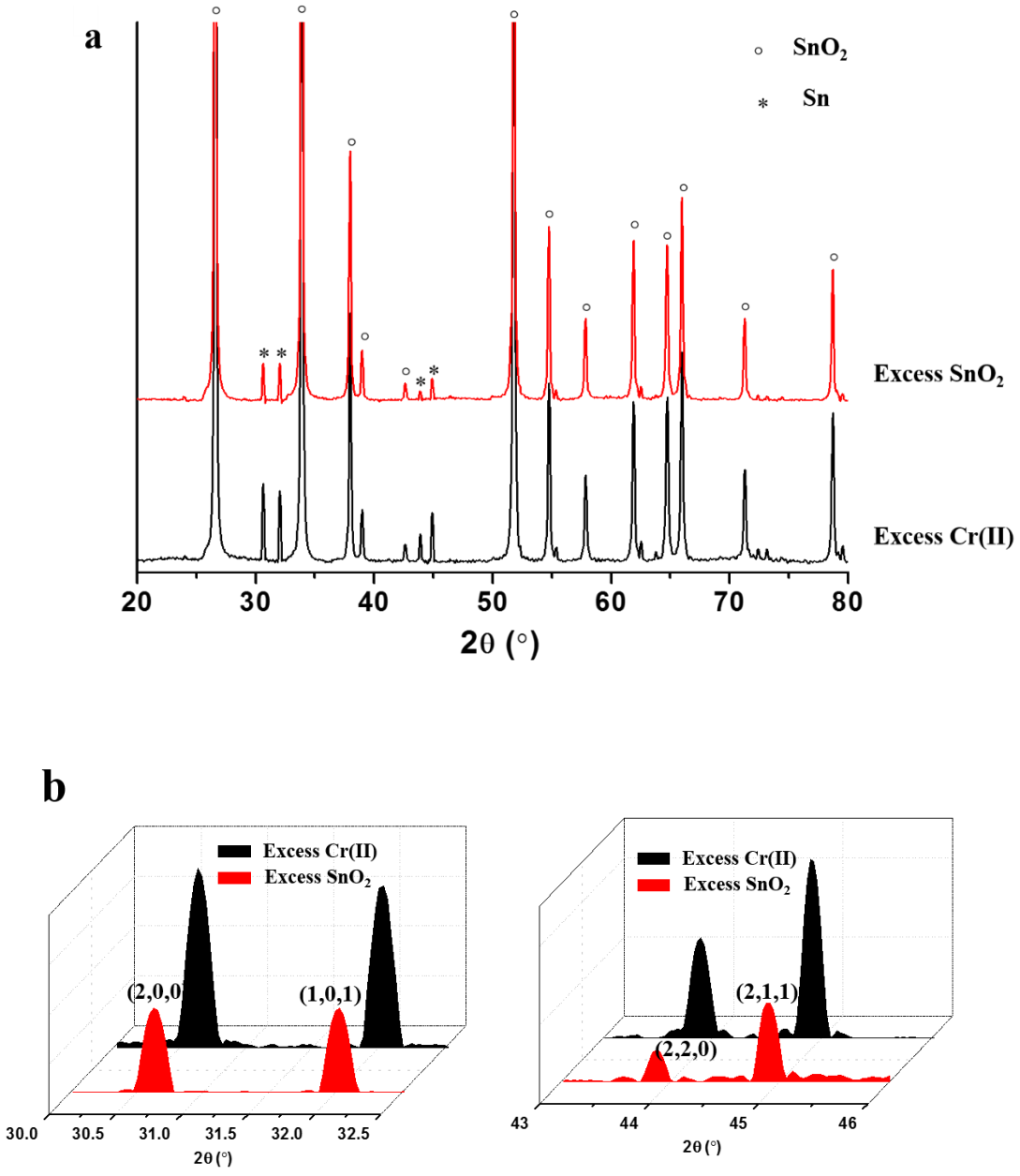

Figure 4.15 (a) XRD patterns for recovery residues in the chloride system, T= 55 ℃ (b) XRD patterns including (h,k,l) for Sn product in the chloride system, T= 55 ℃

4.4 Comparison and Discussion

(1) In all three acidic aqueous systems (chloride, sulfate and MSA), the main product of the recovery test was Sn metal, and very little Sn(II) was produced. The conversion of **Reaction 2** was much higher than that of **Reaction 1** as shown in **Figure 4.16**.

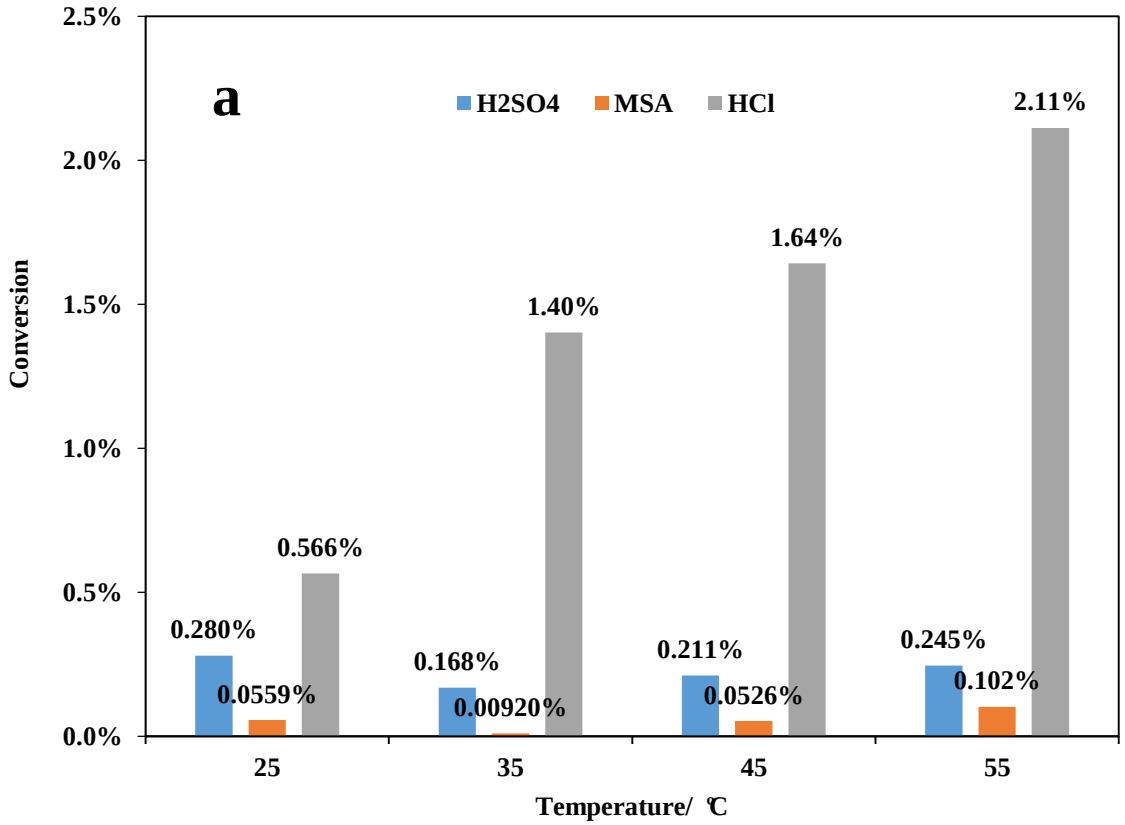

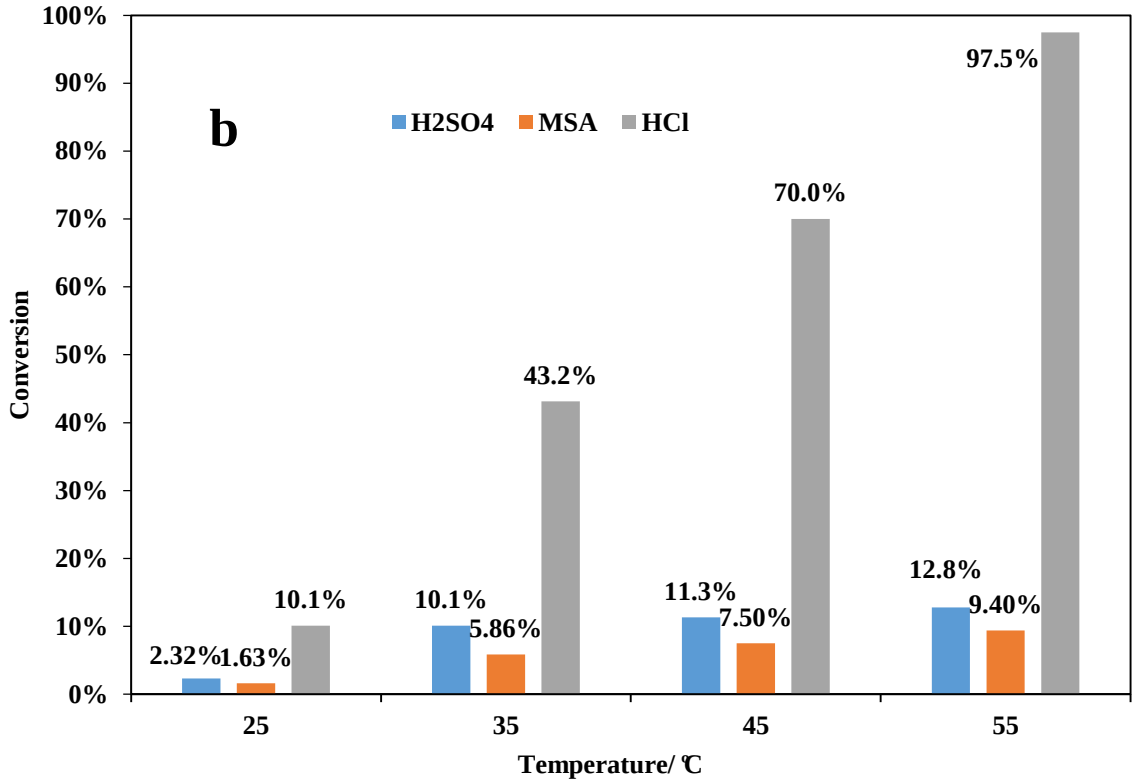

Figure 4.16 (a) Conversion of Cr(II) to make Sn(II), Reaction 1 (b) Conversion of Cr(II) to make Sn metal, Reaction 2

The reason why the conversion of Cr(II) to make Sn(II) was significantly lower than that to make Sn metal may be that the reduction of SnO_2 to Sn metal is via a two-step process. The first step is the reduction of SnO_2 to Sn(II) and the second step is the reduction of Sn(II) to Sn metal. However, the kinetics of Sn(II) to Sn metal is extremely fast. Sn(II) is reduced to Sn metal immediately after its formation from SnO_2. The conditions of this research cannot maintain Sn as the soluble state.

(2) Generally, the recovery process was slow in kinetics and the conversion of **Reaction 1** and **Reaction 2** was low in the sulfate and MSA system. Two possible reasons may

explain this behavior. Firstly, SnO_2 crystallizes with the rutile structure, wherein the tin atoms are surrounded by six oxygen atoms (See **Figure 4.17**).

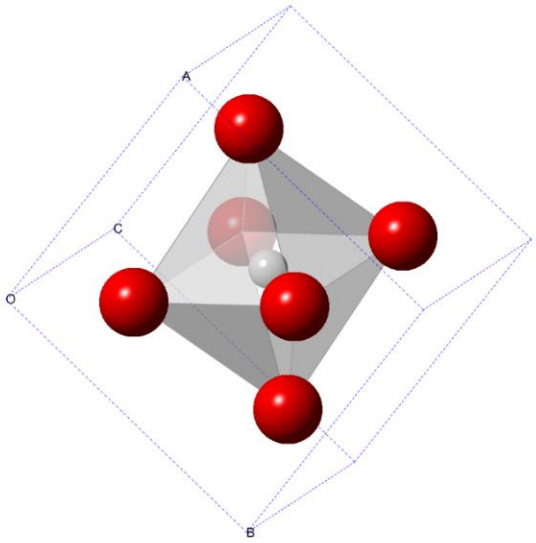

Figure 4.17 Structure of SnO_2, oxygen atom(red) and tin atom(grey)[73]

In order to release Sn from SnO_2, six Sn-O bonds should be broken (See **Figure 4.18**). The bond lengths of Sn-O are 2.0516 ± 0.0039 Å and 2.0577 ± 0.0062 Å[73]. These bond lengths are significantly shorter than that of the rock-salt crystal structure of PbS studied by Kelsall, which is reported to be 2.967 ± 0.0005 Å[74]. The shorter bonds of SnO_2 make it a stable structure and more difficult to reduce, leading to the slow kinetics.

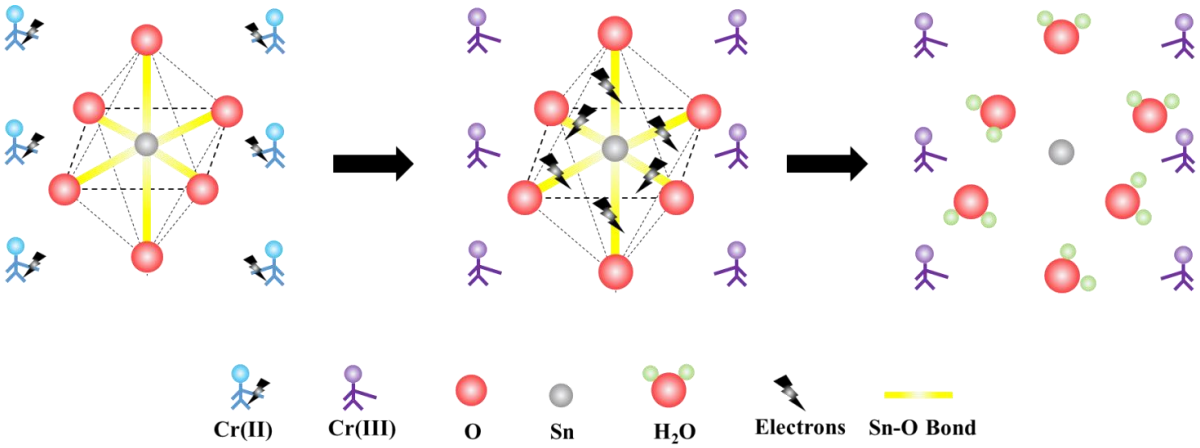

Figure 4.18 Schematic diagram of the tin recovery process

Additionally, as previously reported by Kelsall, for the heterogeneous reactions with Cr(II) ions, a significant decrease in molar volume must accompany the phase transition. Otherwise, the metal formed by topochemical reaction on the solid would cover its surface, inhibiting the recovery reaction[11].

For the case of SnO_2, the oxygen element is being neutralized to liquid water. The decrease in molar volume is calculated to be 5.88 cm^3/mol (27%), resulting from the molar volume difference between SnO_2 and Sn metal. This decrease is smaller than that of PbS studied by Kelsall (ΔV_M =13.2 cm^3/mol, 42%) (See **Section 2.4.2**). The low voidage due to the phase transition from SnO_2 to Sn metal indicates that the surface of SnO_2 can be more possibly covered by the formed Sn metal.

(3) The chloride system showed the best recovery results. Conversion of **Reaction 1** and **Reaction 2** in the chloride system was significantly higher than that in the sulfate and MSA system. This is probably due to the catalysis effect of chloride ions. Chloride ions may participate in the recovery process, acting as a catalyst to accelerate the whole recovery reaction. Taube provided one possible reason for the apparent increased rate in the chloride system[12]. When Cr(II) is associated with Cl^-, by lowering the charge it lowers the energy necessary for the transfer of Cr^{2+} to the surface layer; the recovery rate in the chloride system can be greatly accelerated.

The sulfate and MSA system showed similar recovery results, but a little bit worse for the MSA system. This is likely due to the steric effect of MSA. The $–CH_3$ group in MSA is larger than the –OH group in H_2SO_4. MSA is probably adsorbed on the surface of SnO_2. The larger methyl group would impede the transfer of Cr(II) ions to the SnO_2 surface, increasing the transfer barrier energy of Cr(II) to the surface layer of SnO_2.

Probably, the energy required for the transfer of Cr(II) to the surface layer of SnO_2 is in the order of MSA, sulfate and chloride (See **Figure 4.19**).

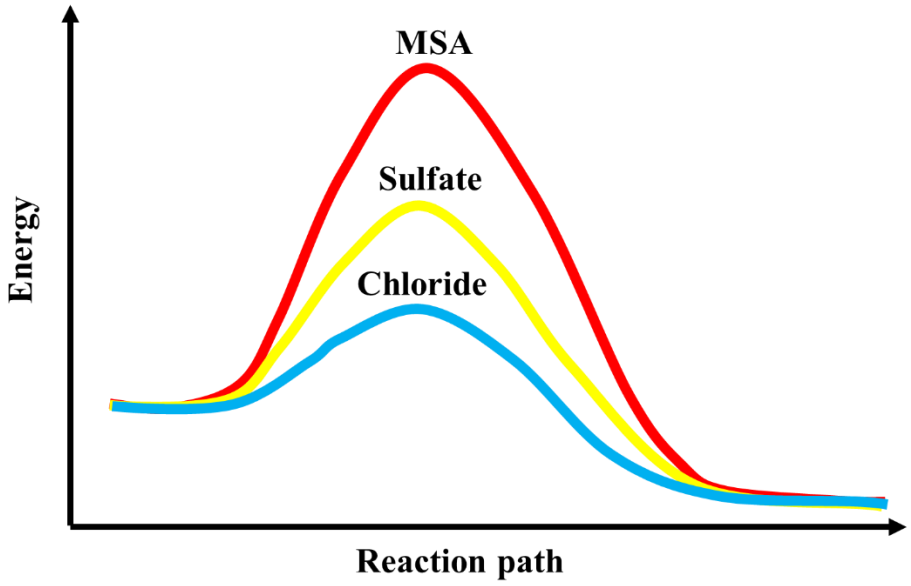

Figure 4.19 Schematic diagram of the energy required for the transfer of Cr(II) to the SnO_2 surface layer

(4) In all three acid systems, the total conversion for the tin recovery test was increasing with temperature. The kinetics of reduction of SnO_2 is faster at higher temperature. High temperature can also accelerate the transfer of Cr^{2+} to the metal oxide surface layer, increasing the recovery kinetics. It is also possible that the Sn metal formed on the SnO_2 surface detaches from the underlying SnO_2 more easily at higher temperature due to the increased reaction rate. This can reduce the impeding effect of formed Sn metal.

(5) The conversion of **Reaction 1** and **Reaction 2** when Cr(II) was in excess was smaller compared to that when SnO_2 was in excess. This may be explained by the fact that excess SnO_2 can provide more surface areas and thus Cr(II) ions have more active reaction sites, especially when some of the SnO_2 are covered by the produced Sn metal during the reduction process.

4.5 Summary

The following conclusions can be summarized from this tin recovery work:

(1) Cassiterite (SnO_2) can react with Cr(II) ions in acidic aqueous solutions, such as hydrochloric acid, sulfuric acid and MSA. In all three acidic aqueous systems, the predominant product of the recovery test is Sn metal. The amount of Sn(II) produced is significantly lower than the Sn metal.

(2) Slow recovery kinetics and low conversion are observed in the sulfate and MSA system. This is probably resulting from the stable rutile structure of SnO_2 and the inhibition of the reaction due to the formation of Sn metal on the metal oxide surface. However, chloride systems show much better recovery results, which is attributed to the catalysis effect of chloride ions on the recovery process.

(3) The recovery kinetics and conversion can be accelerated by elevating the reaction temperature due to the increased energy provided and acceleration of the transfer of Cr(II) to the SnO_2 surface layer.

Chapter 5 Conclusions and Recommendations

5.1 Conclusions

The following overall conclusions can be summarized from this work:

(1) Chromium(III) ions can be electrochemically reduced to synthesize chromium(II) ions in acidic aqueous solutions, such as hydrochloric acid, sulfuric acid and MSA with a high current efficiency and conversion on the graphite felt cathode. Specifically, in the chloride system, the current efficiency can reach a minimum of 0.96 with a conversion of 0.90. In the sulfate system, with a fractional conversion of 0.90, the current efficiency for Cr(III) reduction to Cr(II) can reach a minimum of 0.84 for an initial concentration of 0.1 M Cr(III) in 0.1 M H_2SO_4. In the MSA system, a current efficiency of 0.89 can be achieved when converting 90% of 0.1 M Cr(III) to Cr(II) in 0.2 M MSA solution.

(2) Acid concentration, current density, graphite felt thickness and graphite felt surface condition can affect the electrochemical reduction results. The most obvious influence factor is acid concentration, which has a very significant effect on the electrochemical reduction of Cr(III) in the sulfate and MSA system, while little influence in the chloride system.

(3) Generally, the chloride system shows the best electrochemical reduction results, the sulfate system the worst and the MSA system in between. Additionally, in sulfate and MSA systems, the graphite felt displays a significantly worse electrochemical activity after repeated use, while in the chloride system, the used graphite felt just exhibited slightly worse electrochemical reduction performance. This is mainly due to the pathway difference in the electron transfer between the electrode and the Cr(III) ions.

(4) Cassiterite can react with Cr(II) ions in acidic aqueous solutions, such as hydrochloric acid, sulfuric acid and MSA. In all three acid systems, the predominant product of the recovery test is Sn metal. The amount of Sn(II) produced is significantly lower than that of Sn metal.

(5) Generally, the recovery kinetics is slow and the total conversion is low in the sulfate and MSA system. The total conversion is less than 13% in the sulfate system and less than 10% in the MSA system at the temperature of 55 ℃ for 105 minutes when SnO_2 is in excess. However, chloride system shows much better recovery results. Specifically, the total conversion could reach about 99% at the temperature of 55 ℃ for 105 minutes in excess of SnO_2. This huge difference between the chloride system and the sulfate/ MSA system may be attributed to the catalysis effect of chloride ions.

(6) In the case of excess Cr(II) in the system, the total conversion in the chloride system at 55 ℃ for 105 minutes is about 41% , apparently smaller than that of excess SnO_2 in the system (99%). It is likely due to the fact that excess SnO_2 can provide more surface areas; thus Cr(II) ions have more active reaction sites, especially when some of the SnO_2 are covered by the formation of Sn metal during the reduction process.

5.2 Recommendations for Future Work

(1) Fundamental kinetics of electrochemical reduction of chromium(III) in the sulfate and MSA system should be investigated to explain the reduction difference between these two systems.

(2) Electrochemical reduction of used chromium(III) solution in the chloride, sulfate and MSA system should be performed to evaluate the current efficiency of recycled chromium(III) solution. It was observed that after being oxidized by oxidizing reagents, chromium(II) solution was unable to restore its original state of fresh chromium(III) solution. The recycled chromium(III) solution in chloride, sulfate and MSA systems was found to have a maximum absorbance at around 415 nm, which was different from the wavelengths of fresh chromium(III) solution in these three acid systems. The wavelength difference indicated the change of speciation in the chromium(III) system during the oxidizing process. Therefore, the current efficiency may also alter when the used chromium(III) solution is applied for electrochemical reduction.

(3) The surface condition of the graphite felt after repeated use should be investigated to determine the reason for its short lifetime in sulfate and MSA systems. Better treatment methods should be explored to improve the behavior of used graphite felt in sulfate and MSA systems.

(4) Fundamental kinetics of dissolution of SnO_2 in chloride, sulfate, and MSA systems should be undertaken to elucidate the characteristics and mechanisms. The fundamental difference of the recovery process among these three systems should be investigated.

(5) To define the role that the anion plays during the tin recovery process, quantitative rate studies with ions of different charges and sizes, and with reducing reagents having the first coordination sphere closed (such as $Ru(NH_3)_6^{2+}$) should be performed.

(6) In order to increase the percentage of Sn(II) in the leachate and increase the total conversion, better recovery conditions such as adding additives or catalyst, should be investigated. One possible additive is ethylene glycol tetraacetic acid (EGTA). The stability constant of Sn(II)EGTA (log K=23.85) is significantly larger than that of Cr(III)EGTA (log K=2.54). Due to its strong complexing effect on Sn(II) ions and weak complexing ability on Cr(III) ions, EGTA may be a promising chelating reagent to maintain Sn as the soluble state.

References

1. Louis, H., *Metallurgy of tin*. 1911: McGraw-Hill book Company.
2. Gernon, M., *Environmental benefits of methanesulfonic acid. Comparative properties and advantages.* Green Chemistry, 1999. **1**(3): p. 127-140.
3. Kelsall, G., C. House, and F. Gudyanga, *Chemical and electrochemical equilibria and kinetics in aqueous Cr (III)/Cr (II) chloride solutions.* Journal of electroanalytical chemistry and interfacial electrochemistry, 1988. **244**(1): p. 179-202.
4. Yin, Q., N. Brandon, and G. Kelsall, *Electrochemical synthesis of Cr (II) at carbon electrodes in acidic aqueous solutions.* Journal of applied electrochemistry, 2000. **30**(10): p. 1109-1117.
5. Mantell, C., *Progress in tin metallurgy.* JOURNAL OF METALS, 1965. **17**(5): p. 473-&.
6. Pommier, L.W. and S.J. Escalera, *Processing of Tin from Impure Raw Materials.* JOM, 1979. **31**(4): p. 10-12.
7. Zhao, T., *Non-ferrous extractive metallurgy Manual: mercury, tin and antimony*. 1999.
8. Castro, C. and W. Kray, *The cleavage of bonds by low valent transition metal ions. The homogeneous reduction of alkyl halides by chromous sulfate.* Journal of the American Chemical Society, 1963. **85**(18): p. 2768-2773.
9. Climent, M., et al., *The iron-chromium redox battery.* An. Quim, 1987. **83**: p. 12.
10. Lopez-Atalaya, M., et al., *Optimization studies on a Fe/Cr redox flow battery.* Journal of power sources, 1992. **39**(2): p. 147-154.
11. Kelsall, G. and Q. Yin. *Indirect electrochemical reduction of lead sulfide precipitates*. in *INSTITUTION OF CHEMICAL ENGINEERS SYMPOSIUM SERIES*. 1999. HEMSPHERE PUBLISHING CORPORATION.
12. Zabin, B. and H. Taube, *The reactions of metal oxides with aquated chromium (II) ion.* Inorganic Chemistry, 1964. **3**(7): p. 963-968.
13. Taube, H. and H. Myers, *Evidence for a bridged activated complex for electron transfer reactions.* Journal of the American Chemical Society, 1954. **76**(8): p. 2103-2111.
14. Andreu, R., et al., *The reduction of Cr (III) in concentrated aqueous electrolytes at a DME: The influence of anions.* Journal of electroanalytical chemistry and interfacial electrochemistry, 1986. **210**(1): p. 111-126.
15. Zielińska-Ignaciuk, M. and Z. Galus, *Kinetics and mechanism of the Cr 3+/Cr 2+ electrodereaction in concentrated perchlorates and chlorides.* Journal of electroanalytical chemistry and interfacial electrochemistry, 1974. **50**(1): p. 41-53.
16. Andreu, R., et al., *The reduction of Cr 3+ in NaClO 4 solutions.* Journal of electroanalytical chemistry and interfacial electrochemistry, 1984. **175**(1): p. 251-262.
17. Barr, S.W., K.L. Guyer, and M.J. Weaver, *The dependence of the kinetics of some simple outer-sphere electrode reactions on the nature of the electrode material.*

Journal of electroanalytical chemistry and interfacial electrochemistry, 1980. **111**(1): p. 41-59.
18. Liu, H., J.T. Hupp, and M.J. Weaver, *Surface environmental effects in electrochemical kinetics: outer-sphere chromium (III) reductions at mercury, gallium, lead, and thallium surfaces.* Journal of electroanalytical chemistry and interfacial electrochemistry, 1984. **179**(1): p. 219-238.
19. Jalan, V., H. Stark, and J. Giner, *Requirements for optimization of electrodes and electrolyte for the iron/chromium redox flow cell*, 1981, National Aeronautics and Space Administration, Cleveland, OH (USA). Lewis Research Center; Giner, Inc., Waltham, MA (USA).
20. Hussey, C.L., *Room temperature haloaluminate ionic liquids. Novel solvents for transition metal solution chemistry.* Pure and applied Chemistry, 1988. **60**(12): p. 1763-1772.
21. Hussey, C., G. Mamantov, and A. Popov, *Chemistry of Nonaqueous Solutions: Current Progress.* VCH, New York, 1994: p. 227.
22. Nissen, D., *A Study of the Anode ‐Electrolyte Interface in a Thermal Battery.* Journal of The Electrochemical Society, 1979. **126**(2): p. 176-180.
23. Hussey, C., L. King, and J. Erbacher, *An Electrochemical Study of Chromium in Molten NaCl ‐AlCl3.* Journal of The Electrochemical Society, 1978. **125**(4): p. 561-566.
24. Liu, J.S.Y., et al., *Electrochemical Studies of Chromium (III) and Chromium (II) Chloride Complexes in Basic Aluminum Chloride ‐1 ‐Methyl ‐3 ‐ethylimidazolium Chloride Room Temperature Molten Salts.* Journal of The Electrochemical Society, 1997. **144**(7): p. 2388-2392.
25. Anson, F.C., N. Rathjen, and R.D. Frisbee, *The Absence of a Detectable Potential ‐Dependence of the Transfer Coefficient in the Cr+ 3/Cr+ 2 Reaction.* Journal of The Electrochemical Society, 1970. **117**(4): p. 477-482.
26. Barclay, D.J., E. Passeron, and F.C. Anson, *Multiple-ligand bridging by thiocyanate in the electrochemical oxidation of chromium (II) at mercury electrodes.* Inorganic Chemistry, 1970. **9**(5): p. 1024-1030.
27. Jones, J.G. and F. Anson, *Ligand Bridging in the Oxidation of Chromium (II) at Mercury Electrodes.* Analytical Chemistry, 1964. **36**(6): p. 1137-1138.
28. Tang, T.-W. and F.C. Anson, *Reduction of Cr (edta)(OH) 2− at mercury electrodes as controlled by the rate of its protonation.* Journal of electroanalytical chemistry and interfacial electrochemistry, 1984. **177**(1): p. 183-189.
29. Zhang, X., H. Yang, and A.J. Bard, *Variation of the heterogeneous electron-transfer rate constant with solution viscosity: reduction of aqueous solutions of [(EDTA) chromium (III)]-at a mercury electrode.* Journal of the American Chemical Society, 1987. **109**(7): p. 1916-1920.
30. Walsh, J.H. and J.E. Earley, *Reduction potentials of some chromium (III) complexes.* Inorganic Chemistry, 1964. **3**(3): p. 343-347.
31. Stara, V. and M. Kopanica, *Chromium (III)-complexes of some aminopolycarboxylic acids and their polarographic behaviour.* Journal of electroanalytical chemistry and interfacial electrochemistry, 1974. **52**(2): p. 251-259.

32. Pletcher, D. and J.C. White, *Studies of indirect electrochemical reductions using chromium complexes with polyaminocarboxylate ligands as mediators.* Electrochimica acta, 1992. **37**(4): p. 575-583.
33. Weaver, M.J. and T.L. Satterberg, *The position of the reaction site and the relative reactivities of simple outer-and inner-sphere electrode reactions. The reduction of some chromium (III) amine complexes at mercury electrodes.* The Journal of Physical Chemistry, 1977. **81**(18): p. 1772-1783.
34. Taube, H., H. Myers, and R.L. Rich, *OBSERVATIONS ON THE MECHANISM OF ELECTRON TRANSFER IN SOLUTION1.* Journal of the American Chemical Society, 1953. **75**(16): p. 4118-4119.
35. Aikens, D.A. and J.W. Ross Jr, *EFFECT OF CHLORIDE ON THE KINETICS OF ELECTROÖXIDATION OF CHROMIUM (II) IN ACIDIC PERCHLORATE MEDIUM1.* The Journal of Physical Chemistry, 1961. **65**(7): p. 1213-1216.
36. Ulrich, J.J. and F.C. Anson, *Ligand bridging by halide in the electrochemical oxidation of chromium (II) at mercury electrodes.* Inorganic Chemistry, 1969. **8**(2): p. 195-200.
37. Weaver, M.J. and F.C. Anson, *Distinguishing between inner-and outer-sphere electrode reactions. Reactivity patterns for some chromium (III)-chromium (II) electron-transfer reactions at mercury electrodes.* Inorganic Chemistry, 1976. **15**(8): p. 1871-1881.
38. Tissot, P. and M. Fragniere, *Anodic oxidation of cyanide on a reticulated three-dimensional electrode.* Journal of applied electrochemistry, 1994. **24**(6): p. 509-512.
39. Pletcher, D., et al., *Reticulated vitreous carbon cathodes for metal ion removal from process streams Part I: Mass transport studies.* Journal of applied electrochemistry, 1991. **21**(8): p. 659-666.
40. Pletcher, D., et al., *Reticulated vitreous carbon cathodes for metal ion removal from process streams Part II: Removal of copper (II) from acid sulphate media.* Journal of applied electrochemistry, 1991. **21**(8): p. 667-671.
41. De Leon, C.P. and D. Pletcher, *The removal of Pb (II) from aqueous solutions using a reticulated vitreous carbon cathode cell—the influence of the electrolyte medium.* Electrochimica acta, 1996. **41**(4): p. 533-541.
42. Agarwal, I., et al., *Electrodeposition of six heavy metals on reticulated vitreous carbon electrode.* Water Research, 1984. **18**(2): p. 227-232.
43. Lu, J., D. Dreisinger, and W. Cooper, *Copper electrowinning from dilute cyanide solution in a membrane cell using graphite felt.* Hydrometallurgy, 2002. **64**(1): p. 1-11.
44. Golub, D. and Y. Oren, *Removal of chromium from aqueous solutions by treatment with porous carbon electrodes: electrochemical principles.* Journal of applied electrochemistry, 1989. **19**(3): p. 311-316.
45. Delanghe, B., S. Tellier, and M. Astruc, *The carbon‐felt flow‐through electrode in waste water treatment: The case of mercury (II) electrodeposition.* Environmental technology, 1990. **11**(11): p. 999-1006.
46. Bumroongsakulsawat, P. and G. Kelsall, *Tinned graphite felt cathodes for scale-up of electrochemical reduction of aqueous CO 2.* Electrochimica acta, 2015. **159**: p. 242-251.

47. Engstrom, R.C. and V.A. Strasser, *Characterization of electrochemically pretreated glassy carbon electrodes.* Analytical Chemistry, 1984. **56**(2): p. 136-141.
48. Amatore, C., J. Saveant, and D. Tessier, *Kinetics of electron transfer to organic molecules at solid electrodes in organic media.* Journal of electroanalytical chemistry and interfacial electrochemistry, 1983. **146**(1): p. 37-45.
49. Kamau, G.N., W.S. Willis, and J.F. Rusling, *Electrochemical and electron spectroscopic studies of highly polished glassy carbon electrodes.* Analytical Chemistry, 1985. **57**(2): p. 545-551.
50. Sun, B. and M. Skyllas-Kazacos, *Modification of graphite electrode materials for vanadium redox flow battery application—I. Thermal treatment.* Electrochimica acta, 1992. **37**(7): p. 1253-1260.
51. Puri, B., et al., *Chemisorption of oxygen on activated charcoal and sorption of acids and bases.* Industrial & Engineering Chemistry, 1958. **50**(7): p. 1071-1074.
52. King, A., *307. Studies in chemisorption on charcoal. Part IX. The influence of temperature of activation on the sorption of acids and bases.* Journal of the Chemical Society (Resumed), 1937: p. 1489-1491.
53. Smith, R.N., D.A. Young, and R.A. Smith, *Infra-red study of carbon-oxygen surface complexes.* Transactions of the Faraday Society, 1966. **62**: p. 2280-2286.
54. Banerjee, A., B. Mazumdar, and A. Lahiri, *Action of Permanganate on Coal.* 1962.
55. Taylor, R. and A. Humffray, *Electrochemical studies on glassy carbon electrodes: I. Electron transfer kinetics.* Journal of electroanalytical chemistry and interfacial electrochemistry, 1973. **42**(3): p. 347-354.
56. A. S. Behraman and H. Gustafson, Ind. Eng. Chem, 1935. **27**: p. 426.
57. Puri, B.R., N. Sandle, and O. Mahajan, *932. Fixation of bromine from aqueous solution by outgassed charcoals.* Journal of the Chemical Society (Resumed), 1963: p. 4880-4884.
58. Sun, B. and M. Skyllas-Kazacos, *Chemical modification of graphite electrode materials for vanadium redox flow battery application—part II. Acid treatments.* Electrochimica acta, 1992. **37**(13): p. 2459-2465.
59. Wikipedia. *Tin*. 2015 [cited 2015; Available from: https://en.wikipedia.org/wiki/Tin.
60. Zhang, Y., *Tin and tin alloys for lead-free solder.* Modern Electroplating, 2011. **52**: p. 139.
61. Ardon, M. and R.A. Plane, *The Formation of a Dinuclear Cr (III) Species by Oxidation of Chromous Solutions1*. Journal of the American Chemical Society, 1959. **81**(13): p. 3197-3200.
62. Fraser, R. and H. Taube, *Remote Attack and Ester Hydrolysis on Electron Transfer1*. Journal of the American Chemical Society, 1961. **83**(10): p. 2239-2242.
63. Gordon, G. and H. Taube, *Oxygen tracer experiments on the oxidation of aqueous uranium (IV) with oxygen-containing oxidizing agents.* Inorganic Chemistry, 1962. **1**(1): p. 69-75.
64. Holt G, P.D., Trans. Instn. Min. Metall, 1977. **86**: p. 77.
65. D, P., Trans. Instn. Min. Metall, 1977. **86**: p. 140.

66. P.A, W., *Extractive Metallurgy of Tin*. Second ed. 1982: Elsevier Scientific Publishing Company.
67. Kleinert H, W.H., Heavy metals metallurgy, 1974. **5**: p. 36.
68. L.H, M., Tin Industry Abroad, 1987. **4**: p. 33.
69. Stefanowicz, T., et al., *Tin recovery from an electroplating sludge.* Resources, conservation and recycling, 1991. **6**(1): p. 61-69.
70. Zhou, Y., W. Wu, and K. Qiu, *Recovery of materials from waste printed circuit boards by vacuum pyrolysis and vacuum centrifugal separation.* Waste management, 2010. **30**(11): p. 2299-2304.
71. Huang, K., J. Guo, and Z. Xu, *Recycling of waste printed circuit boards: A review of current technologies and treatment status in China.* Journal of hazardous materials, 2009. **164**(2): p. 399-408.
72. Jha, M.K., et al., *Leaching studies for tin recovery from waste e-scrap.* Waste management, 2012. **32**(10): p. 1919-1925.
73. Baur, W.H. and A.A. Khan, *Rutile-type compounds. IV. SiO2, GeO2 and a comparison with other rutile-type structures.* Acta Crystallographica Section B: Structural Crystallography and Crystal Chemistry, 1971. **27**(11): p. 2133-2139.
74. Noda, Y., et al., *Charge distribution and atomic thermal vibration in lead chalcogenide crystals.* Acta Crystallographica Section B: Structural Science, 1983. **39**(3): p. 312-317.

Appendices

Appendix A Electroplating Tin on Stainless Steel 316 Mesh

The procedures to electroplate tin on stainless steel 316 mesh is described as following.

1. Pretreatment

Stainless steel 316 mesh was first mechanically sanded and then washed by acetone to remove oil on surface. The mesh was then immerged into the strong basic solution containing 80 g/L NaOH, 40 g/L Na_2CO_3, 25 g/L Na_3PO_4, 8 g/L Na_2SiO_3 at 80 ℃ for 30 minutes to chemically remove oil and organics on the surface. Afterwards, it was washed by 37% HCl for 1 minute to activate the surface.

2. Electroplating copper on stainless steel 316 mesh

Under the current density of 200 A/m^2, copper was electroplated on the stainless steel mesh for a minimum of 2 hours to ensure all the surfaces were coated with copper (See **Figure A.1**). The electrolyte was composed of 150 g/L $CuSO_4$ and 60 g/L H_2SO_4. The anode was a pure copper sheet.

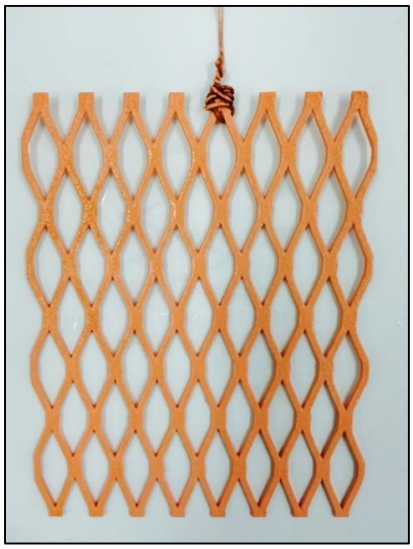

Figure A.1 Copper electroplated SS 316 mesh

3. Electroplating tin on copper coated stainless steel 316 mesh

Under the current density of 200 A/m^2, tin was electroplated on the mesh for a minimum of 2 hours to ensure every site of the mesh was completely coated with tin (See **Figure A.2**). The electrolyte was composed of 0.3 M $K_2[Sn(OH)_6]$, 0.4 M KOH and 0.5 M K_3PO_4. The anode was a pure tin sheet.

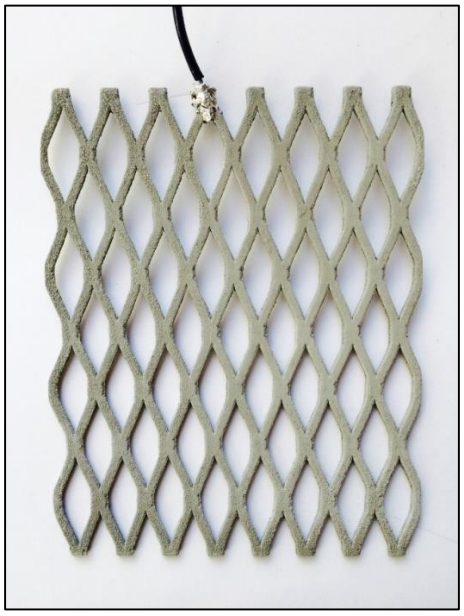

Figure A.2 Tin electroplated SS 316 mesh

4. Painting the mesh

The tin coated mesh was further painted with chemically resistant paint manufactured by Heresite Protective Coatings, Inc. to minimize hydrogen evolution on the mesh surface (See **Figure A.3**).

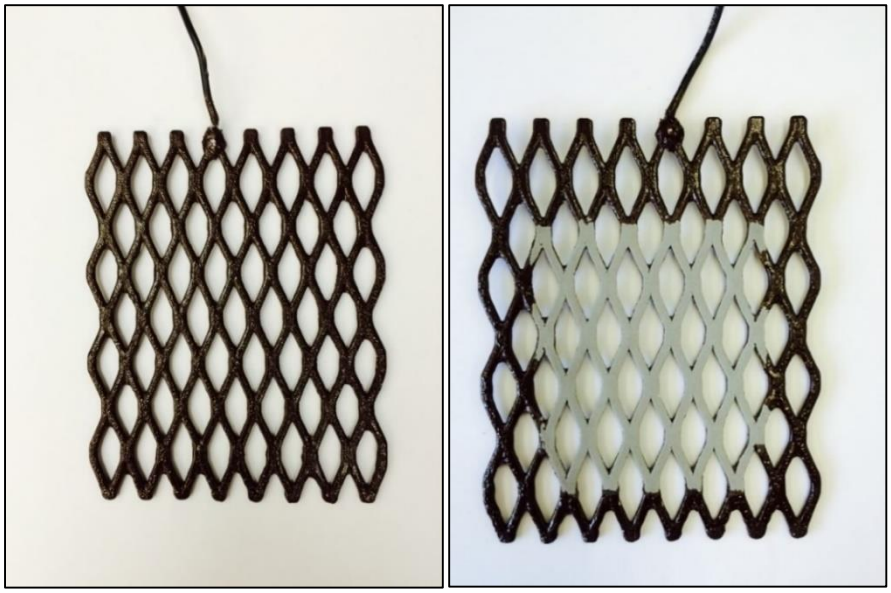

Figure A.3 Chemical resistant paint coated mesh

Appendix B Calibration Curve of Cr(III) in Acidic Aqueous Systems

Chromium(III) in the chloride system has a maximum absorbance at 428 nm. The calibration curve (λ= 428 nm) of Cr(III) in the chloride system is shown in **Figure B.1**.

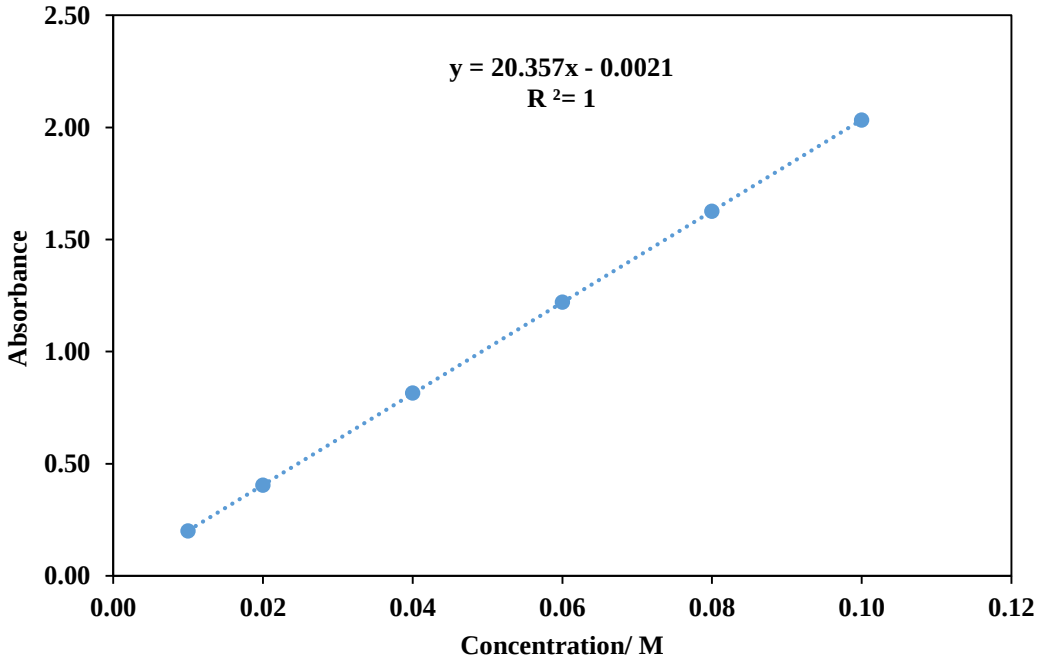

Figure B.1 Calibration curve of Cr(III) in the chloride system

Chromium(III) in the sulfate and MSA system has a maximum absorbance at 407.5 nm. The calibration curve (λ= 407.5 nm) of Cr(III) in the sulfate and MSA system is shown in **Figure B.2**.

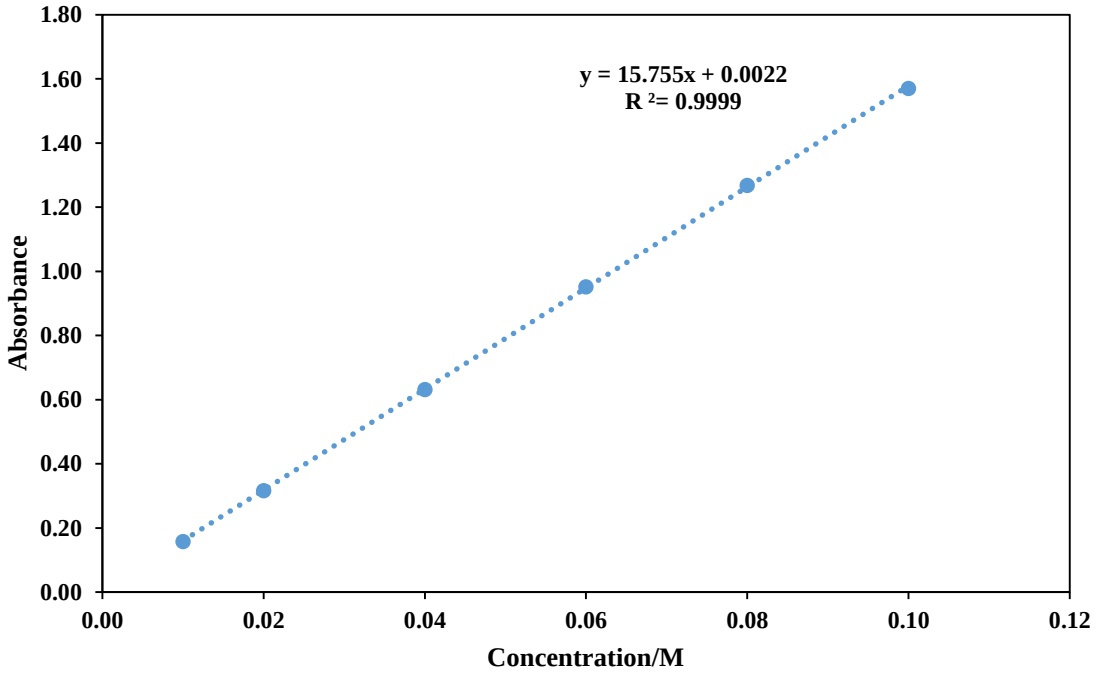

Figure B.2 Calibration curve of Cr(III) in the sulfate and MSA system

Appendix C Mass Determination in Recovery Residues

The mass of metallic tin in the residue can be determined with the principle of mass balance.

Moles of SnO_2 reacted = Moles of Sn in the residue + Moles of Sn(II) in the leachate.

Mass of the residue = Mass of Sn in the residue + Mass of SnO_2 in the residue

For example, 6.0058g SnO_2 were added to the recovery reactor. The recovery residue was 5.7535g. The Sn(II) in the leachate was analyzed by AAS, which indicated that 42.11 mg/L Sn(II) was present in the 0.8 L leachate.

$$\text{Moles of Sn element in } SnO_2 = \frac{\text{Mass of } SnO_2}{\text{Molecular Weight of } SnO_2} = \frac{6.0058\text{ g}}{150.708\text{ g/mol}} = 0.03985\text{ mol}$$

$$\text{Moles of Sn(II) in the leachate} = \frac{\text{Mass of Sn in the leachate}}{\text{Molecular Weight of Sn}} = \frac{42.11\text{mg/L} \times 0.8\text{ L}}{118.71\text{ g/mol}} = 0.0002838\text{ mol}$$

Moles of Sn and SnO_2 in the residue = Moles of Sn element in SnO_2 - Moles of Sn in the leachate = 0.03957 mol

Assume moles of Sn in the residue as α, moles of SnO_2 in the residue as β.

Moles of Sn and SnO_2 in the residue = $\alpha + \beta = 0.03957$ mol

Mass of the residue = Mass of Sn in the residue + Mass of SnO_2 in the residue

= Moles of Sn $\times$ Molecular Weight of Sn + Moles of $SnO_2 \times$ Molecular Weight of SnO_2

= $118.71\alpha + 150.71\beta = 5.7535$ g

$\alpha = 0.006567$ mol, $\beta = 0.03300$ mol

Mass of Sn in the residue = 0.006567 mol $\times$ 118.71 g/mol = 0.7796 g

Appendix D XRD Patterns

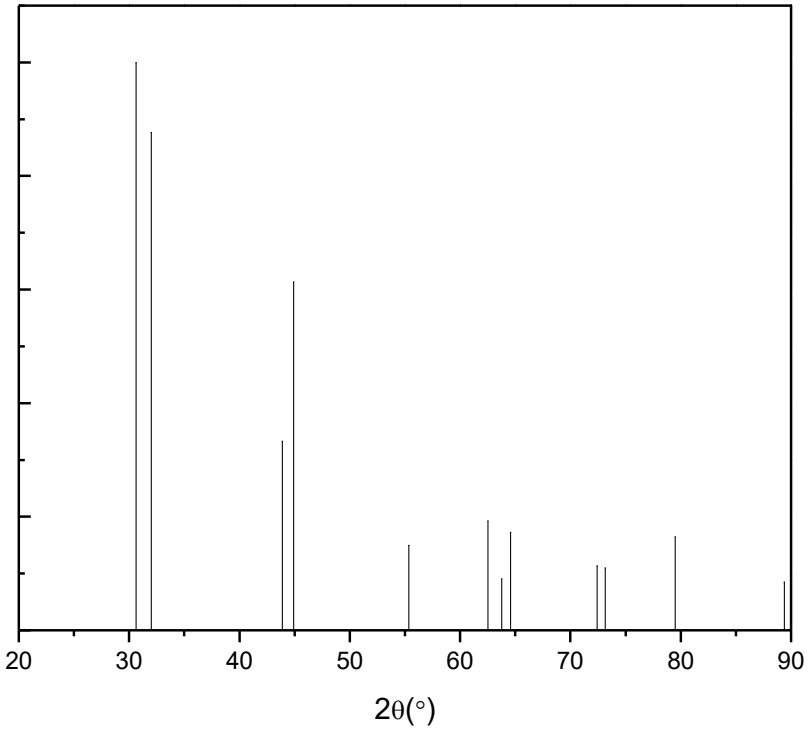

Figure D.1 XRD pattern of metallic β-Sn

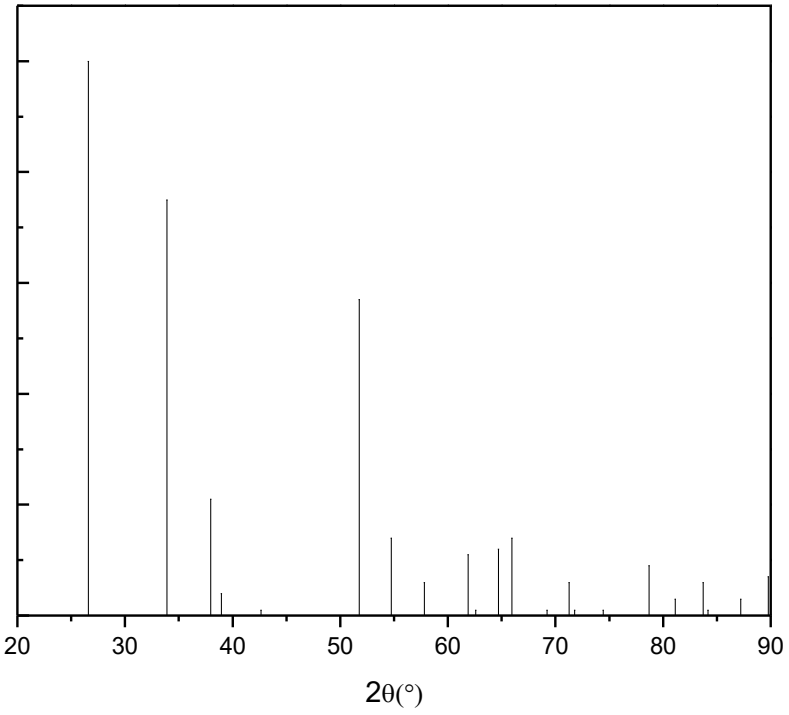

Figure D.2 XRD pattern of cassiterite (syn)